A platform for analysis of *in vitro* neuronal networks for the development of precision therapeutics in *SCN2A* disease

Linghan Jia

0000-0002-5441-8467

Doctor of Philosophy

April 2020

The Florey Department of Neuroscience and Mental Health

Faculty of Medicine, Dentistry and Health Sciences

The University of Melbourne

Submitted in total fulfilment of the requirements for the degree of Doctor of Philosophy

Abstract

Background and Purpose

Developmental and epileptic encephalopathies are a group of devastating neurological disorders in which the patients have developmental impairment as well as refractory seizures. Comorbid states are common and include cognitive and movement disorders. *SCN2A*, which encodes the brain sodium channel $Na_v1.2$, has emerged as one of the most prominent developmental and epileptic encephalopathy genes. Based on the onset of disease, patients with *SCN2A* epilepsy variants can be divided into two major groups. In the early onset group, seizures start within the first three months of life, whereas in the second group, the onset is after three months of age. Sodium channel blockers such as phenytoin are effective in some of the early onset patients. In contrast phenytoin is ineffective and may in fact worsen seizure outcomes in late onset disease. This suggests different molecular pathomechanisms. The lack of efficacious therapies underscores an urgent need for novel treatment strategies.

Experimental Approach

Two knock-in mouse lines were generated carrying Scn2a p.R1883Q and p.R854Q variants corresponding to human SCN2A p.R1882Q and p.R853Q variants. These are the most common recurrent variants found in the early and the late onset group of *SCN2A* developmental and epileptic encephalopathies, respectively. *In vitro* signatures of neuronal network behaviour were assessed using multi-electrode array analysis of the primary cortical cultures obtained from postnatal day 0-1 animals carrying the respective variants up to 28 days *in vitro*. Acute pharmacological effects were evaluated around 22 days *in vitro*.

Key Results

After 2-4 weeks network analysis in culture showed increased activity for neurons harbouring the heterozygous p.R1882Q variant associated with early onset disease. Conversely, a decreased firing rate was observed in cultures in which neurons carried the heterozygous p.R853Q variant associated with late-onset disease. The excitability in both

cultures was reduced by phenytoin, which resulted in shifting the p.R1882Q *in vitro* phenotype towards the wild types and p.R853Q away from the wild types, consistent with clinical observations. Interestingly, the activity of both cultures was changed towards the wild type phenotype by retigabine, indicating potential benefits of this drug for both early and late onset *SCN2A* developmental and epileptic encephalopathies.

Conclusion and Implications

The assumption that early onset *SCN2A* variants are more likely to cause gain-of-function and the late onset *SCN2A* variants to a loss-of-function of the $Na_v1.2$ channel was confirmed for the two studied variants using *in vitro* neuronal cultures. Moreover, the clinical observations regarding the effectiveness of the sodium channel blocker phenytoin in patients with early and late onset seizures was corroborated by our *in vitro* models. Lastly, retigabine was identified as a potential treatment for both early and late onset *SCN2A* developmental and epileptic encephalopathies.

Declaration

This thesis comprises only my original work towards the degree of PhD except where indicated in the preface. Due acknowledgement has been made in the text to all other materials used. This thesis is fewer than 100,000 words in length, exclusive of tables, figures, bibliographies and appendices.

Linghan Jia

April 2020

Preface

All chapters compiled in this thesis correspond to unpublished material and have not been submitted for publication elsewhere. I would like to acknowledge the contribution of my supervisors, Professor Steven Petrou, Associate Professor Christopher Reid, and Dr Snezana Maljevic to the study design and analysis presented in all experimental chapters. I would also like to acknowledge that Dr. Dulini Mendis wrote the custom Matlab script for data analysis.

Acknowledgements

I would like to heartfully thank my supervisor, Professor Steven Petrou for accepting me in the Ion Channels and Human Disease Lab. His scientific vision, determination and resilience have inspired me. I am extremely grateful to my co-supervisors, Professor Christopher Reid and Dr Snezana Maljevic, for their reassurance and support. I am glad I had doors to knock on when I needed discussion of projects or feedback on writing. I would also like to extend my deepest gratitude to Dr. Saul Mullen, my Committee Chair, for his valuable insight, understanding and guidance through the PhD. Also, many thanks to everybody in Ion Channels and Human Disease Lab for your warm help and throughout support.

The last but not least, I would like to thank my family and friends, without whom I could not finish this journey.

Table of Contents

List of figures

List of tables

Abbreviations

ADNFLE	Autosomal dominant nocturnal frontal lobe epilepsy
ADPEAF	Autosomal dominant partial epilepsy with auditory features
AED	Antiepileptic drugs
AIS	Axon initial segments
ANOVA	Analysis of variance
Ara-C	Cytosine arabinofuranoside
ARC	Animal resources centre
ASO	Antisense oligonucleotides
BFNIS	Benign familial neonatal-infantile convulsions
CAE	Childhood absence epilepsy
CHO	Chinese hamster ovary
CNS	Central nervous system
DEE	Developmental and epileptic encephalopathies
DIV	Day(s) *in vitro*
DMSO	Dimethyl sulfoxide
DRG	Dorsal root ganglia
EDTA	Ethylenediaminetetraacetic acid
EEG	Electroencephalogram
EIEE	Early infantile epileptic encephalopathies
FBS	Fetal bovine serum
fMRI	Functional magnetic resonance imaging
GABA	Gamma-aminobutyric acid
GEFS+	Genetic epilepsy with febrile seizures plus
GGE	Generalized epilepsies
GoF	Gain-of-function
GWAS	Genome-wide association studies
HBSS	Hank's balanced salt solution
HEK	Human embryonic kidney
HEPES	4-(2-hydroxyethyl)-1-piperazineethanesulfonic acid
HET	Heterogeneous
Ig	Immunoglobulin
ILAE	International league against epilepsy
I_{NaP}	Persistent sodium current
iPSCs	Human induced pluripotent stem cells
JAE	Juvenile absence epilepsy
JME	Juvenile myoclonic epilepsy
LEV	Levetiracetam
LGS	Lennox-Gastaut syndrome
LoF	Loss-of-function

LTG	Lamotrigine
LTP	Long-term potentiation
MEA	Multi-electrode arrays
MEG	Magnetoencephalogram
MEM	Minimum essential medium
NB	Network bursts
NBA	Neurobasal-A medium
NMDA	N-Methyl-d-aspartate
PDL	Poly-D-lysine
PHT	Phenytoin
P	Postnatal
RTG	Retigabine
SCB	Single channel bursting
SEM	Standard error of the mean
SMEI	Severe myoclonic epilepsy of infancy
SPK	Spiking
SUDEP	Sudden unexpected death in epilepsy
TM	Transmembrane domain
VPA	Valproic acid
VSD	Voltage sensing domain
WT	Wild type

Chapter 1 Introduction

1.1 Epilepsy disorders

The brain activity is determined by neurons transmitting messages through regular electric impulses. Seizures occur when these patterns are disturbed by abnormal, excessive or synchronized neuronal activity. People with recurrent unprovoked seizures are diagnosed with epilepsy, one of the most common neurological disorders that is predicted to affect 3% of the population during their life time [1].

There are major challenges in treating epilepsy. One challenge is that epilepsy can be life-threatening. The incidence of sudden unexpected death in epilepsy (SUDEP) is estimated to be around 1 in 1000 [2]. Another challenge is that one third of the epileptic patients have pharmacoresistant (uncontrolled by medication) seizures [3], which imposes a huge uncertainty and inconvenience to their everyday life. Epilepsy also creates huge burden for patients' families and the society. In the US alone, the annual economic costs of medical expenditures and informal care of epilepsy is estimated to be $9.6 billion dollars [4]. Furthermore, the current focus of antiepileptic drugs (AED) is mainly on seizure control. However, even patients with well-controlled seizures suffer from life-disturbing comorbid cognitive deficits, psychological and psychiatric disorders, and side effects of medications [5].

Investigating the underlying mechanisms of epileptogenesis will, therefore, help to find novel therapeutic strategies. Epilepsy has complex etiologies and a large spectrum of symptoms, including manifestations such as loss of consciousness or awareness, altered emotions, stiffening muscles, involuntary jerking of a body part and a loss of muscle control. Three levels of classifications are undertaken, including the seizure type classification, epilepsy type classification and epilepsy syndrome classification, providing a framework to understand the prognosis and comorbidities of patients and suggesting the treatment directions [6].

1.1.1 Classification

1.1.1.1 Seizure type classification

Based on where in brain they start, seizures can be classified into three groups: generalized onset seizures, focal onset seizures and unknown onset seizures (Figure 1.1) [6, 7]. Seizures that originate from both hemispheres are called generalized seizures, and those primarily generated within networks limited to one hemisphere are termed as focal seizure. The term unknown onset seizures describe seizures that cannot be categorized as either generalized or focal.

Within these categories, seizures can be further grouped depending on the patient's awareness and movement disorders during the seizure. Focal onset seizures can be classified into aware or impaired awareness seizures, and motor or non-motor seizures. In contrast, generalized and unknown onset seizures almost always impair the awareness and their further classification is based on whether movement is involved in seizures or not (Figure 1.1).

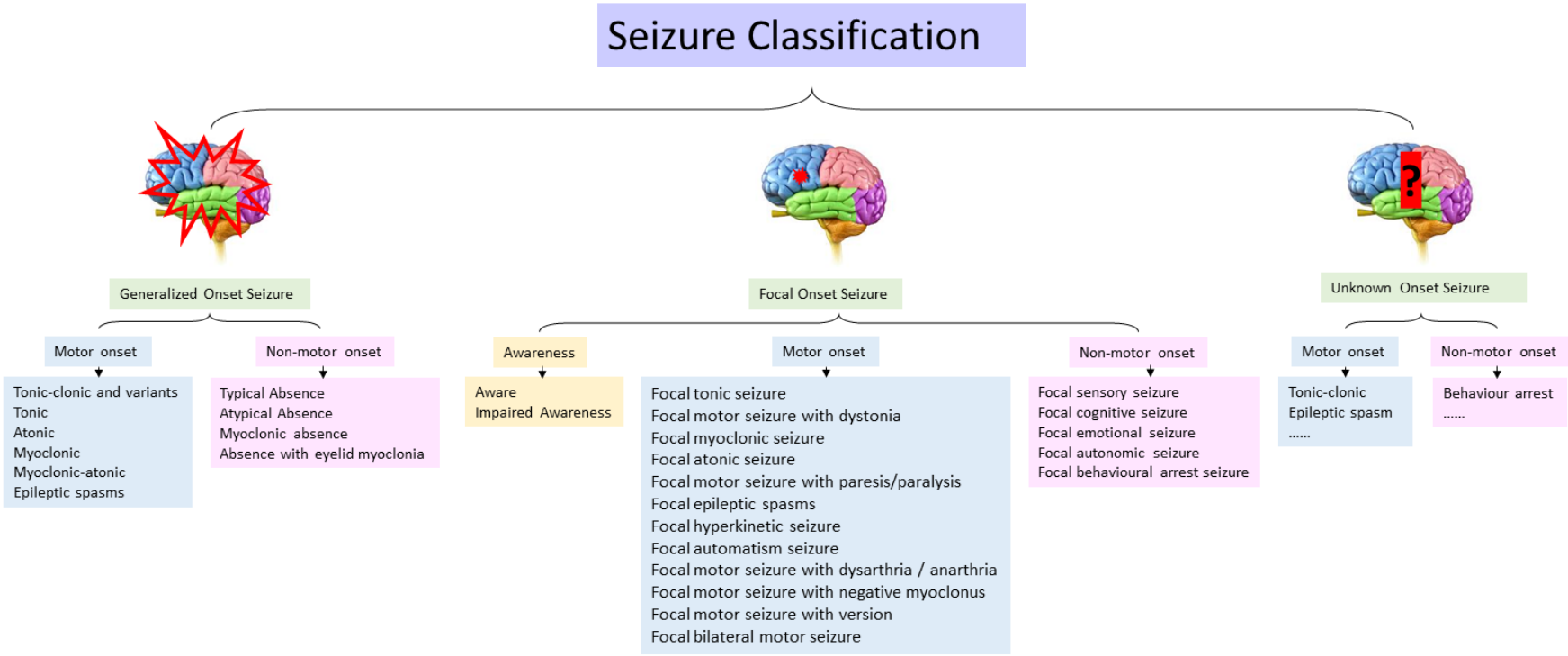

Figure 1.1 The classification of seizure types.

Adapted from, Falco-Walter et al. [6], Brodie et al. [7], and the educational international league against epilepsy (ILAE) website [8].

The most common forms of seizures are as follows [9]. An *absence* seizure is a sudden lapse in awareness and responsiveness. A *tonic* seizure is a brief stiffening of limbs. An *atonic* seizure is a sudden loss of the muscle tone. A *clonic* seizure causes jerking in various parts of the body. A *myoclonic* seizure involves sudden single jerks of a muscle or a group of muscles. A *tonic-clonic* seizure presents with the body stiffens and limbs that begin to jerk rhythmically. An *epileptic spasm* is a sudden flexion, extension or mixed flexion-extension of proximal and truncal muscles.

1.1.1.2 Epilepsy type classification

Diagnosis of epilepsy types is made on clinical grounds, supported by electroencephalogram (EEG) findings [10]. Most patients only have one or two types of seizures. The diagnoses of generalized epilepsy are made if their seizures all fall in the category of generalized seizures, and they normally show generalized spike - wave activity on EEG [10]. In contrast, the diagnoses of focal epilepsy are made if their seizures are classified as focal seizures including unifocal and multifocal seizures, and they normally show focal epileptiform discharges on EEG [10]. The new term "generalized and focal epilepsy" applies if both generalized and focal seizures occur in one patient. And the term "unknown epilepsy" is used when a normal examination presents with insufficient information available from EEG and neuroimaging (Figure 1.2) [6, 7].

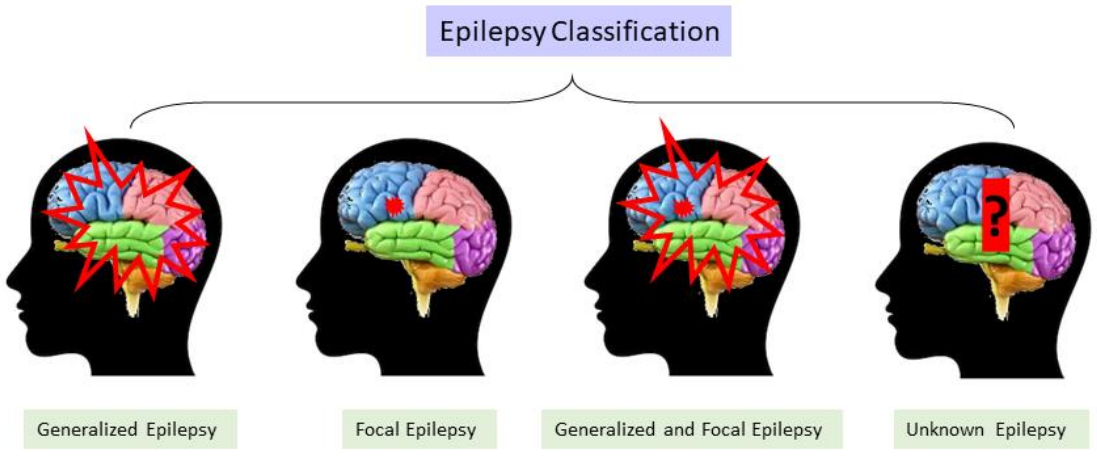

Figure 1.2 The classification of epilepsy types.

Adapted from Scheffer et al. [10], Falco-Walter et al. [6] and the educational ILAE website [8].

1.1.1.3 Epilepsy syndrome classification

Epilepsies that have a unique combination of seizure onset age, seizure types, EEG and brain scan features, are classified as specific syndromes [6]. Other features like family history, causes of seizures, presence or absence of brain abnormalities, progression of the disease, and responses to treatments are also considered during the diagnosis of epilepsy syndromes. The diagnosis of syndromes is very useful because it can suggest etiologies and guide the therapeutic approaches. Based on the seizure onset age, the syndromes are categorized into four main groups - neonatal/infantile, childhood, adolescent/adult and any age - as shown in Figure 1.3.

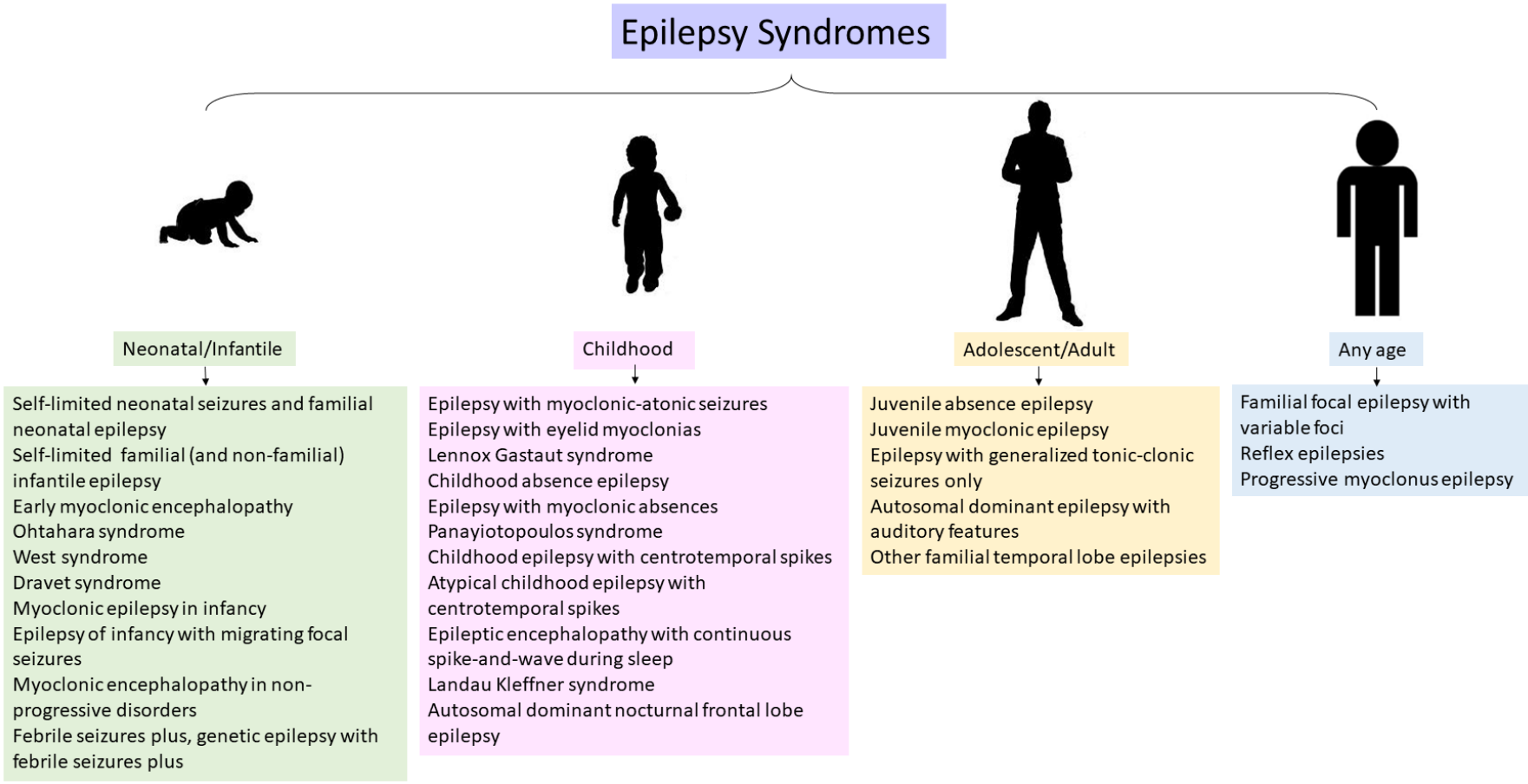

Figure 1.3 The classification of epilepsy syndromes.

Adapted from Berg et al. [11] and the educational ILAE website [8].

1.1.2 Causes of epilepsy

Epilepsy has been recognized as a brain network disorder, caused by structural and functional changes of the neuronal networks. Diverse factors can lead to the alteration of the network activity and result in seizures. They can be classified into six groups: genetic, structural, infectious, metabolic, immune and unknown factors [10].

Genetic factors are now believed to be the biggest cause, implicated in approximately 70-80% of the epilepsies [12]. To understand which genes may affect the function of brain, we need to look at the basis of neuronal networks, where the signalling transduction among nerve cells is conducted by electrical or chemical signalling. The electrical signalling is performed by action potentials that propagate along the neuronal axon toward synapses. Variants in ion channel genes can result in malfunctioning ion channels that alters the resting membrane potential and action potential firing properties [13]. Many variants in voltage gated sodium and potassium channel genes lead to loss or gain of channel function that significantly increase or decrease the excitability of neurons [14, 15]. These changes in individual neurons have an impact on the network activity and can disrupt the balance of excitatory/inhibitory inputs within the central nervous system (CNS). Enhancing the excitatory inputs through increasing the firing of excitatory neurons [16-19] or decreasing the inhibitory inputs by reducing the excitability of inhibitory neurons [20, 21] can both lead to seizures in patients. This is due to the chemical signalling in brain networks performed by neurotransmitters released at synapses between different neurons. The function of a neuronal network can be regulated through synthesis, releasing, reception and degradation of neurotransmitter, which depend on the activity of a single neuron. Moreover, variants in neurotransmitter transporters and receptors, and enzymes or other proteins that involved in synaptic transporting have all been reported in causing epilepsy [22-26]. Overall, enhancing the release of glutamate transmitter or inhibiting gamma-aminobutyric acid (GABA) transmitter can lead to hyperexcitability in CNS and cause seizures.

Except for directly influencing the function, genetic lesions can also change the structure of brain circuits. it has been proposed that sub-mesoscopic structural alterations in

neuronal networks during early development of genetic generalized epilepsy patients may cause long-term seizure susceptibility [27]. Although it is still arguable whether the structural changes are results or causes of epilepsy, long-term subtle structural changes have been found in genetic epilepsy mouse models. Moreover, studies in preclinical models showed that pathogenic variants can set seizure susceptibility into adulthood and influence early development physiology including neuronal differentiation, migration, proliferation and apoptosis [25, 28, 29], as well as dendritic outgrowth, axon guidance and synaptogenesis [30].

Since the first genetic epilepsy gene found in 1995 [31], various genetic variants that give rise to the development of many types of epilepsy have been identified. Developmental and epileptic encephalopathies (DEE, see 1.2) are most commonly caused by *de novo* dominant heterogeneous variants followed by monogenic inheritance [32]. DEE are rare and only represent a small percentage of genetic epilepsy, of which the majority are generalized genetic epilepsies (GGE). GGE have generalized spike-and-wave discharges in EEG that typically start in childhood or adolescence with combinations of absence, myoclonic, or tonic-clonic seizures [33]. The most common GGE syndromes are childhood absence epilepsy (CAE), juvenile absence epilepsy (JAE), juvenile myoclonic epilepsy (JME), and generalized tonic-clonic seizures alone [10]. GGE are rarely caused by single genes. The example of a monogenic GGE is genetic epilepsy with febrile seizures plus (GEFS+), a commonly self-resolved type of childhood epilepsy characterised by the presence of seizures brought on by febrile illness or a fever [24, 25]. Variants in genes such as *SCN1A*, *SCN1B* and *GABRG2* have been found causing GEFS+ [34, 35]. The genetic causes of most GGE are normally complex, where epidemiological, family and twin studies suggested oligo-/polygenic predisposition [36-38]. Genome-wide association studies (GWAS) have identified multiple genome-wide significant risk loci where common variants are associated with GGE, potentially explaining one third of the common GGE cases [39, 40]. Rare variants identified in DEE have also been liked to common GGE, suggesting that precision medicine targeting genetic causes in DEE may also benefit a proportion of common epilepsies [41]. Moreover, some focal epilepsies such as autosomal dominant nocturnal frontal lobe epilepsy (ADNFLE) and autosomal dominant partial epilepsy with auditory features (ADPEAF) have also been associated with genetic factors [42-44]. Identification of the genetic causes of epilepsies emerges as

critical for genetic counselling, selection of treatments in the clinic, as well as for the development of novel therapies.

1.2 Developmental and epileptic encephalopathies

Some epilepsy syndromes present with seizures and developmental delay or regression. These syndromes, commonly denoted as epileptic encephalopathies, have recently been classified DEE [10]. The reason for this is that epileptic encephalopathy implies changes in developmental outcomes caused by the occurrence of seizures. However, genetic changes can affect the development unrelated to seizures, which is what the new nomenclature tries to encompass [10].

DEE are characterized by refractory (i.e. not responsive to treatment) seizures associated with developmental delay and high risk of encephalopathic features that are present before or worsen after seizure onset [10]. DEE occur in infants and children, with the incidence of 1 in 2000 births [45]. Currently, there are no effective therapies for DEE and the available treatments mostly focus on control of seizures and do not target the comorbidities. Compared to other epileptic patients, patients with DEE have little chance of living without constant care because of the severe developmental and intellectual impairment. Therefore, it is of a great importance to gain a deeper understanding of the disease mechanisms underlying these disorders and develop treatments to improve the wellbeing of patients.

1.2.1 Clinical phenotypes

Children with DEE normally have different types of seizures and epileptiform EEG activity. Severe comorbidities include motor, social, language and cognitive delay, intellectual disabilities and movement disorders [46]. Several common DEE syndromes, including Ohtahara syndrome, early myoclonic encephalopathy, West syndrome, Lennox-Gastaut syndrome, Dravet syndrome, epilepsy of infancy with migrating focal seizures and epilepsy with myoclonic-atonic seizures are described below.

Ohtahara syndrome (also known as early infantile epileptic encephalopathies, EIEE) and early myoclonic encephalopathy are DEE that share some common features [47-49]. The

seizure onset time in both syndromes is within the first three months of age. Microcephaly may occur, and abnormal neurological behaviour and severe developmental delay are expected in both syndromes. However, the predominant seizure type in Ohtahara syndrome is tonic seizures, whereas myoclonic seizures are the predominant seizure type in early myoclonic encephalopathy. Abnormal EEG recordings with a burst-suppression pattern (high amplitude spikes followed by very limited brain activity) are also different in the two syndromes. Furthermore, patients with Ohtahara syndrome have a high risk of developing West syndrome or Lennox Gastaut syndrome.

West syndrome [50, 51] is a DEE syndrome characterized by infantile spasms and often described by that term. The onset of spasms is between 3 to 12 months of age. When the spasms occur, the body of the patient suddenly bends forward, and the limbs stiffen while flinging out. These spasms last for only 1 to 2 seconds, but they often happen in clusters that can comprise up to a hundred spasms each time. Global developmental impairment, and an abnormal EEG pattern termed hypsarrhythmia (highly disorganized EEG background with high voltage chaotic slow waves as well as polyspikes and multifocal spikes) are also seen. Epileptic spasms normally stop at the age of five, but in some patients, they next develop into Lennox-Gastaut syndrome.

Lennox-Gastaut syndrome (LGS) is characterised by the occurrence of multiple types of seizures [52-54]. Tonic seizures, atypical absence seizures and atonic seizures are commonly seen. The onset time of seizures is between 1 and 7 (normally 4) years of age. Cognition, behaviour and development are impaired as well. Patients also have abnormal EEG patterns of slow spike-and-wave and paroxysms of fast activity. This syndrome usually persists through childhood and adolescence to adult times.

Dravet syndrome was previously called severe myoclonic epilepsy of infancy (SMEI) [55, 56]. Its seizure onset time is normally between 6 months to 1 year of age, and the initial seizures are often associated with a fever or a sudden temperature change. Prolonged tonic-clonic seizures or clonic seizures on one side of the body are commonly observed as the initial seizures. Other types of seizures develop after 1 year of life, with myoclonic seizures occurring in 85% of all patients. Children with Dravet syndrome have normal development before the seizure onsets, but often from the 2nd year of life they start to show delay or regression in development.

Epilepsy of infancy with migrating focal seizures is a severe form of DEE [57-59]. It is characterized by focal seizures that migrate from one hemisphere to the other. Seizure onset is within first 6 months of life. Daily prolonged seizures with status epilepticus are often developed. By one year of age, most patients develop microcephaly. Although the development of patients before seizure onset may be normal, severe developmental delay and regression are seen after the onset of seizures.

Epilepsy with myoclonic-atonic seizures (previously known as myoclonic-astatic epilepsy or Doose syndrome) is characterised by the presence of myoclonic-atonic seizures [60, 61]. The first seizure normally occurs between 6 months and 6 years of age. Febrile or non-febrile generalized tonic-clonic seizures are often seen before the onset of myoclonic-atonic seizures. Both genders are affected, with a male predilection of 2:1. It is considered as one of the DEE, however the developmental impairment varies from normal intelligence to severe intellectual disabilities. There are other DEE that are difficult to fit in the descriptions of known epilepsy syndromes; these historical names of syndromes are changing rapidly in the face of "genetic diagnosis". When a genetic variant of major effect is identified for DEE, the term encephalopathy can be added after the gene name, such as "*SCN2A* encephalopathy" [10], linking the phenotypic spectrum of these genes.

1.2.2 Underlying mechanisms

DEE were mainly regarded as acquired [62, 63], with genetic factors considered to affect less than 15% of the DEE patients before identification of the first *de novo* variant in *SCN1A* from a patient with Dravet syndrome in 2001 [64]. Since then, with the advancement of next generation sequencing techniques, many of the previously unknown genetic variants in >50 genes have emerged as the major cause of DEE [65]. These variants are mostly heterogeneous *de novo* variants [46], though other genetic abnormalities including structural chromosomal rearrangements and somatic mosaicism can also cause DEE symptoms. The correlation between the rearrangements of chromosomes and epilepsy has been long known, for example seizures occur in 8% of Down syndrome (trisomy 21) patients, and all major type of seizures have been seen in these patients [66]. Recently, germline and somatic mosaicism (indicating that an

individual has at least two genotypically different cell populations) have been found to play an increasingly important role in DEE disorders [67, 68], affecting around 3.5% epilepsy patients carrying pathogenic variants in one of the nine most promising genes. Individuals carrying somatic mosaicism of pathogenic variants can present different level of symptoms or be clinically unaffected [69-73]. It is important to note that parents with germline mosaicism can pass the variant onto their children. Case studies have reported parental mosaicism of pathogenic variants in many genes, including commonly affected epilepsy genes *SCN1A* [74-76], *SCN2A* [77] and *KCNQ2* [78].

With the discovery of more DEE genes, phenotypic heterogeneity and genetic heterogeneity became apparent in this disorder, with variants in one gene causing different syndromes, as well as one syndrome being caused by variants in different genes [46]. For example, the most prominent pathophysiological gene linked to Dravet syndrome is *SCN1A*: variants in *SCN1A* were found in around 80% of Dravet patients [79, 80]. However, Dravet syndrome has been associated with variants in a number of other genes, such as *SCN1B* [81], *SCN2A* [82], *HCN1* [83], *PCDH19* [69], *STXBP1* [84], *GABRA1* [84], *GABRG2* [85] and *GABRB3* [86], indicating genetic heterogeneity. Besides Dravet syndrome, *SCN1A* variants have also been identified in other syndromes, such as generalized epilepsy with febrile seizures plus [87-89] and West syndrome [90], showing phenotypic heterogeneity. Although identifying the genetic variants behind DEE cannot directly categorize patients into traditional syndromes due to phenotypic heterogeneity, it presents a new diagnostic strategy that can direct the treatment [91] and improve our understanding of the pathophysiological mechanisms underlying the disorder.

To date, many DEE genes have been identified and some of them are listed Table1-1 based on the functions of their encoding protein. The most important group of identified genes are encoding ion channels, especially voltage-gated sodium channels, which will be discussed in the next section.

1.2.3 Treatment strategies

Clinical studies have found that the effectiveness of traditional AED is poor in DEE patients. In many cases, AED have either been shown to be non-beneficial or seizure-

worsening [92]. Although in some cases AED reduced the seizures, the devastating comorbidities such as developmental delay, intellectual disability and movement disorders were not improved. New treatment directions that can help with the comorbidities in addition to seizure control are urgently needed in DEE.

Table 1-1 DEE genes grouped by encoded protein functions.

Category	**Protein function**	**Gene**
Voltage-gated ion channel	Voltage-gated sodium channel	*SCN1A, SCN1B, SCN2A, SCN8A, SCN9A*
	Voltage-gated potassium channel	*KCNA2, KCNB1, KCNQ2, KCNT1*
	Voltage-gated calcium channel	*CACNA1A*
	Voltage-gated cation channel	*HCN1*
Ligand-gated ion channel	GABA-A receptor	*GABRA1, GABRB1, GABRB3, GABRG2*
	NMDA receptor	*GRIN1, GRIN2A, GRIN2B, GRIN2D*
Transporter	Neurotransmitter transporter	*SLC1A2, SLC25A12, SLC25A22, SLC6A1*
	Other transporter	*SLC12A5, SLC13A5, SLC2A1*
Enzyme/Enzyme modulator	Enzyme	*AARS, ALG13, ARV1, CDKL5, CHD2, DNM1, GNAO1, GUF1, ITPA, PLCB1, PNKP, SIK1, ST3GAL3, UBA5, WWOX*
	Enzyme modulator	*ARHGEF9, DOCK7, TBC1D24*
Others	Signal transduction/molecule	*FGF12*
	Cell adhesion molecule	*PCDH19*
	Protein trafficking	*STXBP1, FRRS1L*
	Cytoskeletal protein	*SPTAN1*
	Nucleic acid binding	*EEF1A2, GUF1*
	Unclassified	*NECAP1, SZT2*

Adapted from Wang et al. [93] and McTague et al. [46]. NMDA stands for N-Methyl- d-aspartate.

The recent development of next generation sequencing techniques has enabled the detection of genetic changes in patients, whereas functional studies of these variants have helped to understand the underlying pathomechanisms. Together, this has led to the development of precision medicine treatments that are specifically tailored to target the cause of disease in each patient. The quickest way to provide novel treatments is through discovering new application of old approved drugs. For example, quinidine is known to inhibit KCNT1 channels, and has been used to treat cardiac arrhythmias [94, 95]. A number of *KCNT1* variants have been found in DEE patients. Functional analysis of these variants found them to be gain-of-function (GoF), which suggested a potentially beneficial effect of quinidine. After the inhibiting effect of quinidine on the mutant channels was confirmed [96], quinidine was also used in DEE patients carrying *KCNT1* variants and showed limited efficacy, mostly in patients at a very young age but was not beneficial to others [97-100]. Another example is retigabine (RTG), an opener of KCNQ channels [101]. It was approved as add-on treatment for focal epilepsy [102] but then discontinued due to lack of efficacy and some side effects [103]. However, the discovery of *KCNQ2* and *KCNQ3* loss-of-function (LoF) variants in DEE patients, and the observed treatment benefit in some of these patients pointed to the potential utility of RTG or safer potassium channel activators in DEE [104].

Current treatments of DEE are more focused on seizure control and have limited effects on other symptoms. However, development impairment, intellectual disability and movement disorders severely affect the life quality of DEE patients and their family. It is of great importance to improve not only epileptic but also other symptoms in DEE patients. Genetic treatment showed great potential in treating genetic causal disorders, either by correcting the disease-causing variant in genomic DNA or via regulation of expression of the affected gene. CRISPR/Cas9 technique provided the possibility of DNA editing. Apart from ethnical concerns, there are still technical issues with the application of this approach, including off-target effects and use of viral delivery. Another genetic intervention is to control protein levels using specific targeting of mRNA (messenger RNA) expression levels. This approach relies on the use of antisense oligonucleotides (ASO) that have emerged as one of the most promising genetic tools for neurogenetic disorders. ASO therapy has recently been approved to treat spinal muscular atrophy [105, 106]. In DEE, ASO successfully upregulated the expression of *SCN1A* and improved the

excitability of hippocampal interneurons and seizure phenotype in Dravet mouse model [107]. However, technical issues regarding to delivery, efficiency, safety and therapeutic windows are still potential obstacles [108, 109].

1.3 *SCN2A* associated epilepsy

Among the DEE associated genes, ion channels represent the most notable group [46, 110]. Ions are electrically charged atoms or molecules that determine the electrophysiological environment of our bodies. Ion channels are complex pore-forming transmembrane proteins that allow transport of ions through their pores following the concentration gradient. Based on the activation mechanisms, ion channels can be divided into two major groups: voltage-gated ion channels and ligand-gated ion channels. Ion channels are responsible for diverse physiological processes such as nerve impulses, muscle and heart contractions, hormonal secretions, and the homeostasis of salt and water. Dysfunction of ion channels would be expected to affect neural excitability [111, 112], interrupt signal transduction [113, 114], influence cell proliferation, migration and apoptosis [115-117].

With over 700 variants identified in patients with epilepsy, voltage-gated sodium channels have been shown to play an essential role in the genesis and alleviation of this disorder [118].

1.3.1 Voltage-gated sodium channel

1.3.1.1 Structure and function

Voltage-gated sodium channels are responsible for the initiation and propagation of action potentials [119]. There are three conformational states of voltage-gated sodium channels, closed, open/activated and inactivated (Figure 1.4A) [120, 121]. When cells are in the resting state, the channels are mostly closed and do not allow sodium ions to pass through the pore. But a small change of the membrane voltage, such as a slight membrane depolarization caused by excitatory synaptic input, can activate these channels through opening of the activation gates, allowing sodium ions to flow into cytoplasm down the electrochemical gradient and create a rapid membrane depolarization [122]. This process

is called activation. Once activated the channels then inactivate and thereby enter a non-conducting conformation during depolarization of cell membrane. Fast inactivation and slow inactivation are both common for voltage-gated sodium channels. Fast inactivation occurs when sodium ions influx and the extracellular inactivation gates close within milliseconds [121], whereas slow inactivation involves the rearrangement of the pore domain on a longer time scale [123]. The recovery of voltage-gated sodium channels from inactivation is called repolarization, when the inactivation gate reopens and the activation gate closes [123]. It is necessary for the channels to recover and return to resting state before they can open again [123].

Voltage-gated sodium channels are heteromeric integral membrane glycoproteins consist of a pore-forming α-subunit associated with one or two auxiliary β-subunits [124, 125]. The α-subunit, responsible for voltage-dependent ion conductance, comprises of a single ~ 260 kDa polypeptide chain that folds into four homologous repeat domains I-IV (Figure 1.4) [126]. Each domain contains six transmembrane α-helical segments S1-S6 [127]. S1-S4 in each domain form a voltage sensing domain (VSD), with S4 segments serving as voltage sensors [128, 129], while S5 and S6 from the four domains combined to form the ion-conducting pore domain [130]. High concentration Arg/Lys residues on S4 is critical for voltage sensing, facilitated by coordination to acidic and polar residues on S1-S3 [128]. The positively charged residues on S4 can move through the electric field of the membrane towards the outside of cells [131]. The Ile/Phe/Met/Thr motif on the cytoplasmic linker connecting domains III and IV plays an important role in fast inactivation: during the process, this motif is inserted into a hydrophobic cavity enclosed by the end of S6 in domain IV and the linker between S4-S5 in domains III and IV [132]. The Asp/Glu/Lys/Ala residues on hairpin-like loops between S5 and S6 form a narrow filter on the extracellular side of pore domain that controls the ion selectivity [133]; this moderately selective pore allows mistaken passage of potassium ions in 1 in 15 attempts. 10 different isoforms of α-subunits are found in humans, $Na_v1.1$-$Na_v1.9$ and Na_X, encoded by the genes *SCN1A*-*SCN5A* and *SCN7A*-*SCN11A* [134]. Most of the voltage-gated sodium channels are localized in the nervous tissue, with "brain sodium channels" $Na_v1.1$, $Na_v1.2$, $Na_v1.3$ [135, 136], and $Na_v1.6$ mainly expressed in the central nervous system [137, 138], and $Na_v1.7$, $Na_v1.8$, and $Na_v1.9$ primarily found in the peripheral nervous system [139-141]. $Na_v1.4$ are mostly expressed in skeletal muscles while $Na_v1.5$ is

cardiac-specific isoform [142, 143]. Na_X is significantly different in the amino acid sequence from other voltage-gated sodium channels, skeletal muscle, the heart and uterus [144, 145]. β-subunits promote membrane localization of channels and modulate channel properties including the kinetics and voltage-dependence [146]. They are normally between 30-50 kDa large proteins, each composed of an extracellular immunoglobulin (Ig) loop, a single transmembrane domain (TM), and a short intracellular domain [147, 148]. There are four type of β-subunits (β1- β4) in human, encoded by *SCN1B-SCN4B* [149]. All of them can associated with the α-subunit of $Na_v1.2$ [149].

Variants in voltage-gated sodium channels may change the localization, activation, inactivation and repolarization of the channels, and therefore impact on the initiation and propagation of action potentials, and further influence the brain function according to their distribution.

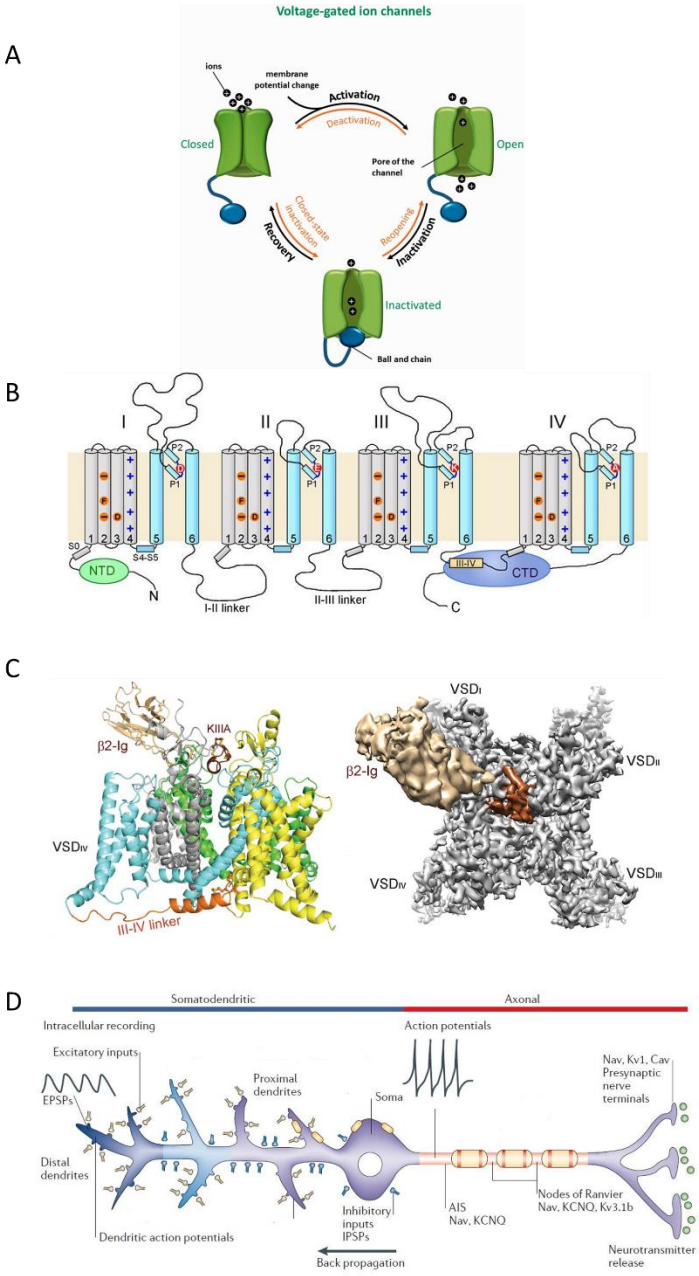

Figure 1.4 Voltage-gated sodium channels architecture and distribution.

(A) Three-state model of voltage-gated ion channels. (B) Topology of human voltage-gated sodium channels α-subunits. (C) The side and extracellular view of human $Na_v1.2$-β2 complex bound to the m-conotoxin KIIIA. KIIIA is shown in brown and β2-Ig is shown in beige. (D) Distribution of brain sodium channels is mainly in axon initial segments, the nodes of Ranvier and presynaptic nerve terminals. Adapted from Hinard et al. [150] Shen et al. [151], Pan et al. [152] and Lai et al. [153].

1.3.1.2 Brain voltage-gated sodium channel $Na_v1.2$-SCN2A

The central pore-forming α-subunit of voltage gated sodium channel $Na_v1.2$, encoded by *SCN2A* [154], is predominantly expressed in the axon initial segments (AIS) and nodes of Ranvier of excitatory neurons in hippocampus and cerebral cortex. During development, $Na_v1.2$ will be partially replaced by $Na_v1.6$ [155, 156]. Specially, during development low-threshold $Na_V1.6$ channels accumulate at the distal part of AIS and the nodes of Ranvier, while high-threshold $Na_v1.2$ channels recede to the proximal AIS [157]. When depolarizing currents generated by synaptic inputs reaches the AIS, low-threshold $Na_v1.6$ channels at the distal AIS will be activated to generate action potentials [157]. The transmembrane currents will then propagate both down the axon and back towards the soma [157]. The back-propagating current will depolarize the membrane and activate high-threshold $Na_v1.2$ to induce back-propagating action potentials [157].

1.3.2 Voltage-gated sodium channel associated epilepsy

1.3.2.1 Brain sodium channel DEE

This complex interplay among different brain voltage-gated sodium channels is critical for neuronal network excitability. Therefore, variants of these channels or their pharmaco-modulation are likely to influence central nervous system networks and cause DEE [158]. Table 1-2 summarises the brain sodium channels linked to DEE together with their phenotypic features and function impact.

Table 1-2 Phenotypic features and pathogenic mechanisms of major single gene encoding brain voltage gated sodium channels causes DEE.

Gene	Chromo-some	Protein	Epilepsy syndrome/s	Seizrue onset age	Seizure onset type		EEG at onset		Development at onset		Survival	Functional impact
					Seizure evolution		EEG evolution		Development evolution			
SCN 1A	2q24.3	$Na_v1.1$	Dravet syndrome, epilepsy of infancy with migrating focal seizures, epilepsy with myoclonic atonic seizures, epilepsy aphasia spectrum, genetic epilepsy with febrile seizures plus	4-15 months	Febrile, tonic clonic, hemiclonic, status epilepticus		Normal, generalized spike-wave, some photosensitive		Normal in most		Death in childhood in some	GoF (rare) LoF
					Refractory Seizure - myoclonic, absence, focal, tonic clonic, febrile, status epilepticus		Generalized spike-wave, polyspike-wave, multifocal, some photosensitive		Normal (rare) to severe developmental delay, neurologic decline in adulthood			
SCN 1B	19q13.1	$Na_v\beta1$	Genetic epilepsy with febrile seizures plus, temporal lobe epilepsy, Dravet syndrome	3–6 months, early childhood in some	Febrile, focal, hemiclonic, absence, myoclonic		Normal		Normal		Death in childhood in some	LoF
					Refractory Seizure - afebrile, absence, tonic–clonic, status epilepticus		Generalized spike-wave, multifocal, slow spike-wave		severe developmental delay			
SCN 2A	2q24.3	$Na_v1.2$	Ohtahara syndrome, epilepsy of infancy with migrating focal seizures, early onset DEE, West syndrome, unclassified DEE, benign familial neonatal-infantile seizures	0-3 months in most, early childhood in some	Focal, tonic, infantile spasms		Burst-suppression, multifocal		N/A or normal in most		Death in early childhood in some	GoF LoF
					Refractory Seizure - focal, infantile spasms, tonic, myoclonic		Multifocal, normal		Severe-profound developmental delay in most, some normal			
SCN 8A	12q13	$Na_v1.6$	Epilepsy of infancy with migrating focal seizures, West syndrome, unclassified DEE	0-22 months	Focal, infantile spasms, tonic		Normal, F, multifocal, hyps		Normal or developmental delay		Death in childhood in some	GoF LoF
					Refractory Seizure in most - focal, tonic, clonic, myoclonic, atypical absence, status epilepticus		Multifocal, slow spike-wave		Moderateprofound developmental delay			

Adapted from McTague et al [46], Oyrer et al [110] and Bouza et al [159].

Variants in *SCN2A* are related to many neurological disorders, including benign epilepsy, DEE, autism spectrum disorders, intellectual disability and schizophrenia [77, 82, 160-164]. Such a broad disease spectrum has become evident for many of the identified epilepsy genes, suggesting common pathways may underlie these neurological conditions [165-170]. *SCN2A* variants first to be identified were linked to benign familial neonatal-infantile convulsions (BFNIS) [171-173]. In the meantime, a number of *de novo* variants have been identified in DEE [82, 174]. Based on their distinct clinical phenotypes and responsiveness to sodium channel blocking antiepileptic drugs (AED), DEE patients with *SCN2A* variants are divided into two groups, the early seizure-onset group and the late seizure-onset group [175]. Patients in the early onset group have a seizure onset time within three months of life and a better response to sodium channel blockers. Conversely, for patients in the late onset group, presenting with a seizure onset after three months of age, sodium channel blockers are rarely effective [92]. The ratio of *SCN2A* variants in each of these groups is at about 50%. Functional analysis of BFNIS variants has suggested gain of channel function as the major molecular mechanism [172]. This was an expected finding as the increased function of sodium channels in the principal cortical neurons would lead to the increased neuronal activity and thus to seizures. However, recent clinical and functional assessments have indicated that both GoF and LoF of *SCN2A* can be linked to DEE. Moreover, it became evident that GoF is common finding in early, and LoF in late onset *SCN2A* DEE [92].

1.4 Disease modeling for developmental and epileptic encephalopathy

Experimental models are essential for studying disease mechanisms and finding potential treatments, especially when the genetic cause is known. Models for genetic epilepsy range from single cells to animal models, commonly including heterologous expression systems, neuronal *in vitro*/*ex vivo* models and *in vivo* animal models [5].

1.4.1 Heterologous expression systems

Heterologous expression systems are often used as first-step models to study the impact a variant has on the function of the protein. Using molecular cloning and site-directed

mutagenesis, variants are inserted into the plasmid carrying the cDNA (complementary DNA, corresponding to the mRNA) of the affected gene. The mutated plasmid and the corresponding wild type control are then expressed in systems that normally don't contain this protein. Functional studies are then performed to identify differences between wild type and mutant proteins.

Xenopus laevis oocytes and mammalian cells such as human embryonic kidney (HEK) 293 cell line and Chinese hamster ovary (CHO) cell line are the most commonly used heterologous expression systems. Two microelectrode voltage clamping of oocytes is often used to study ligand-gated ion channels and voltage-gated potassium channels. For example, in *Xenopus laevis* oocytes, *KCNT1* DEE variants were found to be GoF, and the increased function could be decreased by quinidine [96]. Patch clamping of mammalian cell lines is often used to study voltage-gated sodium channels. For example, in CHO cells, *SCN2A* early onset DEE variant showed GoF while *SCN2A* late onset DEE variant showed LoF [176].

Although electrophysiological analyses using heterologous expression systems is rapid and can provide detailed information about dysfunctional proteins, there are issues regarding post-translational modifications, phosphorylation, trafficking and protein interactions in non-neuronal modelling systems. In some cases, functional findings can be different in neuronal systems and non-neuronal systems. For example, three *SCN2A* epileptic variants were found to be LoF in HEK293 cells [177], but showed GoF in rodent primary cortical neurons [172]. The GoF results matched the effective treatments using sodium channel blockers in the patients carrying these variants, showing advantage of utilizing neuronal systems. Thus, to supplement the insufficiency of heterologous expression systems, other systems with higher physiological similarity are required.

1.4.2 Neuronal *in vitro/ex vivo* models

Currently used neuronal models include rodent brain slices, rodent primary neuronal cultures and human induced pluripotent stem cells (iPSCs) derived neuronal cultures. Efficient methods have been established to obtain brain slices and primary cultures from rodent models. Brain slices can better maintain the morphology of neurons and the structure of neuronal networks, and therefore are more commonly used in acute

experiments. Conversely, primary cultures are easier to manipulate and maintain for longer term recording, showing the advantage in drug screening and studying developing disorders. To study gene variants, these neuronal models can be either transfected or gathered from transgenic rodents. Recently, rapidly developed technologies of stem cells raised the possibility to perform studies with human neuronal cultures. Several DEE variants in different genes have been modelled using patient derived iPSCs, including *SCN1A*, *SCN2A*, *STXBP1* [5, 178]. However, the methodology requires further optimisation, particularly in regard to reproducibility. Moreover, stem cell derived neurons usually do not reach advanced maturity *in vitro*.

Neuronal *in vitro/ex vivo* models can be studied on single neuronal level or neuronal network level. The electrophysiological analysis of single neurons is normally conducted by patch clamp technology and is well established and can reveal changes in firing frequency, properties of action potential, synaptic activity [19]. Studying neuronal networks can provide valuable information about the interactions among different neurons and how the entire neuronal assembly and its function are is affected. However, the analysis of neuronal networks is still in development, with calcium imaging and multi-electrode arrays (MEA) as the two stand-out technologies. Although the utilization of neuronal network analysis in DEE is still rare, calcium imaging and MEA have shown their potential in induced epileptic models [179, 180].

1.4.3 *In vivo* animal models

Zebrafish is an emerging animal model used in epilepsy research. It has the advantage of easier to access *in vivo* brain function. For instance, light sheet calcium imaging in zebrafish larvae provided a different angle to study epileptic activity by assessing the effectiveness of neuronal network though the analysis of synaptic dynamics [181]. pentylenetetrazole and high concentration potassium increased live zebrafish larvae neuronal activity on non-invasive MEA [182], while $Na_v1.1$ (*scn1Lab*) mutant zebrafish exhibited spontaneous abnormal electrographic activity, hyperactivity and convulsive behaviours [183], showing the potential of studying epilepsy in this model. Zebrafish is also easier than other animal models for the application of compounds and shows the potential for higher throughput drug screening [183, 184]. However, behavior methods

for zebrafish are still underdeveloped [185-187] and the clinical translational effectiveness is not well evaluated.

There has been a long history of using rodent models to study epilepsy, and therefore numerous methods have been established, including EEG, behavioral tests and imaging. The rodent models of epilepsy can be grouped into three categories: induced, spontaneous and transgenic. Chemicals and electrical stimulation have been used to create models of chronic epilepsy or acute seizures. For more than 60 years, the anticonvulsant activity in acutely induced epilepsy models, especially the maximal electroshock seizure and pentylenetetrazole seizure models, were widely used in the discovery of AED [188]. However, now it becomes harder for these models to identify AED with novel mechanisms of action or to hint at the unknown pathology of epilepsy. Rodent models carrying spontaneously occurring variants that leads to epileptic phenotype, on the other hand, were helpful in finding novel genes associated with epileptogenesis [189]. Most of these genes are in charge of ion transporting. For example, variants in *Nhe1*, *Cacna1a* and *Cacng2* gene, which encode the sodium/hydrogen exchanger, P/Q-type voltage-gated calcium channel and L-type voltage-gated calcium channel, were found in autosomal recessive slow-wave epilepsy mouse model, tottering mouse model and stargazer mouse model, respectively. Variant of the Ca^{2+} channel β subunit gene *Cchb4* is associated with ataxia and seizures in the lethargic mouse. Many gene knock-out rodent models were also created. For instance, *SCN2A* knockout mice were generated to understand the loss-of-function $Na_v1.2$ in the pathology of epilepsy, autism and schizophrenia. In this knockout line, homozygous mice were lethal within one or two days postnatal, while heterozygous mice exhibited no phenotype except for showing ethosuximide-sensitive absence-like seizures in one study [190]. Recently, the utilization of novel gene editing tools in generation of mouse models has been well established and commercialized, enabling the development of knock-in mouse lines and making transgenic mouse models the most commonly used animal models in DEE. $Scn2a^{Q54}$ is a well-studied epileptic mouse line, presenting spontaneous seizures, EEG focal seizure activity in hippocampus, behavioural arrest, stereotyped repetitive behaviours and shorter lifespan [16]. However, the variant carried by $Scn2a^{Q54}$ was not found in clinic but in laboratory, showing inactivation slow and persistent current enhance in *Xenopus* oocytes. While this helps us understand the physiology and function of *SCN2A*, it is difficult to extrapolate the identified mechanisms

to the disease phenotype seen in patients. To study the mechanisms of DEE, a more useful way may be to create transgenic mouse models based on variants found in patients. For instance, impaired sodium currents in GABAergic interneurons was found by creating a mouse model expressing a truncated *SCN1A* variant found in Dravet patients [191]. In *SCN8A* knock-in model harboring a gain-of-function variant found in DEE patients, frequent spontaneous seizures and sudden unexplained death in epilepsy (SUDEP) were shown. This corresponds to clinical observation, indicating gain-of-function of $Na_v1.6$ leads to a more severe phenotype of DEE [192]. As for *SCN2A*, increased excitability in hippocampal pyramidal neurons was identified in a human BFNIS variant knock-in mouse line that exhibiting frequent seizures and increased mortality [193].

1.4.4 Dissociated neuronal cultures on multi-electrode arrays

As indicated above, the methods to study single cell level and whole animal level are well established. However, there are fewer technologies available for neuronal network level analysis. Here I explore if the analysis of neuronal cultures using MEA can bridge the gap between single cell and animal studies?

MEA are devices that contain multiple electrodes through which electrophysiological signals are obtained. So far, MEA analysis has been commercialized and have found application in toxicity and pharmacology studies [194-197].

Current MEA technology can record neural signals extracellularly, where field potentials of one or multiple neurons are detected by adjacent micro electrodes non-invasively. Although the neuronal signals from patch clamp recordings are more precise, the disruption of cellular membrane causes significant damage to cells and the experiments can only be performed for a short time, which limits their usage. In contrast, extracellular MEA have the advantage of conducting long-term studies including neuronal network developmental studies which may be crucial for the neurodevelopmental disorders, including DEE.

MEA can record spontaneous and evoked activity on any electrogenic tissues, including neuronal and cardiac cultures, brain cultured and acute tissue slices, intact retinas, stem cell derived neurons and cardiomyocytes [198]. Primary dissociated neuronal cultures have two advantages for the study of DEE: (1) the potential for high throughput analysis

and (2) the potential for modelling the development of neuronal networks. During the preparation of the primary cultures, neurons are disconnected and seeded on top of the electrodes. Over time, these neurons form connected neuronal networks with increasing maturity. Hence, long-term experiments can be performed to study both the phenotype changes caused by different genotypes during the development of neuronal networks, as well as to assess the chronic pharmacological or toxic effects of drugs.

1.5 Rationale, hypothesis and aims

DEE is a group of devastating neurological disorders with currently no effective treatments. The motivation for this project is to gain a deeper understanding of the underlying mechanisms of DEE and to identify potential treatments for the patients. *SCN2A* is one of the most prominent disease-causing genes in DEE. Recent studies have raised a paradox of how both GoF and LoF variants in *SCN2A* can lead to DEE. Thus, two most recurrent variants linked to early and late onset DEE were investigated and shown to be gain-of-function and loss-of-function in CHO cells, respectively.

There are three main levels to study the functional change in disease models, including single cell level, neuronal network level and whole animal level. Neuronal network level is important for epileptic studies because epilepsy is a neuronal network disease. Therefore, functional studies of neuronal networks may help to resolve the paradox of *SCN2A* DEE. Compared to the whole animal level, network analysis has the potential for high throughput drug screening that can be beneficial to find new treatments. However, the functional analysis of neuronal networks is being constantly improved. This provided motivation to establish a robust neuronal network analysis method. MEA analysis of neuronal cultures was chosen for this study because it allows the measurement of firing non-invasively for a longer period of time, making them a perfect model system for investigating developmental disorders. Besides, MEA signals allow multiple firing parameters to be extracted that can be used to further characterise disease models and may also be used as markers for drug development.

Hypothesis: MEA analysis of primary neuronal cultures can be used to identify *in vitro* phenotypes of early and late onset *SCN2A* DEE, and this *in vitro* assay can be used to predict and test potential drug therapies for *SCN2A* DEE.

Aim 1 (presented in Chapter 3): Establishing a robust *in vitro* network scale assay based on MEA analysis of primary neuronal cultures.

Aim 2 (presented in Chapter 4): Use MEA analysis of neuronal cultures generated from knock-in mice to model early onset and late onset *SCN2A* DEE.

Aim 3 (presented in Chapter 5): Determine potential drug efficacy in *SCN2A* DEE based on MEA analysis of neuronal cultures from knock-in mice.

Chapter 2 General materials and methods

2.1 Animals

Advanced pregnant wild type C57BL/6 mice were purchased from Animal Resources Centre (ARC).

Mouse lines carrying variants corresponding to human SCN2A p.R1882Q and p.R853Q variants were generated on C57BL/6 background by Cyagen Biosciences (Cyagen Biosciences, Inc, Guangzhou, China). From now on, these mice will be referred to as SCN2A p.R1882Q and p.R853Q mice. Targeted embryonic stem cell clones were microinjected into mice blastocysts (p.R853Q) or ICR surrogates (p.R1882Q). Heterozygous p.R853Q mice were crossed with wild type C57BL/6 mice to generate heterozygous p.R853Q pups and their wild type littermates. SCN2A p.R1882Q mice showed a severe phenotype with seizures and premature death by age P30. When the pups were intracerebroventricular injected with *SCN2A* specific ASO on P1 (Li et al., unpublished data) they could reach maturity, and the treated males were bred with wild type C57BL/6 females to produce heterozygous and wild type pups for *in vitro* experiments. Mice were genotyped by Transnetyx (Transnetyx, Inc, Cordova, US).

Animals were housed in a temperature-controlled environment, maintained at 23 °C with a 12 h light/dark cycle. Tissue extraction from animals was carried out in accordance with the Prevention of Cruelty to Animals Act and the NHMRC Australian Code of Practice for the Care and Use of Animals for Scientific Purposes, and was approved by the Florey Institute Animal Ethics Committee.

2.2 MEA plates preparation

24-well plates with gold electrodes on Flame Retardant 4 were purchased from Multichannel Systems (24W700/100F-288; Multichannel Systems, Inc; Reutlingen, Germany). Each well contains 12 electrodes. The diameter of an electrode is 100 µm and the spacing between neighbouring electrodes is 700 µm. 200 µL of 1% Terg-A-Zyme

(Sigma-Aldrich, St. Louis, MO, USA;), a concentrated anionic detergent with protease enzyme, was added to each well of the MEA plates and left overnight at room temperature. After 24 hrs, the plates were rinsed with distilled water three times and left to dry. Organic matter was removed by plasma cleaning (Femto low-pressure plasma system, Diener Electronic, Nagold, Germany) the plates for 3.5 min to improve the hydrophilicity of the surface. Before the experiment, the MEA wells were coated with 200 µL of 0.1 mg/mL Poly-D-lysine (PDL) (Sigma-Aldrich, St. Louis, MO, USA;) at 4 ^{o}C overnight, followed by 3 washes with distilled water and then ultraviolet light sterilization for 1 h. After sterilization, 35 µL of laminin (20 µg/mL; Sigma-Aldrich, St. Louis, MO, USA) was applied to each well, and incubated at 37 ^{o}C for 3 h before use. PDL and laminin coating were both used to enhance the adhesion of cells. PDL is a chemically synthesized extracellular matrix that promotes electrostatic interaction between the positively-charged culturing surface and the negatively-charged cell membrane. Laminin is an extracellular matrix, heterotrimeric protein, which forms a cross-like structure. This cross-like structure provides a long arm for the cell membranes to bind to. These two treatments are vital for the survival of the primary cortical neurons once they are seeded on the plates.

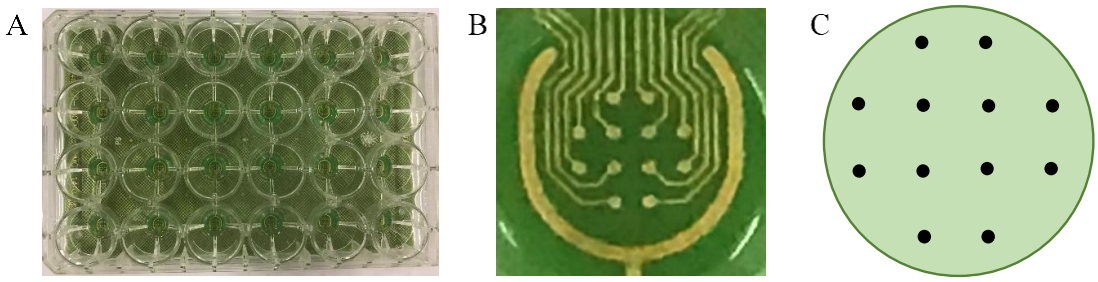

Figure 2.1 Layout of wells and electrodes.

A) Image of a 24-well MEA plate. B) Enlarged image of the base of a single well from panel A. C) Schematic of the layout of the 12 electrodes in one well. The electrodes are represented by black dots.

2.3 Culturing media preparation

Three different solutions were made for preparing and culturing primary cultures: a HBSS/HEPES solution, a MEM/FBS solution, and an NBA/B27 solution.

To make up the HBSS/HEPES solution, 10 mM HEPES (Sigma-Aldrich, St. Louis, MO, USA) was added to Hank's balanced salt solution (HBSS) (Sigma-Aldrich, St. Louis, MO, USA) and the pH was adjusted to 7.3 using sodium hydroxide.

For the MEM/FBS solution, 6 g/L D-(+)-Glucose (Sigma-Aldrich, St. Louis, MO, USA), 10 mM HEPES, 10% fetal bovine serum (FBS) (Sigma-Aldrich, St. Louis, MO, USA) and 1% of penicillin/streptomycin (Thermo Fisher Scientific, Inc., Waltham, MA, USA) were added to MEM (Sigma-Aldrich, St. Louis, MO, USA) solution and the pH was adjusted to 7.3 using sodium hydroxide.

The NBA/B27 solution was made by combining neurobasal-A medium (Thermo Fisher Scientific, Inc., Waltham, MA, USA) with 2% B-27 supplements (Thermo Fisher Scientific, Inc., Waltham, MA, USA), 1% GlutaMaX (Thermo Fisher Scientific, Inc., Waltham, MA, USA), 1% of penicillin/streptomycin and 10 mM HEPES.

2.4 Primary cortical neuron preparation and maintenance

P0-P1 pups were decapitated with sharp scissors. The brains were extracted using forceps and placed into a cold HBSS/HEPES solution. Cortices were dissected under a microscope (Olympus, SZX7) using forceps and blades, then transferred into 50 mL tubes filled with pre-warmed 0.25% Trypsin-EDTA (ethylenediaminetetraacetic acid, Thermo Fisher Scientific, Inc., Waltham, MA, USA; 1 mL per cortex), and placed in a water bath at 37^{o}C for 6 min. 500 µL/cortex of 0.032% deoxyribonuclease I (Sigma-Aldrich, St. Louis, MO, USA) was then added and the tissue was incubated in a water bath for a further 4 min. 10 mL/cortex of MEM/FBS media was used to wash the tissue. The supernatant was removed after 5 min centrifugation at 1500 rpm. Another 10 mL/cortex MEM/FBS was added, and the cell pellets were gently triturated using 1 mL tips and then passed through 42 µm cell-strainers (Thermo Fisher Scientific, Inc., Waltham, MA, USA) to dissociate the cells into a single cell preparation. A Countess automated cell counter (Thermo Fisher Scientific, Inc., Waltham, MA, USA; C10310) was used to calculate cell

numbers and after a further centrifugation step, for 5 min at 1500rpm, the pellets were resuspended in MEM/FBS to achieve a cell suspension of 2500 cells/μL. Laminin was removed from the plates and 120 μL/well (300000 cells/well) cell suspension was seeded into each well of the MEA plates. After 2-4 hours incubation at 37°C, the media was changed to NBA/B27 (500 μL/well) and the culture age noted as day(s) *in vitro* (DIV) 0. Cytosine arabinofuranoside (Ara-C) is anti-mitotic that inhibits the proliferation of glia cells. It is important to keep the number of glia cells at a level where they support the connection between the neurons, without allowing them to overgrow and disrupt neuronal proliferation. On the third day (DIV3), 5 μM Ara-C (Sigma-Aldrich, St. Louis, MO, USA) was added to the media, and remained present until DIV5. The NBA/B27 media was then changed every 2 days. The experiments were performed under class II biosafety cabinets to keep the cultures sterile.

2.5 MEA electrophysiology

2.5.1 Data acquisition

The 24-well MEA plates were taken from the incubator and placed in an enclosed recording chamber with 1 L/min CO_2 flow on a 37 °C Multiwell-MEA headstage (Multichannel Systems, Inc; Reutlingen, Germany). 10 min recordings were performed using Multiwell-Screen software (Multichannel Systems, Inc; Reutlingen, Germany). As shown in Figure 2.2, the sampling rate was 20 kHz and a high-pass 300 Hz was applied to filter the signal. Each electrode is considered as a recording channel.

2.5.2 Elements and parameters of MEA

Spikes, bursts, and network bursts (NB) are the three main elements of MEA (shown in Figure 2.3 together with two parameters).

2.5.2.1 Spikes

Upward and downward excursions beyond 6 times of standard deviation of noise were detected as spikes [199]. The essence of a spike is an action potential and it is recorded by the nearest electrode. The electrodes are able to detect spikes that initiate from one or

more neurons. The amplitude, frequency and synchronization are important features of spikes.

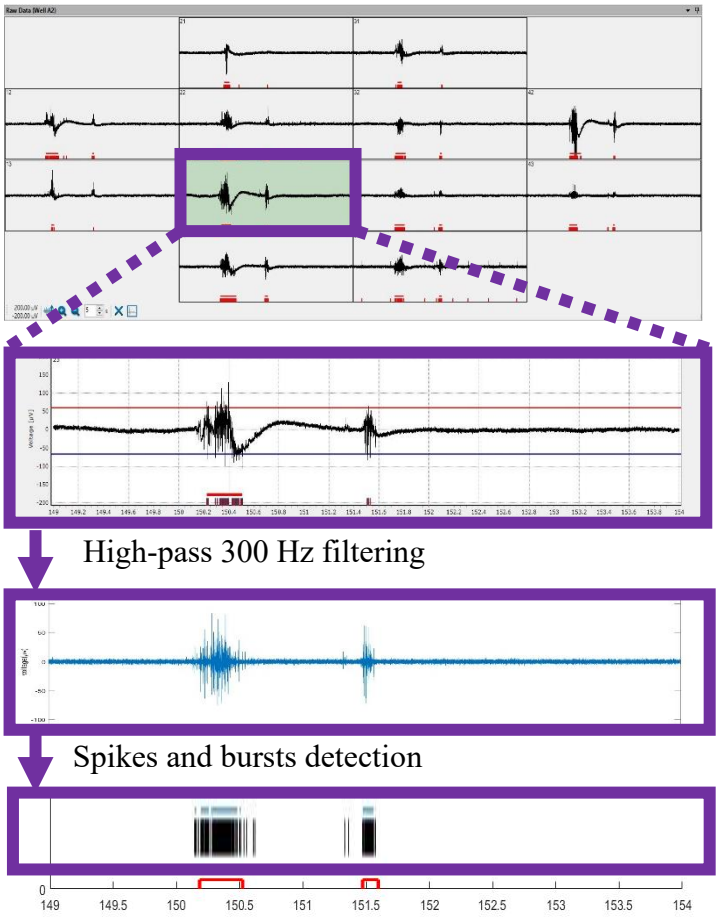

Figure 2.2 Generation of raster plot from raw data.

Raw data acquired from a single well showing the recording period 149 s to 154 s. Each well contains 12 electrodes. The signal from electrode No. 5 is enlarged below the raw data array. Then 300 Hz high pass filter is applied to the raw data to detect spikes (middle panel). Raster plot of electrode No. 5 below the filtered signal shows spikes and bursts happen in 5 seconds (bottom panel). Raster plot of the whole well is displayed below the single electrode raster plot showing the network formed in this well.

The peak of the action potential is the amplitude of the spike, and the time point of the peak is considered as the timestamp of the spike. The amplitudes reflect cell viability and distances to electrodes. The frequency of spikes is reflected by firing rate, which is the average number of spikes per second in one electrode. It shows the overall neuronal

activity level of the culture. Kappa is the measurement of temporal synchronization of spikes across all electrodes in one well. The time of each channel was divided into 10 ms bins. If one or more spikes occur in the bins, they were marked as 1. If no spikes occur, the bins were marked as 0. For all pairs of active electrodes, the agreement coefficient, Cohen's Kappa, was calculated. This measures the degree of coincidence of spikes on both electrodes exceeding the chance-expected coincidence assuming uncorrelated spikes. The range of Kappa is from -1 (completely unsynchronized) to +1 (perfectly synchronized).

2.5.2.2 Bursts

A fast progression of 3 or more spikes in a single electrode with short inter-spike intervals was defined as a burst, also known as a single channel burst[200]. The threshold of the inter-spike intervals was calculated based on the mean firing rate of this electrode. The time duration and the size of bursts are important features of bursts.

The time duration of a burst is from the timestamp of the first spike in the burst to the timestamp of the last spike in the burst. The size of a burst is the average number of spikes in single channel bursts over all bursting channels.

2.5.2.3 Network bursts

A network burst is a synchronized bursting activity happening across multiple channels. Such activity was detected when more than 15 % of the single channel bursts overlapped in time. The frequency, time duration, interval, participation proportion are important features of network bursts.

The number of network bursts per second is termed as network bursting rate, representing the frequency of network bursts. The time duration of a network burst is from the timestamp of the first spike of the network burst to the timestamp of the last spike in the network burst. The average of intervals between successive network burst starts is called meanNBSI. The average of intervals between the end of one network burst to the start of the next network burst is called meanInbis. The averaged intervals between the furthest starts of single channel bursts participating in a network burst is called meanJitter. The average number of channels that participate in network bursts is termed as avgChansInNB.

2.5.2 Elements and parameters of MEA

Spikes, bursts, and network bursts (NB) are the three main elements of MEA (shown in Figure 2.3 together with two parameters).

2.5.2.1 Spikes

Upward and downward excursions beyond 6 times of standard deviation of noise were detected as spikes[170]. The essence of a spike is an action potential and it is recorded by the nearest electrode. The electrodes are able to detect spikes that initiate from one or more neurons. The amplitude, frequency and synchronization are important features of spikes.

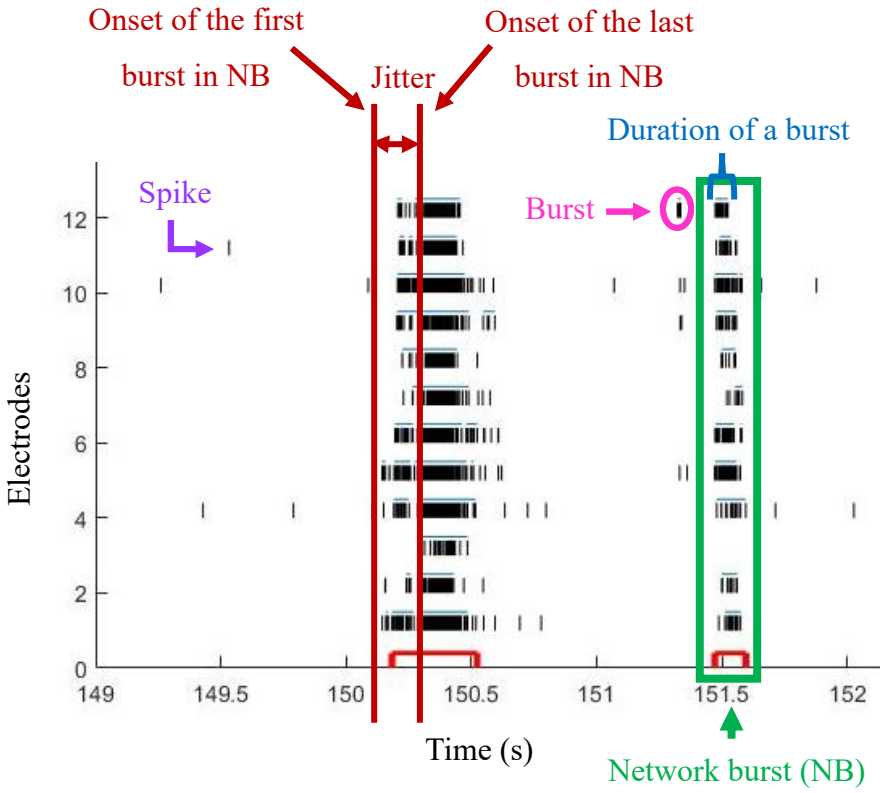

Figure 2.3 Raster plots illustrate the dynamics of a neuronal network.

Each row represents one electrode (1 to 12). Each vertical tick represents an action potential/spike (purple arrow). A burst (pink arrow), constitutes a succession of spikes in close temporal proximity. The time duration of a burst (blue). Bursts occurring across different electrodes is termed as a network burst (green arrow). Jitter is the time interval between the onset of the first and last bursts in a network burst (dark red arrows).

40 network characteristics in terms of spiking (SPK), single channel bursting (SCB) and network bursting (NB) parameters were extracted using custom MATLAB script [200] (Table 2.1).

Table 2-1Orders and descriptions of extracted parameters shown in iris plots

No.	Classification	Abbreviation of parameters	Description
1	Spiking features (SPK)	mfrAll	Mean firing rate (number of spikes per second in a channel)
2		mfrIn	Mean firing rate inside bursts.
3		mfrOut	Mean firing rate outside bursts
4		mfrRatio	Ratio between mfrIn to mfrOut (mfrIn/mfrOut)
5		avgAmp	Mean amplitude of all spikes
6		noOfSpikingChans	Number of channels that shows spiking
7		Kappa	A measurement of synchronization between spikes (1 means a complete synchronization)
8	Bursting features (SCB)	meanSCBDuration	Mean duration of all single channel bursts in all bursting channels
9		stdSCBDuration	Standard deviation of meanSCBDuration
10		cvSCBDuration	Coefficient of variation of meanSCBDuration
11		rangeSCBDuration	Range of meanSCBDuration
12		meanSCBSize	Mean number of spikes in single channel bursts in all bursting channels
13		stdSCBSize	Standard deviation of meanSCBSize
14		cvSCBSize	Coefficient of variation of meanSCBSize
15		rangeSCBSize	Range of meanSCBSize
16	Network bursting features (NB)	NBRate	Number of network bursts per second
17		meanDuration	Mean duration of network bursts
18		stdDuration	Standard deviation of meanDuration
19		cvDuration	Coefficient of variation of meanDuration
20		rangeDuration	Range of meanDuration
21		meanNBSI	Mean interval between successive network burst starts
22		stdNBSI	Standard deviation of meanNBSI
23		cvNBSI	Coefficient of variation of meanNBSI
24		rangeNBSI	Range of meanNBSI
25		meanInbis	Mean inter network burst interval
26		stdInbis	Standard deviation of meanInbis
27		cvInbis	Coefficient of variation of meanInbis
28		rangeInbis	Range of meanInbis
29		meanJitter	Mean interval between the furthest starts of single channel bursts participating in a network burst

30	Network bursting features (NB)	stdJitter	Standard deviation of meanJitter
31		cvJitter	Coefficient of variation of meanJitter
32		rangeJitter	Range of meanJitter
33		totNBAmp	Sum of amplitudes of all spikes included inside a network burst averaged across all network bursts
34		avgNBPeakAmp	Mean amplitude of spikes included in a network burst
35		avgNBTimeAmp	Time-wise mean of the amplitudes of spikes included in a network burst (totNBAmp/NB Duration)
36		totNoOfSpikes	Number of spikes included inside a network burst averaged across all network bursts
37		avgSpikesInNB	Mean number of spikes included in a network burst
38		%spikesInNBs	The percentage of detected bursts that are located inside a network burst
39		avgChansInNB	Average number of channels that participate in network bursts
40		%chansInNBs	noOfChansInNB/noOfSpikingChansX100

2.6 Statistical analysis

Mann-Whitney test, Friedman test and Kruskal-Wallis test in GraphPad Prism 8 were applied to line or bar graphs. Wilcoxon rank sum test (equivalent to Mann-Whitney test) in Matlab was applied to iris plots. Analysis has been performed on raw data between heterozygous and wild types, whereas drug effect was analysed between normalized changes after the application of drugs and vehicle control. Detailed descriptions can be found in figure legends and n represents culture wells. Results were presented as mean ± SEM. $*p < 0.05$, $**p < 0.01$, $***p < 0.001$, $****p < 0.0001$.

Chapter 3 Development of MEA assay for *in vitro* neuronal network analysis

3.1 Introduction

In brief, brain function can be studied on different levels, including single cell level, neuronal network level, and the whole brain level (*in vivo* studies). In epilepsy, seizures are believed to occur when regular electrical impulse patterns in neuronal networks are disturbed by abnormal, excessive or hypersynchronized activity [194]. Therefore, to understand the underlying pathomechanism of epilepsy it is important to study this disease at the neuronal network level. Another purpose of our study is to find potential treatments for DEE. The ability to screen compounds on a large scale is required for drug discovery. Hence, *in vitro* neuronal network systems are preferred over *in vivo* models because they are highly accessible to electrical stimulation, pharmacological manipulation and observation. However, robust high throughput neuronal network functional analyses have not yet been established for epilepsy.

The currently available technologies to study *in vitro* neuronal networks include MEA recording and calcium imaging [198]. MEA are arrays of micro electrodes through which extracellular voltage changes of single neurons or small clusters of neurons can be detected and recorded in parallel [201]. Calcium imaging measures calcium changes using fluorescent indicators, to reflect neural activity [202]. MEA have high temporal resolution to detect action potentials and relatively low spatial resolution to detect signals occurring only in the proximity of electrodes. Compared to MEA, calcium imaging has a lower temporal resolution that cannot detect action potentials and a lower signal-to-noise ratio, although its spatial resolution is higher [203-205].

Primary neuronal cultures develop complex spontaneous network activity that can be highly sensitive to their chemical environment and this can be recorded on MEA [206]. So far, dissociated neurons grown on MEA have been shown to be a successful method to perform toxicological profiling and functional pharmacological screening [194-197].

Moreover, because networks on MEA can survive for a long period of time and be recorded from non-invasively, they are also used to study synaptic plasticity [207, 208], neuronal assemblies [209] and *in vitro* learning [210, 211]. These have made MEA a potential platform for understanding the developmental deficit aspects of DEE and for searching for novel treatments.

However, despite the benefits of extracellular MEA recordings in primary dissociated neuronal cultures, high biological and technical variabilities were observed and became obstacles for high throughput MEA studies. For example, recent publications have pointed out that culture media changing schedule and techniques, as well as the stabilization time before recording on the MEA headstage, can affect the output of MEA recordings [201, 212-214]. Although this is less a problem for 'before and after' pharmacological studies it poses a particular issue for the comparison of disease phenotypes between different cultures. Moreover, there's no parameter based golden standard of what's a good culture or what are the conditions required to obtain a good culture. Therefore, in this chapter, I investigated these variabilities and identified conditions necessary for the establishment of a reproducible and robust *in vitro* neuronal network model in our lab.

3.2 Methods

The methods used in this chapter have been described in Chapter 2, apart from those presented in "3.3.1 Culture handling" while testing the impact of different conditions. In 3.3.1.1, the cells were obtained from hippocampus or cortex. In 3.3.1.2, the neurons were obtained from P0/P1 or P2 mouse pups. In 3.3.1.3, the cell seeding densities were 200000 cells/well, 300000 cells/well and 375000 cells/well. In 3.3.1.4, the culture media were changed 0 hour, 12 hours, 24 hours, 36 hours and 48 hours before MEA recordings. For the rest of the chapter, all cultures were obtained from P0/1 mouse cortices, seeded at 300000 cells/well, and media was changed 2 days before recordings. Moreover, all the animals were wild type C57/BL6 mice.

3.3 Results

3.3.1 Culture handling

To minimize the impact of different culture handling conditions I firstly examined the variability caused by; the region that brain region cells are extracted from, the age of the animals, the cell seeding density and the time of media change before the recordings.

Six main parameters reflecting the spike activity (firing rate and firing rate inside of bursts), network activity (network bursting rate and duration of bursts) and the synchronization of cultures (Jitter and kappa) are showed.

3.3.1.1 Brain region

SCN2A is highly expressed in hippocampus and throughout the cerebral cortex [215-217]. Both of these regions are also closely related to epilepsies. The involvement of cortex is known from EEG recordings in patients and studies in rodent models. Generalized seizures simultaneously involve the entire cortex. Also, the cortex is the only brain region where epileptiform activity arises with any frequency [218]. Confirming the role of the hippocampus in epilepsy, it is known that over 50% of epileptic patients have a damaged hippocampus, although it is not certain whether that is a cause or a result of seizures. However, surgical removal of the hippocampus has been found to reduce seizures [219].

Here primary cultures obtained from either cortical or hippocampal tissue were tested. As shown in Figure 3.1, the activity of hippocampal neurons was stronger and more synchronized. Hippocampal cultures had an increase in overall firing rate of 5 ± 1 Hz, compared to the 2.8 ± 0.5 Hz of cortical cultures (Figure 3.1 C, $p > 0.05$). And the firing rate inside bursts of hippocampal neurons was 41 ± 4 Hz, significantly higher (Figure 3.1 D, $p < 0.05$) than the 15 ± 1 Hz of cortical neurons. No significant differences were observed in network bursting features including network bursting rate and the duration of bursts. As for synchronization, the Jitter (time interval between the start of the first and last bursts in a network burst) of cortical cultures was 1.4 fold larger (91 ± 5 ms versus 67 ± 13 ms) than the hippocampal cultures (Figure 3.1 G, $p < 0.05$), and the Kappa (the measurement of temporal synchronization of spikes across all electrodes in one well) value of hippocampal cultures increased 2.0 fold (0.12 ± 0.02 versus 0.059 ± 0.009) compared to the cortical cultures (Figure 3.1 H, $p < 0.05$).

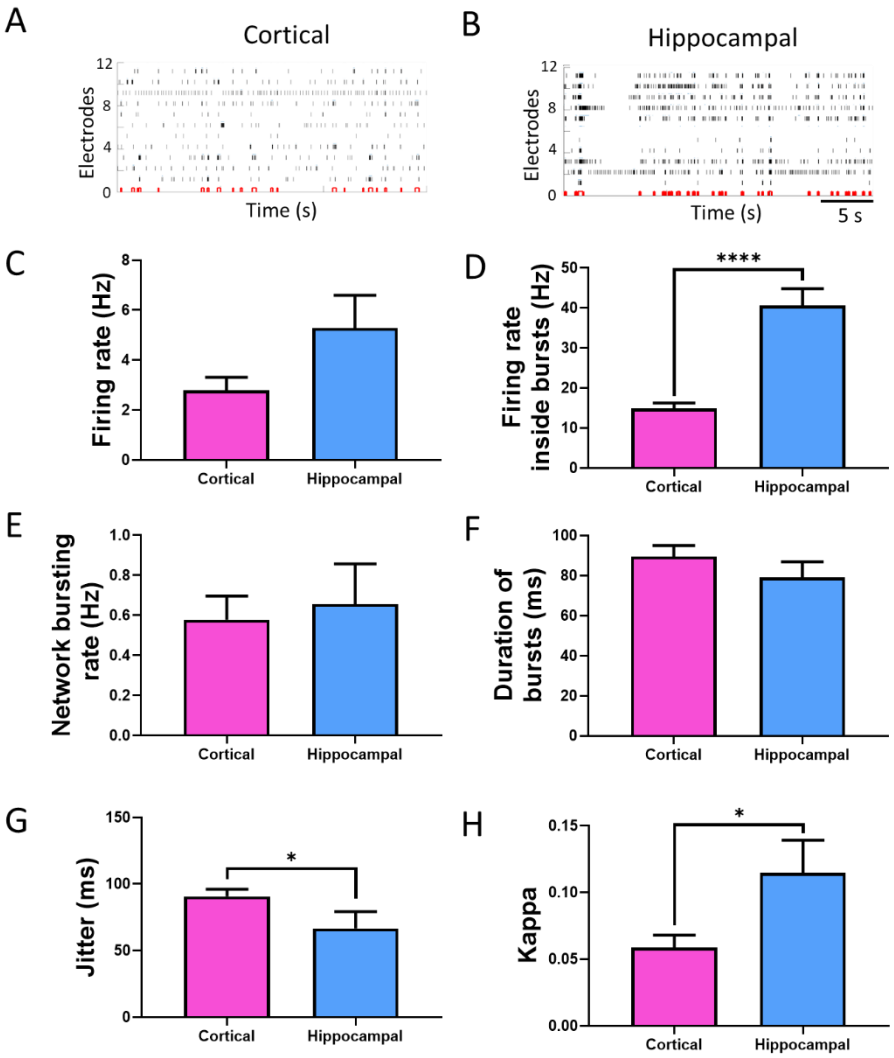

Figure 3.1 *In vitro* network activity of mice cortical and hippocampal neurons.

*Representative raster plots of A) cortical, B) hippocampal cultures are shown. Comparisons of the average of C) firing rate, D) firing rate inside of bursts, E) network bursting rate, F) duration of bursts, G) Jitter, and H) Kappa between cortical (n = 19) and hippocampal (n = 9) cultures. A Mann-Whitney test was applied to test the significant differences. Results are presented as mean ± SEM. *p < 0.05, ****p < 0.0001.*

While these data were an interesting comparison for the purposes of establishing a high throughput method, the cortex is the more suitable brain region to study *SCN2A* DEE as the yield of cells is much higher (the hippocampus has only about 1% of the volume of the cortex [220] and the yield of hippocampal cells account for approximately 10% of cortical cells per animal [221].

3.3.1.2 Animal age

The age of animals at the time of brain tissue harvesting is a factor that profoundly influenced the *in vitro* cell viability. The older the animal, the more developed the neurons are, and thus are less robust following extraction [222]. Compared to the commonly used embryonic neuronal cultures [223], culturing postnatal neurons is more complex. However, there are distinct benefits to using postnatal neurons, as time pairing of the breeders required for embryonic cultures can be challenging if the animals are hard to breed, it can also be very time consuming and more costly. In addition, to extract the embryos the breeder is usually sacrificed, increasing the number of requested animals. In postnatal culturing, the breeder and part of the litter can be saved for further breeding or other purposes. Finally, postnatal mouse provides more cells than the embryos.

Comparing the cultures obtained at different postnatal days, it has been found that the long-term cellular viabilities were altered between cultures obtained from P0/1 and P2 pups. As shown in Figure 3.2, although the cultures were similar at DIV14, the P2 cultures were significantly less active and less synchronized at DIV21/22 and DIV28 compared to P0/1cultures.

The overall firing rate of P0/1 group increased up to 17.3 ± 0.9 Hz during development, while the P2 group declined to 4.8 ± 0.3 Hz (Figure 3.2 C, $p < 0.0001$). Like firing rate, the network bursting rate of P2 cultures was also lower than in the P0/1 cultures. At DIV28, the network bursting rate was 0.63 ± 0.04 Hz in P0/1 group, and 0.21 ± 0.02 Hz in P2 group (Figure 3.2 E, $p < 0.0001$). For the Jitter that shows the synchronization of network bursts, the biggest difference was observed at DIV28: the average Jitter of P0/1 was 81 ± 3 ms versus 119 ± 5 ms seen in P2 cultures (Figure 3.2 G, $p < 0.0001$). The largest difference for Kappa (which represents the synchronization of the spikes) was found at DIV28. The average Kappa of P0/1 was 0.33 ± 0.01 versus 0.20 ± 0.02 of P2 cultures (Figure 3.2 H, $p < 0.0001$). Therefore, P0/1 mouse pups were selected.

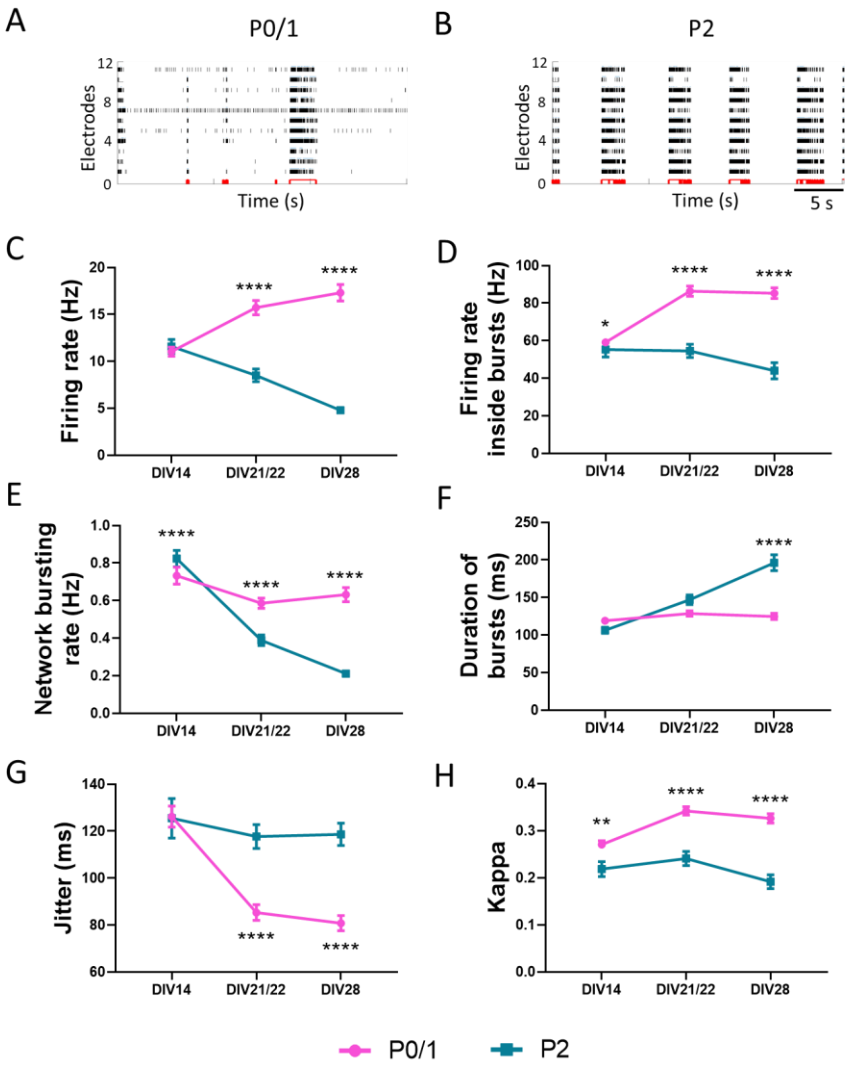

Figure 3.2 MEA properties of cortical neurons obtained from P0/1 and P2 mice pups between DIV14 to 28.

*Representative raster plots of A) P0/1, B) P2 obtained cultures at DIV21/22 are shown. Comparisons of the average of C) firing rate, D) firing rate inside of bursts, E) network bursting rate, F) duration of bursts, G) Jitter, and H) Kappa between cortical cultures obtained from mice pups at P0/1 (n = 241) and P2 (n = 131), from DIV14 to 28. Experiments are performed sequentially on the same cells. A Mann-Whitney test was applied to test the significant differences. Results are presented as mean ± SEM. *p < 0.05, **p < 0.01, ****p < 0.0001.*

3.3.1.3 Cell seeding density

The next observation was that the density of plated cells has a massive effect on the results of MEA analysis. Compared to cultures with lower numbers of plated cells, denser cultures present more spikes and faster maturation. Also, sufficient cell density is required to exhibit globally synchronized bursts, and the pattern of bursts varies dramatically based on the cell density [212].

To find the suitable seeding density for a *SCN2A* DEE *in vitro* MEA model, based on the literature and previous data obtained in our lab, three seeding densities were tested: 200000 cells/well, 300000 cells/well and 375000 cells/well. As shown in Figure 3.3, 200000 cells/well caused significant differences in firing rate (Figure 3.3 D, $p < 0.0001$), firing rate inside of bursts (Figure 3.3 E, $p < 0.0001$), duration of bursts (Figure 3.3 G, $p < 0.0001$), Jitter (Figure 3.3 H, $p < 0.0001$) and Kappa (Figure 3.3 I, $p < 0.01$) compared to the density of 300000 cells/well. Whereas 300000 cells/well showed increased firing rate inside of bursts (Figure 3.3 E, $p < 0.0001$) and time duration of bursts (Figure 3.3 G, $p < 0.0001$) compared to the 375000 cells/well group, though the network bursting rate of 300000 cells/well cultures was lower than that of 375000 cells/well cultures (Figure 3.3 F, $p < 0.0001$). As for synchronization, the Jitter of 300000 cells/well cultures was significantly bigger than that of 375000 cells/well cultures (Figure 3.3 H, $p < 0.01$). However no significant difference was detected in Kappa between the seeding density of 300000 cells/well and 375000 cells/well (Figure 3.3 E, $p < 0.001$). Overall, these results suggested similar activity levels and maturity of 300000 and 375000 cells/well groups. I therefore selected 300000 cells/well as the seeding density for mouse cortical neurons.

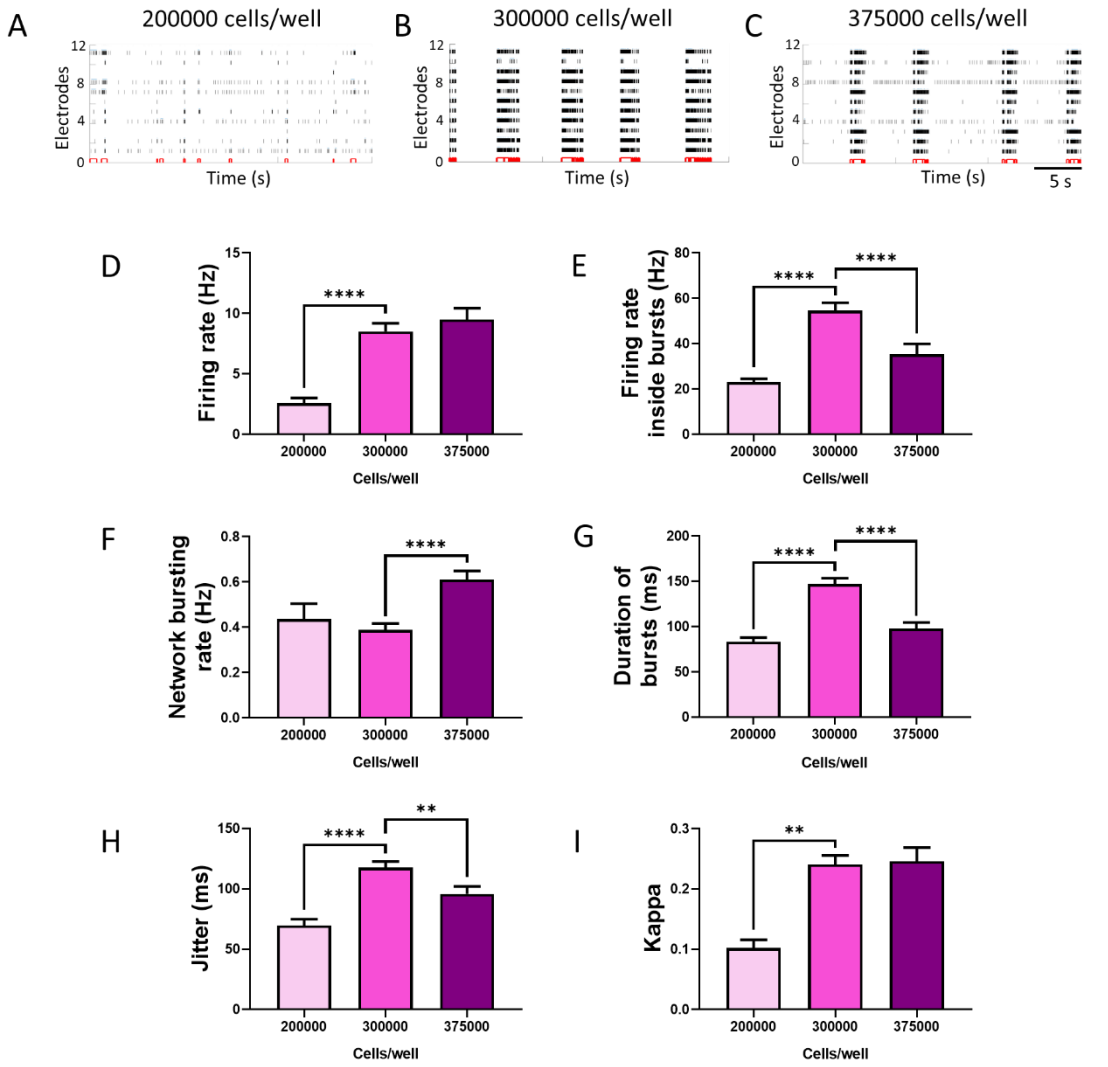

Figure 3.3 MEA properties of cortical neurons in different seeding densities.

*Representative raster plots of A) 200000 cells/well, B) 300000 cells/well and C) 375000 cells/well seeding densities are shown. Comparison of the average of D) firing rate, E) firing rate inside of bursts, F) network bursting rate, G) duration of bursts, H) Jitter, and I) Kappa among different cell seeding densities, 200000 cells/well (n = 19), 300000 cells/well (n = 131) and 375000 cells/well (n = 44). A Mann-Whitney test was applied to test the significant differences. Results are presented as mean ± SEM. **p < 0.01, ****p < 0.0001.*

3.3.1.4 Media change time

A media change can disturb the electrophysiological performance of primary cultures [224, 225].To test the changes in neuronal network activity caused by media change, MEA recordings were performed in 31 wells before media change, and 0 hour (immediately), 12 hours, 24 hours, 36 hours and 48 hours after media change. As a result of the media change, the activity of cultures escalated while the synchronization was perturbed. As shown in Figure 3.4, the firing rate (Figure 3.4 G) increased about 50% immediately after the media change, while the network bursting rate was elevated by over 150% 12 hours after (Figure 3.4 I). The level of activity recovered 24 hours after the media change, however dramatic declines of firing rate inside of bursts (Figure 3.4 H) and synchronization (Figure 3.4 L) were observed immediately after the media change and took longer time to stabilize.

Based on these results, for the purpose of minimizing the impact of media change and obtaining stable readouts from the primary neuronal cultures using MEA, I decided to always change the media 48 hours before the data acquisition and perform recordings every two days to track the development of the cultures.

To summarise, the optimal activity for our assay was obtained from cortical neurons isolated from P0/P1 mice and plated at the seeding density of 300000 cells/well, with the media change carried out 2 days before MEA recordings.

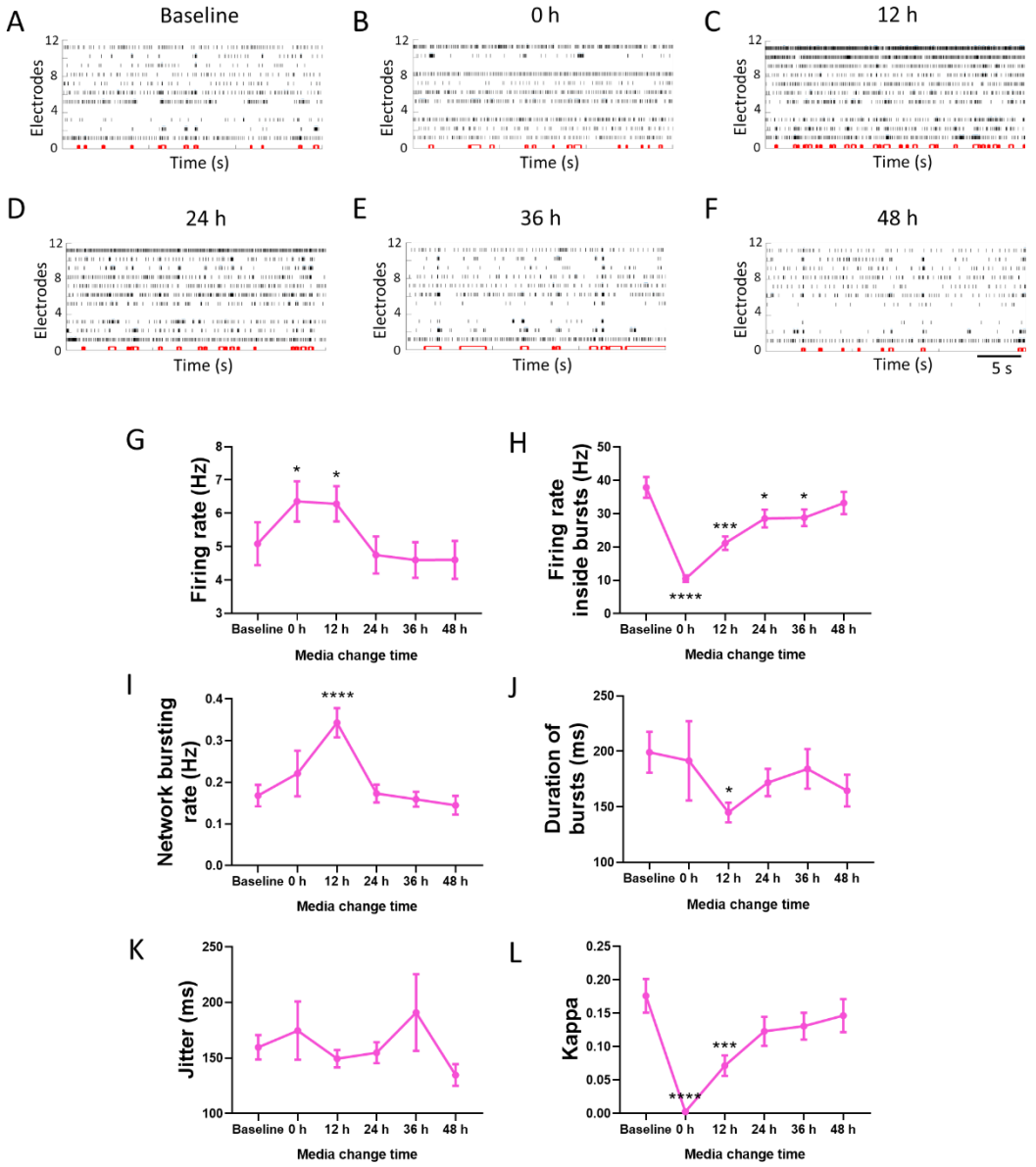

Figure 3.4 Changes in neuronal network activity caused by media change.

*A baseline was measured right before the media change. Representative raster plots of A) baseline, B) 0 h, C) 12 h, D) 24 h, E) 36 h and F) 48 h after media change are shown. G) firing rate, H) firing rate inside of bursts, I) network bursting rate, J) duration of bursts, K) Jitter, and L) Kappa. (n = 31) are shown. Experiments are performed sequentially on the same cells. A Mann-Whitney test was applied to test the significant differences compared to baseline. Results are presented as mean ± SEM. **p < 0.01, ****p < 0.0001.*

3.3.2 Characterization of wild type cortical cultures WT developmental features

Under these conditions, the development of wild type cultures between DIV14 to 28 was investigated as the base of our research.

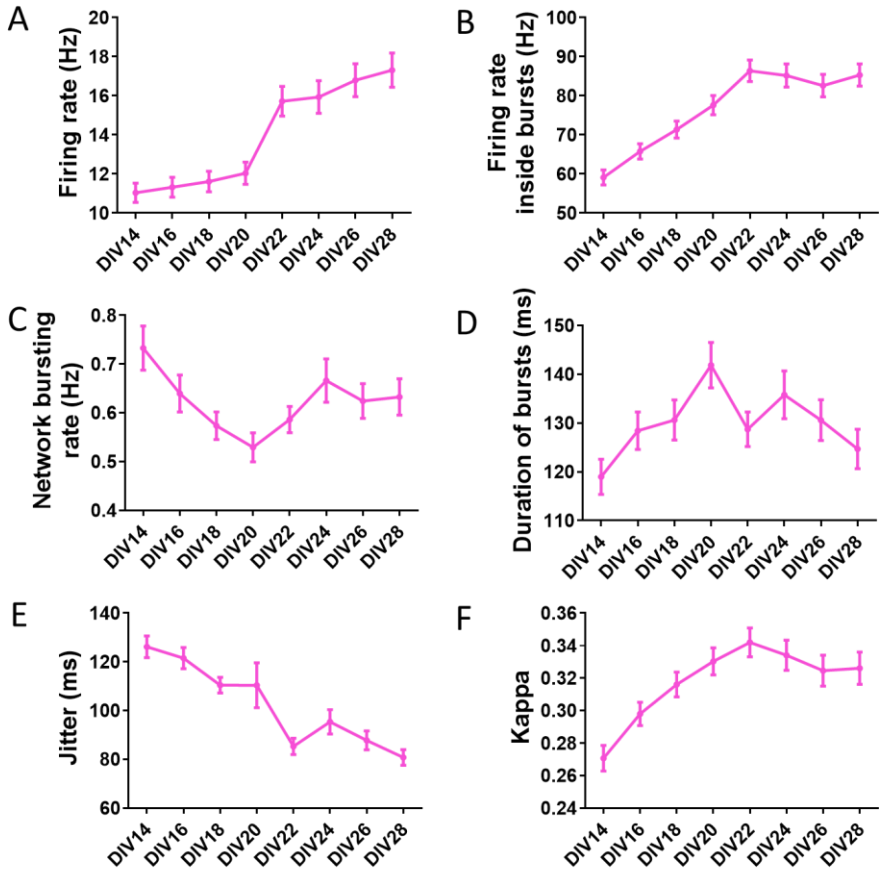

Figure 3.5 The developmental features of WT cortical neurons from DIV14 to 28.

The average of A) firing rate, B) firing rate inside of bursts, C) network bursting rate, D) duration of bursts, E) Jitter and F) Kappa at DIV14, 16, 18, 20, 22, 24, 26 and 28. The primary cortical cultures were obtained from wild type C57/BL6 mice pups at P0/1 (n = 241). Experiments are performed sequentially on the same cells. Results are presented as mean ± SEM.

3.3.3 Variability of MEA recordings

MEA cultures have been shown to have considerable variability including well-to-well, plate-to-plate, animal-to-animal and litter-to-litter [212, 213, 226]. In this part of the thesis, these differences were investigated using firing rate.

3.3.3.1 Well-to-well variability

Cultures were obtained from the same animal and seeded onto six different MEA wells on the same plate. Each well is represented by a different colour. The firing rates of eight recording points from DIV14 to 28 are shown in Figure 3.6. Overall, 10 out of 13 analysed conditions showed significant differences using a Friedman test. 6 representative figures are shown in Figure 3.6. Figure 3.6 A and B illustrate the non-significant variation. Figure 3.6 C ($p < 0.05$), D ($p < 0.01$), E ($p < 0.001$) and F ($p < 0.0001$) illustrate the significant differences seen between different wells. To eliminate the well-to-well variability, it became obvious that the number of wells used per condition needed to be increased.

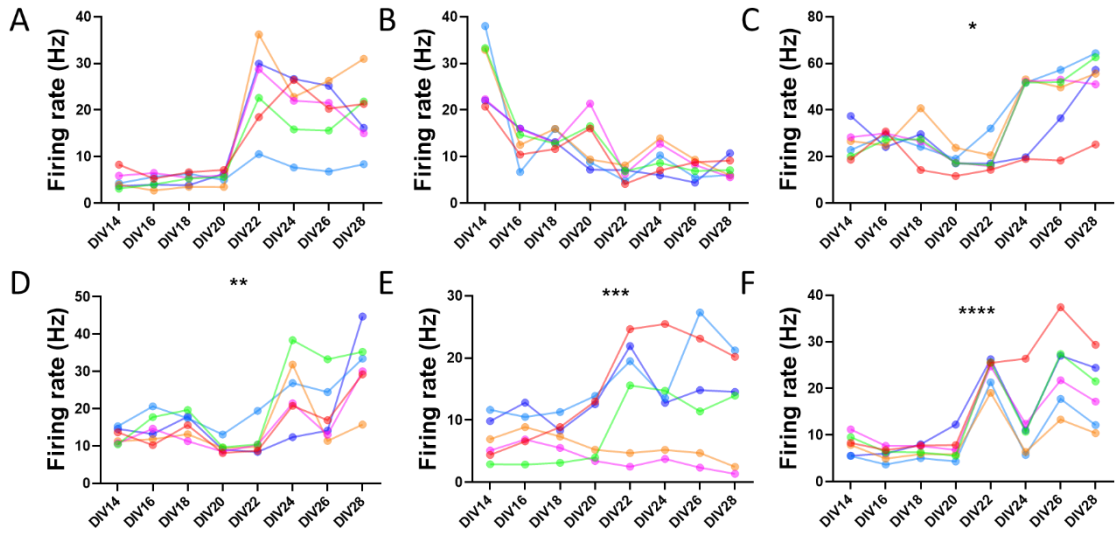

Figure 3.6 Well-to-well variability shown by firing rates.

*The firing rates recorded in individual wells from the same plate, when the primary cortical cultures were obtained from the same wild type animal. Experiments are performed sequentially on the same cells. A Friedman test was applied to test the significant differences. *$p < 0.05$, **$p < 0.01$, ***$p < 0.001$, ****$p < 0.0001$.*

3.3.3.2 Plate-to-plate and animal-to-animal variability

After the well-to-well variability of MEA recordings, the plate-to-plate and animal-to-animal changes were investigated (Figure 3.7). Data obtained from 12 wild type animals at DIV22 were analysed. The primary cortical neurons obtained from each animal were seeded on two plates at six wells per plate. The firing rates are shown in Figure 3.7. Each animal is marked in a unique colour. A Mann-Whitney test was applied to test the differences between the plates for each animal. No significant differences were observed, indicating limited variance among MEA plates. Among the cultures obtained from different animals, the Kruskal-Wallis test revealed significant differences ($p < 0.0001$).

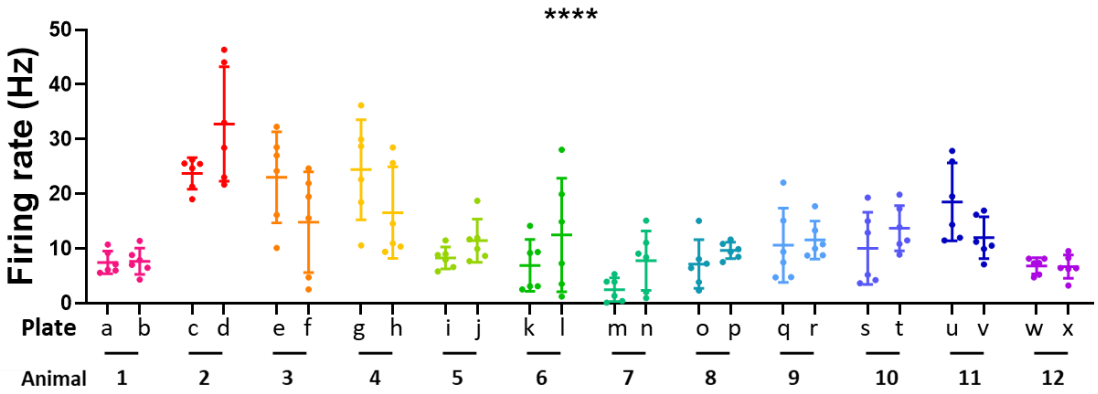

Figure 3.7 Plate-to-plate, and animal-to-animal variability shown by firing rates.

*The firing rates of 12 different wild type animals are shown in different colours. Cells were seeded on two different plates for each animal, and the firing rate of individual well is shown as a dot. A Student's t-test was applied to test plate-to-plate differences. A Mann-Whitney test was applied to test plate-to-plate differences in each animal. A Kruskal-Wallis test was applied to test animal-to-animal differences. Results are presented as mean ± SEM. ****$p < 0.0001$.*

3.3.3.3 Litter-to litter-variability

During the experiments, differences in MEA features were also found to exist among different litters. As shown in Figure 3.8, the mean firing rates of three different litters from DIV14 to 28 showed significant differences ($p < 0.05$). These differences were not only caused by the variability among individual animals, but probably also by the age of the litter and other factors that I could not control during the preparation of the primary

neurons. Although the harvest time of the brains from mice pups was set at P0 to P1, differences still exist within this time frame. This increased the difficulty of identifying phenotypic differences between different genotypes on MEA because the observed variability can mask the phenotypic differences. To address this concern, it is necessary to always use controls from the same litter. Therefore, for the phenotype studies, the mutants were normalized to their wild type littermates recorded within the same experiment.

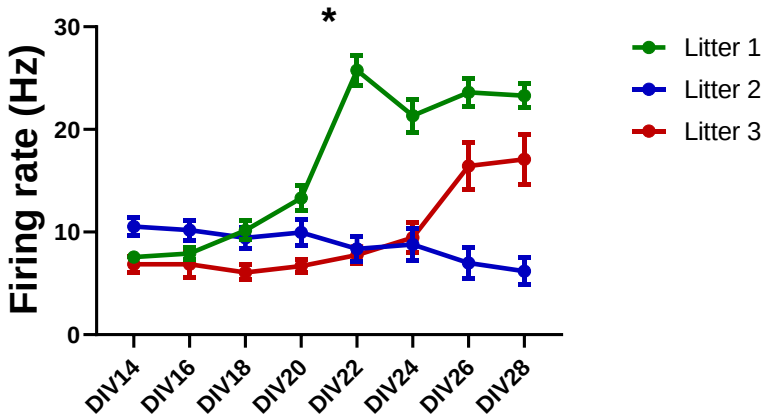

Figure 3.8 Litter-to-litter variability shown by variability of firing rates.

*The average firing rates of the wild type cultures from three different litters recorded between DIV14 and 28 are shown in different colours. Experiments are performed sequentially on the same cells. A Friedman test was applied to test the significant differences. Results are presented as mean ± SEM. *p < 0.05.*

3.3.4 Power analysis

After the experimental conditions were settled, wild type primary cultures at DIV22 were examined. The mean values and standard deviations of 40 parameters were calculated (n=241), revealing the variability of the parameters. Therefore, we were curious to know the sample size needed to pick up a 30% reduction between two equally sized groups to be significant ($p < 0.05$, power 0.8). The calculated sample sizes needed per group for each parameter are listed in Table 3-1, using an unpaired Student's *t*-test on GPower 3.1.

Table 3-1 Power analysis results.

No.	Abbreviation of parameters	Sample size	No.	Abbreviation of parameters	Sample size
1	mfrAll	99	21	meanNBSI	88
2	mfrIn	44	22	stdNBSI	60
3	mfrOut	163	23	cvNBSI	30
4	mfrRatio	344	24	rangeNBSI	70
5	avgAmp	7	25	meanInbis	107
6	noOfSpikingChans	4	26	stdInbis	61
7	Kappa	30	27	cvInbis	41
8	meanSCBDuration	34	28	rangeInbis	75
9	stdSCBDuration	44	29	meanJitter	66
10	cvSCBDuration	15	30	stdJitter	82
11	rangeSCBDuration	43	31	cvJitter	25
12	meanSCBSize	25	32	rangeJitter	71
13	stdSCBSize	34	33	totNBAmp	187
14	cvSCBSize	13	34	avgNBPeakAmp	8
15	rangeSCBSize	43	35	avgNBTimeAmp	63
16	NBRate	92	36	totNoOfSpikes	123
17	meanDuration	56	37	avgSpikesInNB	116
18	stdDuration	44	38	%spikesInNBs	6
19	cvDuration	20	39	avgChansInNB	20
20	rangeDuration	45	40	%chansInNBs	3

An unpaired Student's t-test was used to assess significance between two equal sample size groups. The significance criterions were p <0.05 and the power was 0.8, with the magnitudes of the effects of 30% reductions. The sample sizes showed were sample sizes per group.

MfrAll (mean firing rate) and NBRate (network bursting rate) are two of the most important parameters to describe MEA cultures. As shown in the table, the sample size required for mean firing rate was 99 and the sample size required for mean network bursting rate was 92. These sample sizes are big but larger changes are also normally seen in these parameters. Conversely, the sample size needed for %chansInNBs (percentage of channels participating in network bursts) was only 3 and the sample size needed for noOfSpikingChans (number of channels that spikes) was 4. However, global spontaneous network activity is normally developed in primary cortical cultures at DIV22. The

percentage of channels participating in network bursts was often close to 100% and the number of channels that spikes is often close to 12 (all the electrodes). If 30% reduction occurred to these two parameters, a more dramatic reduction would probably be seen for the mean firing rate and network bursting rate. Hence, with the increase of magnitudes of the effects, the sample size required for mean firing rate and network bursting rate would drop. The largest sample sized needed appeared in mfrRatio. This parameter is a ratio between mfrIn (mean firing rate inside of bursts) and mfrOut (mean firing rate outside of bursts). The ratio of spikes participating in bursts or not is an important feature used to describe MEA cultures. However, the variability of this parameter was found to be very high and it was difficult to obtain a stable mfrRatio. Therefore, in most cases mfrIn and mfrOut were looked into separately instead of investigating mfrRatio.

3.4 Discussion and conclusion

To study DEE and bridge the gap between single cell and whole brain analysis, a functional neuronal network research model was optimized based on the use of MEA technology. In this chapter, the sources of variability affecting the MEA analysis of neuronal networks were investigated and they are discussed below. Different conditions were tested and the ones that seemed optimal for our experimental questions were selected. However, the optimization wasn't done in a series that I only performed the next optimization after the first one is settled.

The differences in preparation and handling of cultures has been recognised as a source of variability [201, 212-214]. Primary cultures obtained from different brain regions have been found to display different activity patterns on MEA [212], which is why harvesting cells from the same brain region can reduce the inter-culture variability. It was shown that the cultures originating from different regions sometimes respond differently to compounds due to their higher affinity to the cellular components which were enriched or reduced in a given region of the nervous system [227, 228]. Spinal cord culture was commonly used in early MEA pharmacological studies because of the smaller variability in terms of network dynamics [201]. However, cortical culture has been found to be more sensitive, adaptive and complex, which can enable the establishment of an advanced drug screening system [212, 229]. Network dynamics of cortical cultures and hippocampal

cultures were tested because they are both closely related to epilepsy. The decision to use cortices over hippocampi was based on the fact that they provided larger number of cells that can be used for high throughput analysis. However, in the tested conditions hippocampal cultures were more active and synchronized and would be a useful system, especially for the analysis of genotype-phenotype correlations. It will be interesting to perform our experiments using hippocampus cultures in future study.

The age of the tissue used to generate primary cultures has a profound impact on MEA features. Neurons in younger animals are less developed and therefore more robust during the handling of *in vitro* culture preparations [222]. Therefore, embryonic neurons are more commonly used [223]. However, it was decided to establish the model based on postnatal neurons to gain more cells while sacrificing fewer mice. Previous studies used primary cultures obtained from P0-P2 [200]. However, large differences were observed between P0/P1 and P2 cultures. Cultures from younger mice showed higher activity at both single channel level and global network level during *in vitro* development, as well as more synchronization, suggesting this was a better model for MEA analysis. Also, because the development of cultures obtained from different postnatal time have shown large variation, normalization of the parameters obtained in MEA recordings from mutants to those from wild types is important [230].

The plating density of cortical cultures has been found to affect maturation of *in vitro* cultures because of the faster axonal outgrowth in dense cultures compared to sparse ones [212, 229]. The denser the cultures were, the more spikes detected, and the quicker they were to exhibit bursting behaviours [212]. Also, sufficient cell density was required to form globally synchronized bursts [212]. In this study, three different seeding densities were tested and this confirmed that the denser cultures had more spikes and more channels participating in network bursts. Denser cultures were found to be more synchronized. However, the network bursting rate of cultures was not necessarily linear with the seeding density. The cultures of higher density can have less frequent but longer network bursts. This confirmed a former study showing that the pattern of bursts varies dramatically based on the cell density [212]. Taking the activity and efficiency into consideration, 300000 cells/well were chosen for our experiments.

The impact of media change on recorded MEA activity has been reported in the literature for wash-in drug applications [231, 232], but its importance in phenotype studies has not been well addressed. This study focused on the transient effects of media change. As with pharmacological studies, investigating changes normalized to the baseline of the same culture is more powerful, although we cannot exclude the impact of the development of the culture during the experiment. Therefore, the spontaneous activity of the same cultures was compared before and after media changes. It was found that freshly changed media stimulated the cultures to fire more but become less synchronized. After 48 hours after a media change, the cultures were mostly stabilized and back to synchronization. Another study performed by Wagenaar et al. compared the spontaneous activity of different cultures derived from the same tissue at different time points after the media change. This approach eliminated the impact of the *in vitro* development but introduced the variability of plating. They have found that the variability from long-term media changes (up to 7 days) was not significantly larger than the variability from different plating, but media change 12 hours before recordings was needed to prevent the transient effects [212]. Taken these results into consideration, having a standardized 48 hours media changing schedule before recordings can reduce variability when multiple recordings are performed during long-term studies, enabling more reproducible MEA recordings and a comparison of results across different experiments.

Studies from different groups have found that the fundamental resource of the variability of *in vitro* network on MEA is the variable nature of cortical neurons, especially when obtaining them from different animals [232-234]. According to Wagenaar et al., variability in cortical cultures existed among recordings of the same culture on consecutive days [212]. Our study also confirmed the MEA well-to-well variability during the development over two weeks. Moreover, MEA studies on brain slices have found that slices from the same animal displayed higher similarity compared to tissues originating from different animals [231]. It has also been found that the variability inherited from different animals was much larger than the variability caused by different MEA plates. However, the reason behind the variability of cortical neurons in culture is still unclear. Reducing synaptic inputs by pharmacologically blocking synaptic receptors has been known to reduce the variability [235]. However, studying neuronal networks without synaptic inputs is not very useful, which is why the number of animals used in

the experiments was increased to eliminate the biological variation arising from different animals. To further understand the behaviour of primary cultures and establish baseline recordings under our conditions, the wild type cultures between DIV14 to DIV28 were investigated. The increase in firing and synchronization during development suggested our protocol can produce robust and healthy primary cultures.

In conclusion, different conditions were tested to develop a robust model of *in vitro* networks on MEA, despite variability caused by a number of different factors. Determining the impact of experimental variables on neuronal culture function has provided an insight into the important factors that need to be considered when developing these assays. This optimisation was demonstrated to be a necessary step in establishing MEA analysis of primary neuronal cultures. In doing so I have provided a framework that can be used by different laboratories and for similar research questions.

Chapter 4 Characterization of *SCN2A* DEE variants

4.1 Introduction

With the advances in genetic testing, variants in *SCN2A* have emerged as a major cause of neurogenetic disorders. Numerous variants have been identified [236] and linked to a broad clinical phenotypic spectrum , including benign epilepsy [77, 82, 160-164], DEE [17, 237, 238], autism [239, 240], schizophrenia [241], ataxia [242], and intellectual disability without seizures [242]. The associated clinical phenotypes range from mild to very severe, indicating a complex role that dysfunction in $Na_v1.2$ channels play pathologically.

To assess the functional impact of detected variants, heterologous expression of mutant and wild type channels combined with whole cell patch clamping to study their electrophysical properties is a common approach [5, 243]. Studies in these expression systems have shown that the *SCN2A* variants can be classified into two major groups – one linked to GoF changes in the biophysical properties, the other group including variants which result in LoF. These changes in cellular function can be caused by alterations in selectivity, voltage dependence, gating (including faster/slower activation or inactivation), and changes in regulation, trafficking or apoptosis of the channel [244]. A recent study suggested there is a good correlation between the clinical phenotype and biophysical properties of the $Na_v1.2$ channel. *SCN2A* variants found in BFNIS [172, 237, 242, 245, 246] and ataxia [245] have been shown to be GoF, whereas variants found in autism patients all caused LoF [17, 175]. In DEE, the GoF variants were linked to the early seizure onset phenotype (<3 months), and corresponded to a relatively good responsiveness, reducing seizures in these patients when treated with sodium channel blockers [92, 174, 176]. In contrast, the variants which are LoF associate with the late seizure onset DEE [176, 247, 248]. However, this classification is not always straightforward. Firstly, some variants show a combination of biophysical changes indicating both gain and loss of function and making it difficult to assess their overall impact on neuronal excitability. Moreover, discrepancies in the effect seen for the same

variants expressed in non-neuronal cell lines have also been reported. While expression of three BFNIS variants in HEK293 cells showed that they cause $Na_v1.2$ LoF [177], transfecting the same variants into cultured rat cortical neurons revealed that they enhance $Na_v1.2$ function [172]. Interestingly, the result seen in neurons matched the observed efficacy of sodium channel blockers in the patients carrying these variants [172], suggesting the advantage of using neuronal cultures. This suggests that testing genotype-phenotype correlations for *SCN2A* disorders requires use of different experimental models and levels of analysis.

SCN2A p.R1882Q (located at the C-terminal domain of $Na_v1.2$) and p.R853Q variants (located at the S4 of domain II of $Na_v1.2$) are the most recurrent variants identified in patients with early and late seizure onset DEE, respectively [92, 152]. A previous voltage clamp study in our lab, using a non-neuronal expression system, has found that p.R1882Q channels showed a shift in both activation and inactivation curves and slower fast inactivation, whereas p.R853Q channels exhibited a negative shift of the steady-state inactivation and an enhanced entry into slow inactivation [176]. This evidence supports the hypothesis that early onset DEE are caused by $Na_v1.2$ channel GoF variants, whereas late onset DEE are caused by LoF variants. To further test this idea, our lab generated two mouse models carrying variants corresponding to the two human variants. The p.R1882Q mice showed a very severe phenotype, with spontaneous seizures and premature death by the age P30, whereas the p.R853Q mice had no spontaneous seizures, no EEG abnormalities or other obvious behavioural changes and was even less prone to develop chemical induced seizures (Li et al., unpublished data). The lack of disease phenotype in p.R853Q mice may be due to the compensatory effects in a complex animal model. Testing the genotype-phenotype correlations using behavioural and seizure tests in mouse models may be more challenging than anticipated and suggest that other levels of analysis are needed. The central question that arose was how the presence of *SCN2A* variants affected the properties of neurons and networks they form. Single neuronal properties can be assessed using patch clamp recordings in brain slices; however, this does not provide intact networks, or the ability to monitor neuron activity from multiple recording sites. Therefore, the aim of this work was to study network activity using primary neuronal cultures derived from the two mouse models and assess the impact of the two disease variants with MEA analysis.

4.2 Methods

The methods used in this chapter are described in Chapter 2 with modifications listed below.

As shown in Figure 4.1, *in vitro* neuronal network cultures were obtained from the cortices of P0 or P1 mice at a seeding density of 300000 cells/well on multiwell MEA. 10-minute recordings of spontaneous neuronal activity were conducted from DIV14 to 28 with a sampling rate of 20 kHz. After filtering the signals with a high-pass 300 Hz, 40 network parameters were extracted in terms of spiking, single channel bursting and network bursting activity using a custom MATLAB script. Data normalized to wild type littermates are presented in line graphs. It should be noted that the normalization of Kappa used the after-drug value to minus the baseline value of the same well due to the existing minus values in Kappa, whereas division was used on all the other parameters.

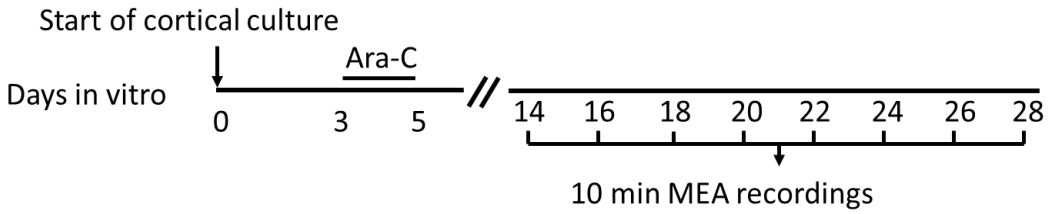

Figure 4.1 Schematic of the experimental design of *SCN2A* DEE variants characterization.

P0 or P1 mice cortices were dissected and put into culture on DIV0, followed by Ara-C (5 µM) treatment from DIV3 to 5. For phenotype characterization, 10 minute MEA recordings were performed every second day between DIV14 and 28.

4.3 Results

In order to understand the underlying mechanism of *SCN2A* DEE, spontaneous network activity in primary cortical cultures obtained from mouse models carrying either a LoF or a GoF variant were investigated. From previous studies performed on wild type cortical cultures (Chapter 3), we learned that *in vitro* global network activity that started to appear after two weeks, sometimes vanished after four weeks and was most stable and

synchronized after three weeks (DIV21). Therefore, although MEA recordings were conducted from two to four weeks *in vitro*, the representative raw traces were selected from DIV22 recordings (Figure 4.2). These raw traces show 30 second recordings on a single electrode to emphasize the differences among cultures generated from wild type, SCN2A p.R1882Q and p.R852Q heterozygous mice. Compared to wild type, the cultures with p.R1882Q variant showed higher activity, while the cultures obtained from p.R853Q mice were less active.

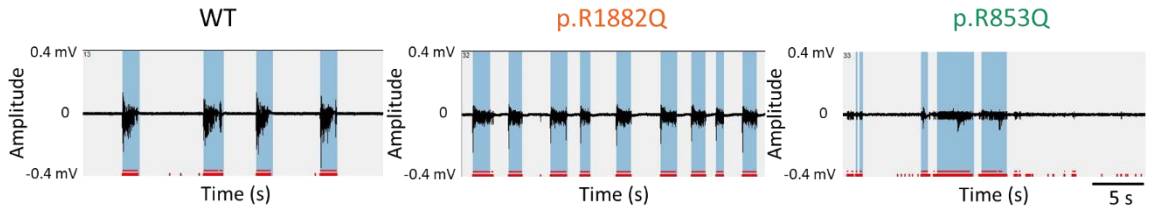

Figure 4.2 Representative raw traces of *SCN2A* DEE variants.

Representative raw signals of the spontaneous activity in wild type culture (left), SCN2A p.R1882Q mutant culture (middle) and SCN2A p.R853Q mutant culture (right) recorded for 30 s on one electrode at DIV22.

The raw MEA signals were then filtered and detection of spikes, single channel bursts and network bursts was conducted using custom MATLAB script. Representative raster plots relative to the raw traces are shown in Figure 4.3, exhibiting the network activity of 12 electrodes in each well. Each row represents signals received and analysed from one electrode, and each short horizontal line represents a spike. Compared to wild type cortical cultures, SCN2A p.R1882Q variant increased the overall neuronal activity, whereas p.R853Q variant decreased the activity as well as the synchronization (see below).

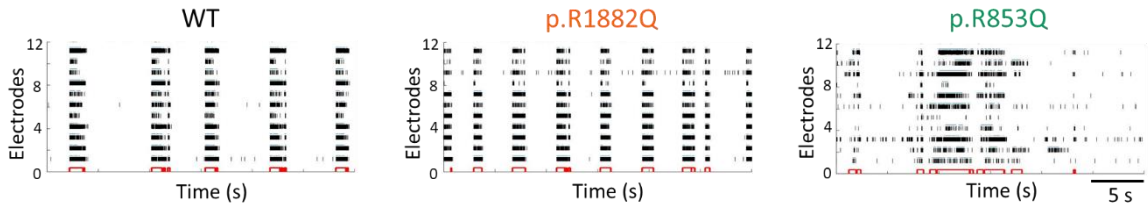

Figure 4.3 Representative raster plots of *SCN2A* DEE variants.

Representative raster plots of the spontaneous activity in wild type culture (left), SCN2A p.R1882Q mutant culture (middle) and SCN2A p.R853Q mutant culture (right) recorded for 30 s in one well at DIV22.

The changes were quantified by extracting information from all the recordings and calculating the parameters of the *in vitro* networks derived from wild type and *SCN2A* heterozygous animals as described in Chapter 2. All the data were normalized to the average data of the wild type littermates recorded on the same day and looked at six major parameters to gain a better understanding of the network features.

Firstly, the spike activity was analysed using two main parameters (Figure 4.4). The normalized mean firing rates of p.R1882Q heterozygous cultures were significantly higher than in wild type cultures, starting from 1.58 ± 0.09 ($p < 0.0001$) at DIV14, reaching the peak at 2.4 ± 0.1 ($p < 0.0001$) at DIV20, and then dropping to 1.26 ± 0.07 ($p > 0.05$) at DIV28. On the contrary, the average firing rates recorded from p.R853Q cultures were significantly lower than in cultures derived from their wild type littermates. However, the trend of normalized firing rate in p.R853Q group is like in the p.R1882Q group - lower at the start and end recording time point, higher at three weeks *in vitro*. At the first and last recording point, the values were 0.53 ± 0.03 ($p < 0.0001$) and 0.51 ± 0.04 ($p < 0.001$) fold, respectively. The highest value appeared at DIV22 as 0.78 ± 0.06 ($p < 0.01$) fold. The normalized firing rate inside bursts showed mostly consistent decrease in p.R853Q cultures, from 0.83 ± 0.05 ($p > 0.05$) at DIV14 to 0.54 ± 0.04 ($p < 0.0001$) at DIV28, compared to the wild type. In contrast, a significant increase was observed in p.R1882Q cultures. The largest increase was seen at DIV16 when the mean firing rate inside bursts of p.R1882Q was 1.51 ± 0.07 fold ($p < 0.001$) of wild type. The smallest increase was observed at DIV22, with the mean firing rate inside p.R853Q bursts reaching 1.12 ± 0.05 fold ($p > 0.05$) of the wild type. Changes of the average firing rate confirmed that p.R1882Q variant increased the overall spontaneous activity, while p.R853Q variant decreased the activity. The changes in firing rate inside of bursts further showed that heterozygous SCN2A p.R1882Q and p.R853Q action potential properties were affected.

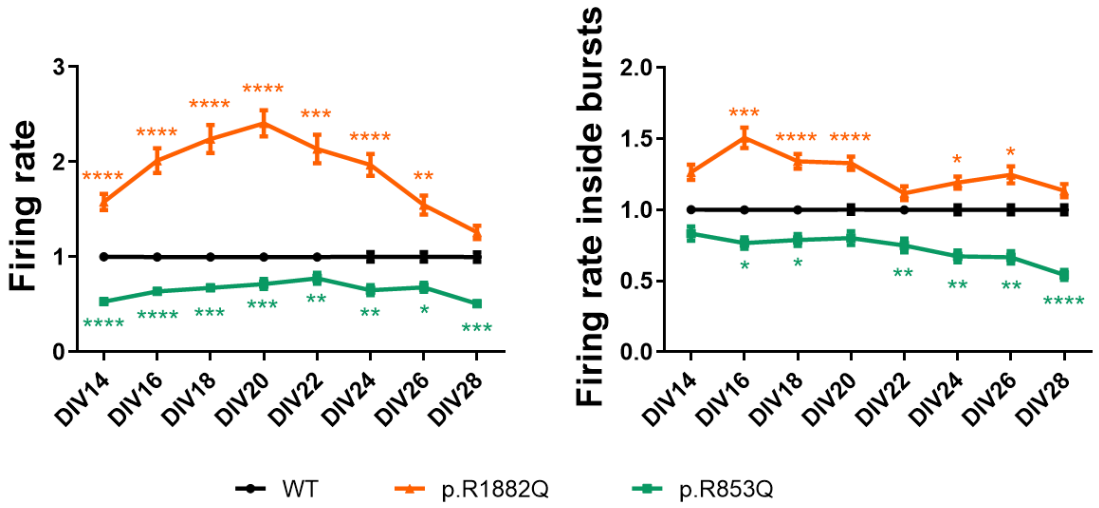

Figure 4.4 Spike parameters of *SCN2A* DEE variants.

*Line graphs of two selected parameters of SCN2A p.R1882Q and p.R853Q cultures normalized to their wild type littermates from DIV14 to 28 showing firing rate (left) and the firing rate inside of bursts (right). p.R1882Q group is shown in orange, p.R853Q group is shown in green, and the wild type group is shown in black. p.R1882Q heterozygous n=104, p.R1882Q wild type littermates n=143, p.R853Q heterozygous n=81, p.R853Q wild type littermates n=98. Experiments are performed sequentially on the same cells. A Mann-Whitney test was applied on raw data to test the significant differences between the heterozygous and wild type at each time points. Results are presented as mean ± SEM. *p < 0.05, **p < 0.01, ***p < 0.001, ****p < 0.0001.*

Secondly, network activity was investigated (Figure 4.5): the normalized network bursting rate showed a significant increase in cultures with *SCN2A* p.R1882Q variant, and a significant reduction in cultures with p.R853Q variant. For p.R1882Q cultures, the normalized network bursting rate started from 1.388 ± 0.082 ($p < 0.0001$) at DIV14 and was elevated and stable from DIV20 to 24, showing values of 2.7 ± 0.3 ($p < 0.0001$), 2.6 ± 0.3 ($p < 0.0001$) and 2.6 ± 0.3 ($p < 0.0001$) fold, respectively. At DIV28, the value reduced to 1.3 ± 0.2 fold, but was still significantly higher than the wild type ($p < 0.05$). In p.R853Q cultures, the normalized network bursting rate increased from 0.56 ± 0.05 ($p < 0.0001$) at DIV14 to 0.77 ± 0.04 ($p > 0.05$) at DIV28. These results indicate GoF for p.R1882Q mutant, and LoF of p.R853Q, at the network activity level. I also assessed the features of bursts. Cultures with p.R1882Q variant had shorter normalized duration of

bursts, while cultures with p.R853Q variant showed longer duration. During development, the normalized duration of bursts in p.R853Q networks decreased from 1.50 ± 0.09 ($p < 0.0001$) at DIV14 to 1.09 ± 0.04 ($p < 0.01$) at DIV28. For p.R1882Q networks, the lowest normalized duration happened at DIV24, 0.70 ± 0.07 ($p < 0.0001$).

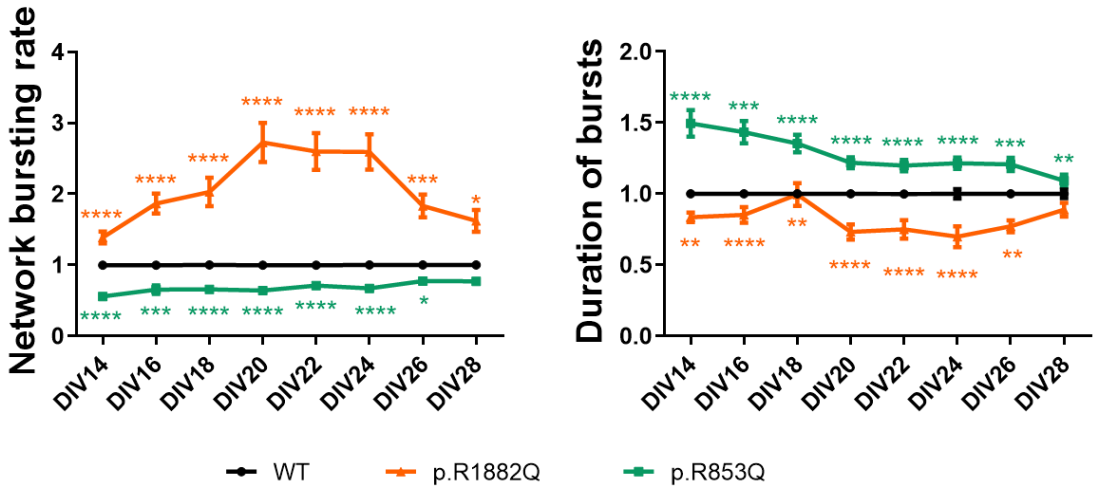

Figure 4.5 Bursts parameters of *SCN2A* DEE variants.

*Line graphs of two selected parameters of SCN2A p.R1882Q and p.R853Q cultures normalized to their wild type littermates from DIV14 to 28 showing the network bursting rate (left) and the time duration of bursts (right). p.R1882Q group is shown in orange, p.R853Q group is shown in green, and the wild type group is shown in black. p.R1882Q heterozygous n=104, p.R1882Q wild type littermates n=143, p.R853Q heterozygous n=81, p.R853Q wild type littermates n=98. Experiments are performed sequentially on the same cells. A Mann-Whitney test was applied on raw data to test the significant differences between the heterozygous and wild type at each time points. Results are presented as mean ± SEM. *p < 0.05, **p < 0.01, ***p < 0.001, ****p < 0.0001.*

Lastly, I analysed the synchronization of cultures (Figure 4.6). Jitter is the time duration from the start of the first burst in a network burst, to the start of the last burst in the network burst. It shows the synchronization of a network burst. Compared to the wild type, the mean Jitter of p.R853Q cultures was increasing from DIV14 to DIV28, indicating the p.R853Q variant showed less synchronized networks during development. At two weeks of *in vitro*, the normalized average Jitter of SCN2A p.R853Q cultures was 1.15 ± 0.06 ($p > 0.05$). After an additional two weeks *in vitro*, this number increased to

1.58 ± 0.06 ($p < 0.0001$). As for the cultures derived from p.R1882Q heterozygous mice, the average of Jitter showed only limited elevation.

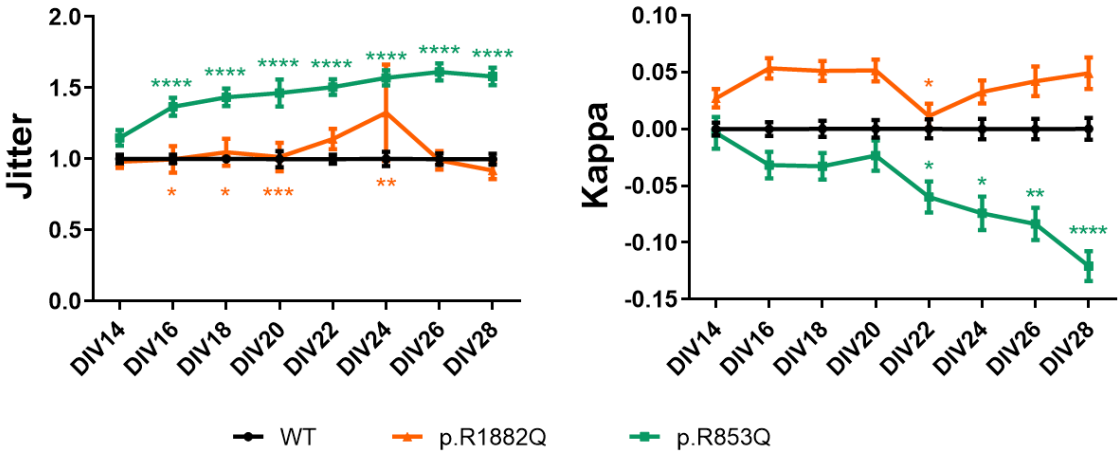

Figure 4.6 Synchronization parameters of *SCN2A* DEE variants.

*Line graphs of two selected parameters of SCN2A p.R1882Q and p.R853Q cultures normalized to their wild type littermates from DIV14 to 28 showing the Jitter (left) and the Kappa (right). p.R1882Q group is shown in orange, p.R853Q group is shown in green, and the wild type group is shown in black. p.R1882Q heterozygous n=104, p.R1882Q wild type littermates n=143, p.R853Q heterozygous n=81, p.R853Q wild type littermates n=98. Experiments are performed sequentially on the same cells. A Mann-Whitney test was applied on raw data to test the significant differences between the heterozygous and wild type at each time points. Results are presented as mean ± SEM. *p < 0.05, **p < 0.01, ***p < 0.001, ****p < 0.0001.*

Kappa is the measurement of temporal synchronization of spikes across all electrodes in one network. To calculate Kappa, the time of the recording on each electrode was first divided into 10 ms bins. If one or more spikes occur within the bins, they are marked as 1. If no spikes occur, the bins are marked as 0. The agreement coefficient Cohen's Kappa is calculated for all pairs of active electrodes. It measures the degree of coincidence of spikes on both electrodes exceeding the chance-expected coincidence assuming uncorrelated spikes. Bigger kappa means more synchronized. Compared to the wild type cultures, cultures with SCN2A p.R1882Q variant had bigger Kappa value in most of the recordings. The biggest increase occurred at DIV16, 0.054 ± 0.009 ($p > 0.001$). In cultures

with SCN2A p.R853Q variant, an insufficient development in synchronization was seen that got worse over time. At DIV28, the reduction in Kappa was 0.12 ± 0.01 ($p < 0.0001$).

Iris plots are heat maps of p values from Wilcoxon rank sum test (Figure 4.7) and used as a network signature of a mutant culture. In the left iris plot, 40 parameters of p.R1882Q cultures were compared with wild type cultures at DIV14, 22 and 28. 7 parameters of spiking features, 8 parameters of single channel bursting features and 25 parameters of network bursting features were included (Orders and definition of the parameters were shown as Table 2.1). Compared to the parameters of wild type, the increase in a given parameter for mutant cultures is shown in red, while a decrease is shown in blue. The iris plot on the right showed the changes of p.R853Q cultures. Looking at the two iris plots together, it is obvious that the cultures with SCN2A p.R1882Q variant and p.R853Q variant show the opposite changes compared to the wild type.

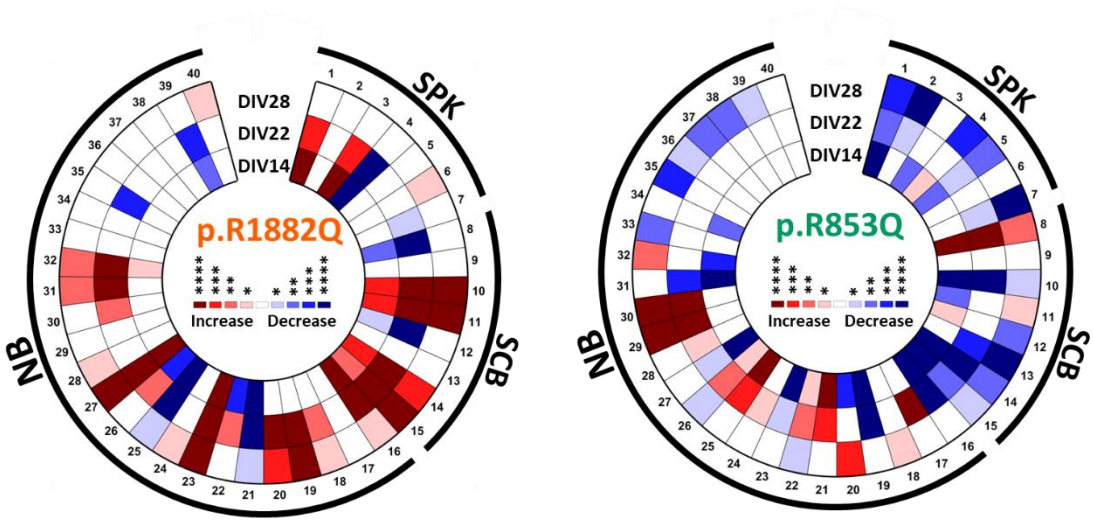

Figure 4.7 Iris plots of *SCN2A* DEE variants.

*Iris plots (Wilcoxon rank sum test p value heat map of 40 parameters) of the differences between SCN2A p.R1882Q heterozygous culture and wild type culture (left), and between SCN2A p.R853Q heterozygous culture and the wild type littermates (right) at DIV 14, 22 and 28. The increase compared to the wild type, is shown in red, whereas the decrease is shown in blue. p.R1882Q heterozygous n=104, p.R1882Q wild type littermates n=143, p.R853Q heterozygous n=81, p.R853Q wild type littermates n=98. Experiments are performed sequentially on the same cells. Results are presented as mean ± SEM. *p < 0.05, **p < 0.01, ***p < 0.001, ****p < 0.0001.*

4.4 Discussion and conclusion

Using MEA analysis, I showed that neuronal networks derived from mouse models of early and late onset DEE had two distinctive *in vitro* phenotypes, corresponding to gain and loss of function reported in previous functional analysis in non-neuronal expression systems. p.R1882Q neuronal networks exhibited dramatic increases in firing rate and network bursting rate, showing enhanced activity in both individual spiking and global bursting. These indicated hyperexcitability at the neuronal network level, and matched the prediction made by patch clamp and dynamic patch clamp experiments [176]. Furthermore, the elevation in Kappa showed hypersynchronization at the overall spiking level, and the reduction in Jitter showed hypersynchronization at the network activity level. Altered busting features were also observed. Although the time duration of bursts was reduced in p.R1882Q neuronal networks compared to the wild type, the frequency of firing in bursts increased. This indicates that the p.R1882Q neurons have shorter "cool down" time before they can fire again (quicker recovery), which was not reported in single cell patch clamping in CHO cells where the mutant showed a similar recovery time compared to the wild type [176]. These results show that GoF in $Na_v1.2$ leads to enhanced spontaneous activity in neuronal networks. The observed hyperexcitability, hypersynchronization and altered bursting features in neuronal networks could present the *in vitro* phenotype of SCN2A p.R1882Q epilepsy.

In SCN2A p.R853Q neuronal networks, the frequency of firing and network bursting were both decreased, indicating impaired excitability at the network level, and matching the results of patch clamp and dynamic clamp analysis in non-neuronal cells [176]. Reduced Kappa and enlarged Jitter in the p.R853Q cultures both imply lack of synchronization. The decrease in excitability and synchronization corroborates LoF in p.R853Q neuronal networks. It is still not clear how less frequent firing and lack of rhythm in neuronal activity can cause seizures. One possible explanation could be prolonged burst duration seen in p.R853Q network activity, indicating that the bursts were harder to stop. Less frequent presence of spikes in bursts suggests the p.R853Q neurons need more time to recover before they can fire again. This was not found in single cell patch clamp recordings performed in CHO cells that showed similar recovery time from inactivation compared to the wild type [176].

$Na_v1.2$ is mainly present in excitatory neurons at the AIS and the nodes of Ranvier. Early in development this is the only sodium channel expressed at these sites indicating $Na_v1.2$ is essential for the generation and propagation of action potentials early in life. The augmented $Na_v1.2$ currents will therefore result in highly excitable neurons, and cause hyperexcitability in neuronal networks that leads to seizures. This may be the explanation why early onset seizures occur in p.R1882Q DEE patients and why the patients have a better response to sodium channel blockers. In contrast, p.R853Q variant impairs the $Na_v1.2$ function and causes decrease in neuronal network excitability. This might be why p.R853Q patients do not have seizures in early development but does not answer the question of how LoF variant causes seizures later in development. Two possible hypotheses suggest altered formation and maturation of neuronal circuits, or imbalance of excitatory and inhibitory inputs. It has been shown that altered excitability in brain can affect developmental processes. For instance, changes in synaptic connectivity, indicating changes of synaptic strength rather than the topography of circuits, can affect the formation and maturation of cortical circuits [249]. Moreover, bursting was shown to play a role in establishing appropriate circuit connections [250], especially in inducing synaptic plasticity [251]. Recently, $Na_v1.2$ was found to be expressed in dendrites throughout development as well as in mature brains, with an enrichment near postsynaptic densities in spines using immuno-electron microscopy [252]. A recent study also suggested that consistent $Na_v1.2$ function is required to maintain dendritic excitability, which is crucial for sufficient synaptic strength [253]. A LoF *SCN2A* variant would be expected to reduce dendritic excitability and networking activity, leading to a decrease in synaptic strength and therefore altered the formation and maturation of neuronal circuits. In mature brains, $Na_v1.6$ replaces $Na_v1.2$ in distal AIS and nodes of Ranvier, and is then in charge of initiating and propagating action potentials. Therefore, when $Na_v1.6$ emerges in already malfunctioning brain circuits, seizures may occur. This may explain why late onset seizures occur in DEE patients with *SCN2A* LoF variants, and offer an explanation for why developmental delay occurs before seizures. The alternative hypothesis suggests an imbalance in excitatory/inhibitory inputs based on the expression of $Na_v1.2$ channels in axons of unmyelinated mossy fibres in mature brains [92, 156, 237]. Because mossy fibres predominately target inhibitory basket cells [254], LoF $Na_v1.2$ channels would decrease the activity of mossy fibres that leads to inhibitory input reduction, and therefore

can cause hyperexcitability in brain. However, the fact that p.R853Q mouse model does not develop spontaneous seizures suggests these mechanisms could be different in human and mouse.

Iris plots show changes in all parameters, and they can be used as network signature of a variant. Comparison of iris plots of p.R1882Q and p.R853Q cultures indicates opposite effects caused by these two *SCN2A* variants. It should be noted that presenting p-values from the statistical tests in iris plots is different than showing the magnitude of the effect, and it is possible that multiple testing may have contributed to the observed associations as correction for multiple comparisons was not performed. However, we were attempting to interpret the overall pattern of results rather than any specific estimate in isolation, and the purpose of using iris plots is to create a pattern for visualizing different phenotypes.

Although the symptoms of patients carrying p.R1882Q and p.R853Q have a lot in common, the pathologies behind them are very distinct. Categorizing these disorders as one and treating the patients with the same strategy would be harmful. This has already been observed in the clinic, as sodium channel blockers were found partially beneficial for early onset patients to compensate the GoF of Nav1.2. However, the same treatment could potentially worsen the epileptic phenotype in late onset patients with SCN2A LoF variants. This implies that patients should be considered individually based on their genotype and not just based on the clinical phenotype. The following chapter will address the predictive value of MEA network activity for potential novel treatments for *SCN2A* variants (p.R1882Q and p.R853Q).

Chapter 5 Investigating pharmacology treatments for *SCN2A* DEE

5.1 Introduction

DEE are severe disorders where patients present with seizures, developmental disability and other comorbidities that have an extremely poor overall prognosis. Currently, there are no effective treatments available, highlighting a huge unmet clinical need. In recent years *de novo* variants have been identified as the main cause of DEE and they account for about 70% of all DEE cases. To date, more than 50 genes have been linked to DEE [46]. Analysis of the genetic causes is important for both diagnosis as well as for the development of precision medicine therapies for these patients. Identifying the gene variant and determining the functional consequences of that variant is vital when selecting the appropriate treatment for individual patients as some of the available antiepileptic drugs (AED) have been known to exacerbate patients' symptoms. This phenomenon became apparent when Dravet patients, carrying *SCN1A* variants, were prescribed sodium channel blockers which caused them to have more seizures [110]. The deleterious effect of prescribing sodium channel blocker for Dravet patients is that *SCN1A* is predominantly expressed in inhibitory interneurons and variants in this gene commonly cause LoF channels, therefore blocking these channels will lead to disinhibition resulting in increased seizure frequency which is clearly not therapeutically beneficial.

Recent studies have identified two groups of patients with *SCN2A* DEE, an early onset group and a late onset group [92]. Patients with early onset DEE have a seizure onset, typically focal seizures, within the first three months of life and developmental delay emerges after the onset of seizures. Late onset DEE patients start having seizures from three months onwards. These patients often experience spasms and developmental delay before the onset of their actual seizures [176]. One important difference between these two groups is that early onset DEE patients are more likely to respond well to sodium channel blockers, while patients with late onset DEE either show no response at all or experience increased seizure frequency [92]. This is supported by functional data,

including my data presented in Chapter 3, showing that the early onset DEE *SCN2A* variants result in GoF phenotypes and late onset DEE variants result in LoF phenotypes.

Previously published data illustrated in Table 5 shows the effectiveness of fifteen FDA (Food and Drug Administration) approved AED commonly prescribed for patients with both early onset and late onset *SCN2A* DEE. For the early onset group, the commonly prescribed sodium channel blocker phenytoin (PHT), is effective in reducing seizures in 71.4% of patients (20 out of 28) when compare to other sodium channel blockers which only reduce seizure frequency in 53.3% of patients (16 out of 30). Since its introduction in 1936, PHT has proved to be one of the most successful AED on the market [255]. PHT preferentially binds to the inactive form of the sodium channel and blocks the channels in a voltage-dependent and frequency-dependent manner, which is evident from the increase in the ratio of inactive channels and the repetitive firing with increasing membrane depolarization [256]. The picture for patients carrying the *SCN2A* p.R1882Q heterozygous variant is not as promising because only 2 of 5 patients prescribed PHT experienced alleviation of their seizures and their symptoms were made worse by the other sodium channel blockers. There was only one patient that showed a positive response and they were prescribed carbamazepine.

In the late onset group, patients showed negative responses to sodium channel blockers, however, only 28.3% of the patients exhibited seizure reduction (13 out of 46) when prescribed sodium channel blockers. In SCN2A p.R853Q patients, PHT was found to exacerbate seizures [176]. However, levetiracetam (LEV) was more effective compared to the other drugs, alleviating symptoms in 72.2% (13 out of 18) of patients. LEV controls seizures by inhibiting the release of excitatory neurotransmitter through synaptic vesicle protein 2A [257], producing positive cognitive side effects [258, 259]. LEV has not been reported to be used in p.R853Q patients (lamotrigine (LTG), but was mistaken for LEV in one case in Wolff's paper [92], which was originally published by Kazuyuki [160]). LEV had no effect in one p.R1882Q patient from the Wolff's study. However, another early onset DEE case became seizure free after the LEV treatment [92].

Although PHT is able to improve the seizure status for some of the early onset *SCN2A* DEE patients, for the majority of patients, this treatment has no impact on their seizure frequency [92]. Moreover, of the seven patients identified to be carrying a p.R1882Q

variant, treatment with PHT was ineffective. Interestingly, of twelve patients identified to be carrying a p.R853Q variant, only one patient treated with LTG ceased to have any ongoing seizures [160]. However, for another two p.R853Q patients, who also received LTG, no beneficial effect was observed [176]. These data suggest that there is an urgent need to find new effective treatment strategies to help these patients.

Based on these data, we decided to test the *in vitro* predictability and efficacy of PHT and LEV in both of our *in vitro* model of early and late onset *SCN2A* DEE. The neuronal culture models developed in Chapter 4 provided the basis for the network scale analysis to enable us to determine the impact of drugs in *SCN2A* disease.

Table 5-1 Previously published data illustrating the responses to clinical treatment in *SCN2A* early onset DEE patients.

Medicine	Mechanism	Seizure free or reduction	No effect or seizure worsen
Carbamazepine (CBZ)	Sodium channel blocker	6	3
Lacosamide (LCM)	Sodium channel blocker	3	2
Lamotrigine (LTG)	Sodium channel blocker	5	3
Oxcarbazepine (OXC)	Sodium channel blocker	1	2
Phenytoin (PHT)	Sodium channel blocker	20	8
Rufinamide (RUF)	Sodium channel blocker	0	1
Zonisamide (ZNS)	Sodium channel blocker	1	3
Valproate (VPA)	Sodium channel blocker and GABA enhancer	5	11
Topiramate (TPM)	Sodium and calcium channel blocker	7	14
Ethosuximide (ESM)	T-type calcium channel blocker	0	0
Phenobarbital (PB)	GABA receptor enhancer	1	18
Benzodiazepines (benzo)	$GABA_A$ receptor enhancer	2	8
Levetiracetam (LEV)	Modulation of synaptic neurotransmitter release	2	17
Sulthiame (ST)	Carbonic anhydrase inhibitor	0	2
Vigabatrin (VGB)	GABA aminotransferase inhibitor	2	9

This table gathered data from Wolff et al. [92, 176].

Table 5-2 Previously published data illustrating the responses to clinical treatment in *SCN2A* late onset DEE patients.

Medicine	Mechanism	Seizure free or reduction	No effect or seizure worsen
Carbamazepine (CBZ)	Sodium channel blocker	2	6
Lacosamide (LCM)	Sodium channel blocker	0	2
Lamotrigine (LTG)	Sodium channel blocker	6	12
Oxcarbazepine (OXC)	Sodium channel blocker	1	7
Phenytoin (PHT)	Sodium channel blocker	0	4
Rufinamide (RUF)	Sodium channel blocker	2	3
Zonisamide (ZNS)	Sodium channel blocker	2	3
Valproate (VPA)	Sodium channel blocker and GABA enhancer	10	10
Topiramate (TPM)	Sodium and calcium channel blocker	7	9
Ethosuximide (ESM)	T-type calcium channel blocker	1	4
Phenobarbital (PB)	GABA receptor enhancer	2	9
Benzodiazepines (benzo)	$GABA_A$ receptor enhancer	11	4
Levetiracetam (LEV)	Modulation of synaptic neurotransmitter release	13	5
Sulthiame (ST)	Carbonic anhydrase inhibitor	2	5
Vigabatrin (VGB)	GABA aminotransferase inhibitor	3	6

This table gathered data from Wolff et al. [92, 176].

$K_v7.2$ and $K_v7.3$ are known to colocalized with voltage-gated sodium channels at the AIS and the nodes of Ranvier [260, 261]. Like $Na_v1.2$, LoF and GoF variants of K_v7 were also identified in DEE patients [262-266]. These K_v7 channels are responsible for the M current [267], which is critical for controlling neuronal excitability [268]. It contributes to the medium and slow afterhyperpolarizations of action potentials caused by bursts [269-271], as well as regulating resting membrane potential and synaptic functions [268, 269, 271-273]. It also plays a role in shaping action potential firing properties, including spike frequency adaptation [274]. More specifically, at AIS, K_v7 channels inhibit the initiation of action potentials by counteracting the afterdepolarizations generated by Na_v channels. However, at the nodes of Ranvier, K_v7 channels also enhance the conduction of the action potentials by increasing Na_v channel availability [275]. Essentially,

enhancing the function of these potassium channels may increase or decrease the excitability of neuronal networks in different circumstances.

Retigabine (RTG), also known as ezogabine, is a potassium channel opener which specifically targets K_v7 channels. This drug was approved as an add on therapy to treat patients suffering from focal epilepsies [102] but it has since been discontinued due to deleterious side effects resulting in a blue discolouration of the skin and eye abnormalities [103]. While companies are striving to modify the chemical properties of RTG with the aim of reducing unwanted side effects, the compound is still used as a good experimental tool to study the effect of enhancing activity of potassium K_v7 channels. We hypothesized that both mechanisms of RTG may in different ways be beneficial for GoF and LoF SCN2A DEE. In the GoF DEE, K_v7 channel opening could potentially serve as the break for burst firing increased due to the p.R1882Q variant. SCN2A LoF indicates a reduced number of functional sodium channels. RTG in this case may increase the availability of the sodium channels by hyperpolarizing the membrane potential and facilitating the recovery from inactivation for the available Na_v channels.

In this chapter, I will explore the utility of MEA network analysis for the development of better treatments for *SCN2A* DEE patients. To this aim, I will first examine if the efficacy of two clinically applied AED (PHT and LEV) can be reproduced in our *in vitro* neuronal network models that carry the p.R1882Q and p.R853Q variants. Further, I will explore the effectiveness of RTG in these models through its ability to adjust bursting patterns and hyperpolarize membrane potential.

5.2 Methods

The methods used in this chapter are based on methods described in Chapter 2. Specific applications are described below.

5.2.1 Preparation of investigational compounds

Investigational compounds were purchased from commercial companies: PHT (Sigma-Aldrich, St. Louis, MO, USA); LEV (Sigma-Aldrich, St. Louis, MO, USA); RTG (Sigma-

Aldrich, St. Louis, MO, USA). Compounds were dissolved in Dimethyl sulfoxide (DMSO) (Sigma-Aldrich, St. Louis, MO, USA) to obtain stocking solutions, which were diluted in H_2O to reach the concentration of 50 X of the working solutions with 1‰ DMSO. H_2O containing 5% DMSO was used as 50 X vehicle control.

5.2.2 Application of investigational compounds

As shown in Figure 5.1, cultured neuronal networks were obtained from P0 or P1 mice and seeded as 300000 cells/well on multiwell MEA plates. Cultures were kept until DIV21 or 22 for pharmacology studies, and the media was changed two days before the test. The first 10 minutes of MEA recordings were performed and used as baselines. Then 10 µL of a 50 X working solution of the tested chemical was added per well. After 5 minutes of incubation, spontaneous activity was recorded on the MEA for another 10 minutes as the after-treatment effect.

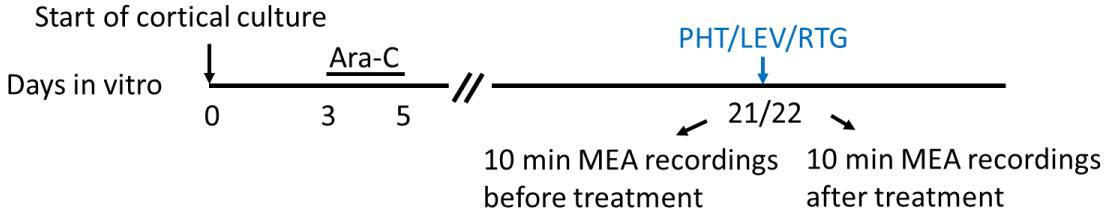

Figure 5.1 Schematic of the pharmacology experimental design.

P0 or P1 mice cortices were dissected and plated into culture on DIV 0, followed by Ara-C (5 µM) treatment from DIV3 to 5. For pharmacology tests, a 10-minutes MEA was recorded as baseline on DIV 21 or 22. Chemicals were added in small volume immediately after the baseline recording. 5 minutes after the addition of chemicals, another 10-minutes MEA recording was performed to measure the impacts of the chemicals.

5.2.3 Data analysis of the efficacies of investigational compounds

In Chapter 4, the *in vitro* network signatures of cultures derived from mutant mice that were identified as different from the wild type are shown as iris plots in Figure 4.7. In this chapter, these signatures are used to evaluate the pharmacological effects of commonly

used antiepileptic drugs. In addition, three main parameters are chosen to represent the changes caused by the applied compounds. They are firing rate, network bursting rate and duration of bursts. Compounds with beneficial effects are expected to reverse the changes caused by the mutants and revert the signatures of mutant cultures back to wild type.

Three different concentrations were used for each drug. Parameters changes were calculated by averaging the values after the treatment normalized to the values before treatment for each well. These changes were then compared with to the vehicle to determine the effect of the drug. It should be noted that the normalization of Kappa used the after-drug value to minus the baseline value of the same well due to the existing minus values in Kappa, whereas division was used on all the other parameters.

Three parameters including mean firing rate, network bursting rate and duration of bursts are chosen due to their commonly usage in antiepileptic drug research [276-278].

5.3 Results

5.3.1 Phenytoin (PHT)

PHT is known to have the best clinical outcome in early onset *SCN2A* DEE patients [92]. Therefore, this sodium channel blocker was applied to the primary cultures obtained from pups carrying SCN2A p.R1882Q and p.R853Q variants at three weeks *in vitro*, the time point when the cultures were more stable. As the raw traces in Figure 5.2 show, the activity of both p.R1882Q and p.R853Q cultures was suppressed after the application of 100 µM PHT. Especially in cultures with the late onset DEE variant, PHT almost abolished all the activity.

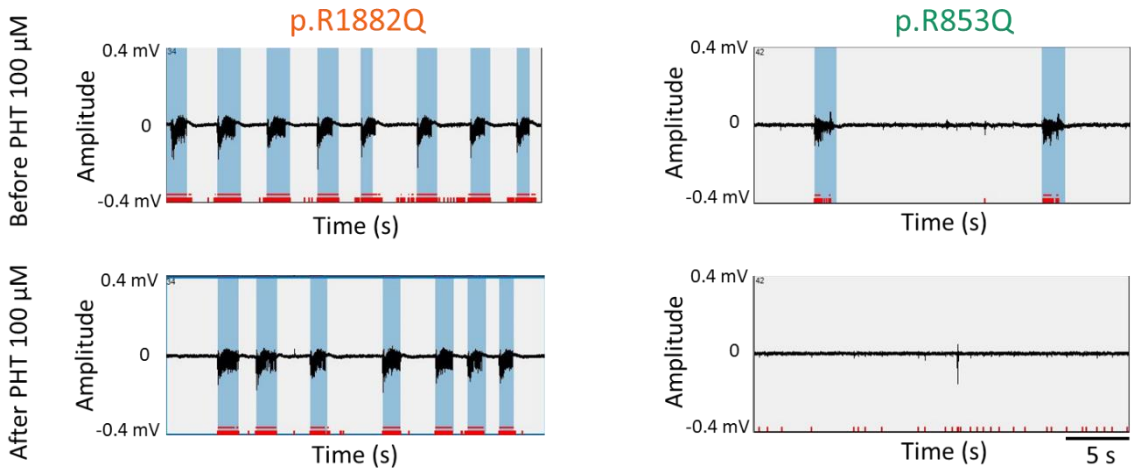

Figure 5.2 Representative raw traces before and after the application of PHT.

Effect of PHT was tested on DIV21 or 22 primary cortical cultures derived from SCN2A p.R1882Q (left) and p.R853Q (right) heterozygous mice. 30 seconds representative raw traces of neuronal activity before (top) and after (bottom) the application of 100 µM PHT in one electrode are shown.

The raster plots show 30 s long network activity, sampled by 12 electrodes per network. As shown in Figure 5.3, in the cultures carrying p.R1882Q variant, the network activity decreased, as well as the overall firing activity. In p.R853Q network, the bursts almost disappeared, leaving the single spikes at the rate similar to the baseline recording.

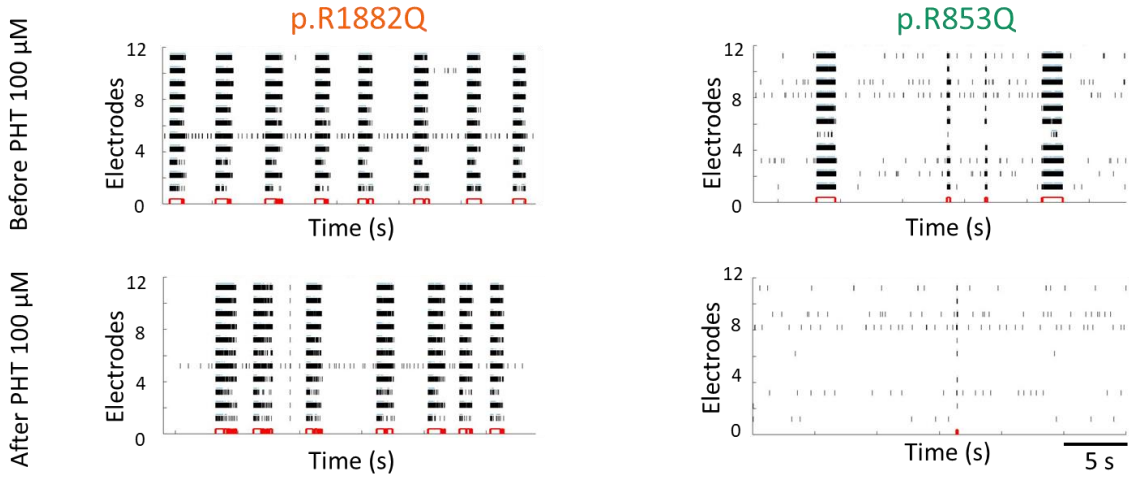

Figure 5.3 Representative raster plots before and after the application of PHT.

Effect of PHT was tested on DIV21 or 22 primary cortical cultures derived from SCN2A p.R1882Q (left) and p.R853Q (right) heterozygous mice. 30 seconds representative raster plots of neuronal activity before (top) and after (bottom) the application of 100 µM PHT in one well are shown.

The PHT effects were quantified as previously described (Figure 5.4).

For the culture carrying *SCN2A* DEE early onset variant p.R1882Q, the application of 30 µM, 50 µM and 100 µM PHT caused nonsignificant reduction of firing rate of 19 ± 3% ($p > 0.05$), 24 ± 9% ($p > 0.05$) and 34 ± 8% ($p > 0.05$), respectively. There was also no significant change in network bursting rate, but the normalized network bursting reduced as the dose of PHT increased. From low to high dose, the normalized percentage of network bursting rate were 107 ± 22% ($p > 0.05$), 93 ± 21% ($p > 0.05$) and 80 ± 14% ($p > 0.05$). No significant changes were seen in the duration of bursts. With the increase of concentration of PHT, the normalized percentage of bursts duration was 132 ± 29% ($p > 0.05$), 115 ± 16% ($p > 0.05$) and 182 ± 77% ($p > 0.05$).

For the cultures carrying the late onset variant p.R853Q, significant differences were observed in all three parameters. Dramatic decrease ($p < 0.0001$) was seen in firing rate. The highest and medium dose of PHT caused over 80% (84 ± 2%) and 50% reduction (51 ± 5%), respectively. Even application of the drug at lowest dose decreased the firing rate by over 40% (40 ± 5%). Network bursting rates were also reduced significantly, with

the percentage change similar to the firing rate. The percentages of reduction of the network bursting rate were 42 ± 7% ($p < 0.01$), 58 ± 4% ($p < 0.0001$) and 84 ± 3% ($p < 0.0001$) after the treatment with 30 µM, 50 µM and 100 µM PHT, respectively. In contrast to these two parameters, the duration of bursts was increased by acute application of 30 µM, 50 µM and 100 µM PHT. From the lowest dosage to the highest dosage, the elevations were 71 ± 25% ($p < 0.05$), 61 ± 18% ($p < 0.05$) and 136 ± 66% ($p > 0.05$), respectively.

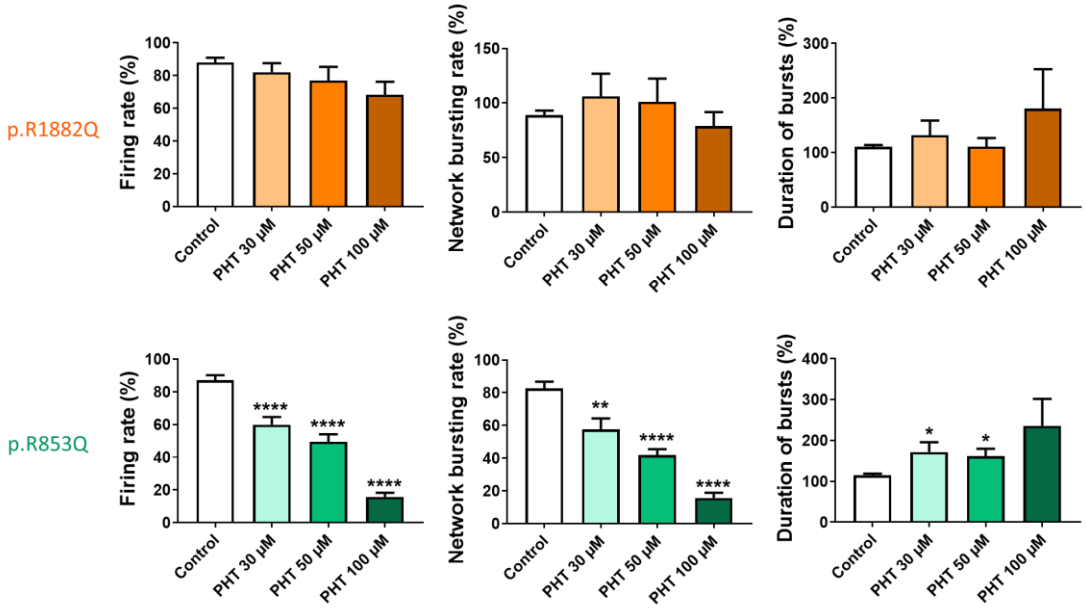

Figure 5.4 The effect of PHT on firing rate, network bursting rate and duration of bursts in cortical neuronal networks carrying SCN2A p.R1882Q and p.R853Q variants.

*Bar graphs on the top row show the drug effect by presenting percentage changes of mean firing rate, mean network bursting rate, and mean duration of single channel bursts of p.R1882Q cultures before and after the application vehicle control, 30 µM, 50 µM and 100 µM PHT. Bar graphs on the bottom row show the percentage changes in p.R853Q cultures. p.R1882Q heterozygous for vehicle control, 30 µM, 50 µM and 100 µM PHT n=38, 18, 18, and 18. p.R853Q heterozygous for vehicle control, 30 µM, 50 µM and 100 µM PHT n=54, 19, 23, and 22. A Mann-Whitney test was applied on percentage changes to test the significant differences between the drug group and vehicle control group. Results are presented as mean ± SEM. *p < 0.05, **p < 0.01, ****p < 0.0001.*

As shown in Figure 5.5, the left iris plot described the *p* value of Wilcoxon rank sum test comparing the changes after application of three concentrations of PHT with changes after application of vehicle control in SCN2A p.R1882Q in cultures after three weeks *in vitro*. The changes of *in vitro* network signature caused by PHT were minor, with only 6 out of 40 parameters changing. The right iris plot in Figure 5.5 shows comparison of changes in SCN2A p.R853Q cultures. PHT significantly decreased the activity (including firing rate, both inside and outside of bursts), the number of electrodes that fired and the percentage of bursts that participated in network bursts. Also, the synchronization of the culture was further impaired at the high concentration of PHT.

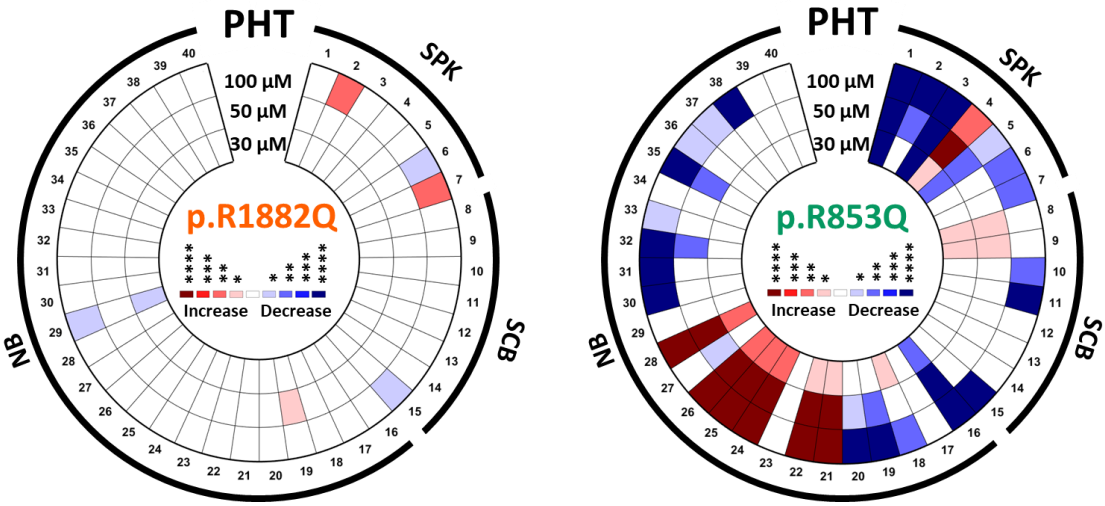

Figure 5.5 The effect of PHT on SCN2A p.R1882Q and p.R853Q networks shown by iris plots.

*The ratio changes of individual culture before and after the application vehicle control, 30 µM, 50 µM and 100 µM PHT were calculated. Using Wilcoxon rank sum test, the iris plot on the left shows the differences between the ratio change of vehicle control and the ratio change of 30 µM, 50 µM and 100 µM PHT in SCN2A R1882Q culture. The iris plot on the right shows the SCN2A p.R853Q ratio change of control compared to different concentrations of PHT. p.R1882Q heterozygous under vehicle control, 30 µM, 50 µM and 100 µM PHT n=38, 18, 18, and 18. p.R853Q heterozygous under vehicle control, 30 µM, 50 µM and 100 µM PHT n=54, 19, 23, and 22. Results are presented as mean ± SEM. *p < 0.05, **p < 0.01, ***p < 0.001, ****p < 0.0001.*

5.3.2 Levetiracetam (LEV)

Currently, there is no effective drug treatment for late onset DEE patients. Among the drugs given to late onset DEE patients, LEV showed somewhat positive outcomes. Therefore, we tested the efficacy of LEV in our *in vitro* network system. The representative raw traces were shown in Figure 5.6. The application of LEV did not have a dramatic impact on the mice primary cultures carrying variant relative to human SCN2A p.R1882Q variant, whereas it decreased the activity in cultures carrying variant relative to human SCN2A p.R853Q variant.

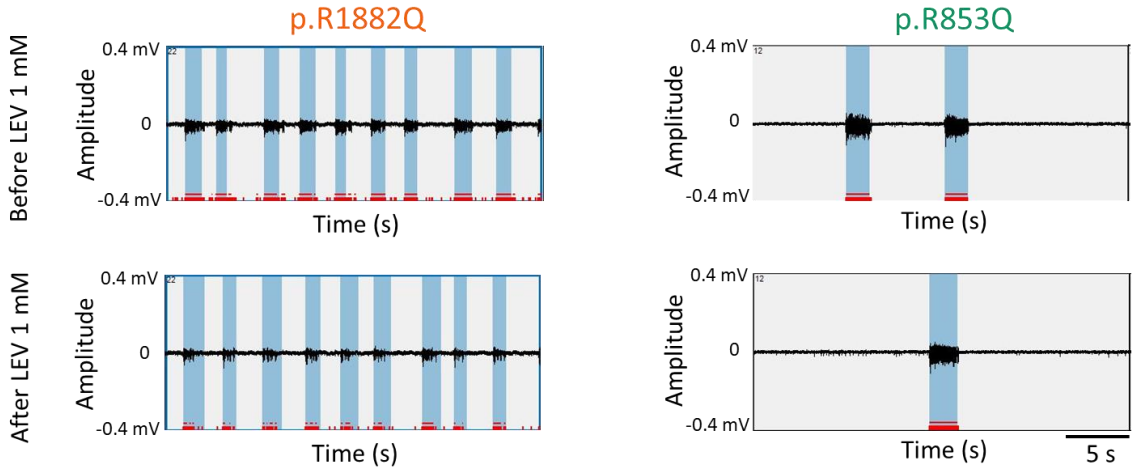

Figure 5.6 Representative raw traces before and after the application of LEV.

Effect of LEV was tested on DIV21 or 22 primary cortical cultures derived from SCN2A p.R1882Q (left) and p.R853Q (right) heterozygous mice. 30 seconds representative raw traces of neuronal activity before (top) and after (bottom) the application of 1 mM LEV in one electrode are shown.

The representative raster plots are presented in Figure 5.7. Compared to the baseline before the application of 1 mM LEV, neither the frequency nor the synchronization of the spontaneous neuronal network activity of p.R1882Q culture changed obviously. As for the p.R853Q cultured network, LEV inhibited the network bursting, although the single spikes outside of bursts did not seem to be affected.

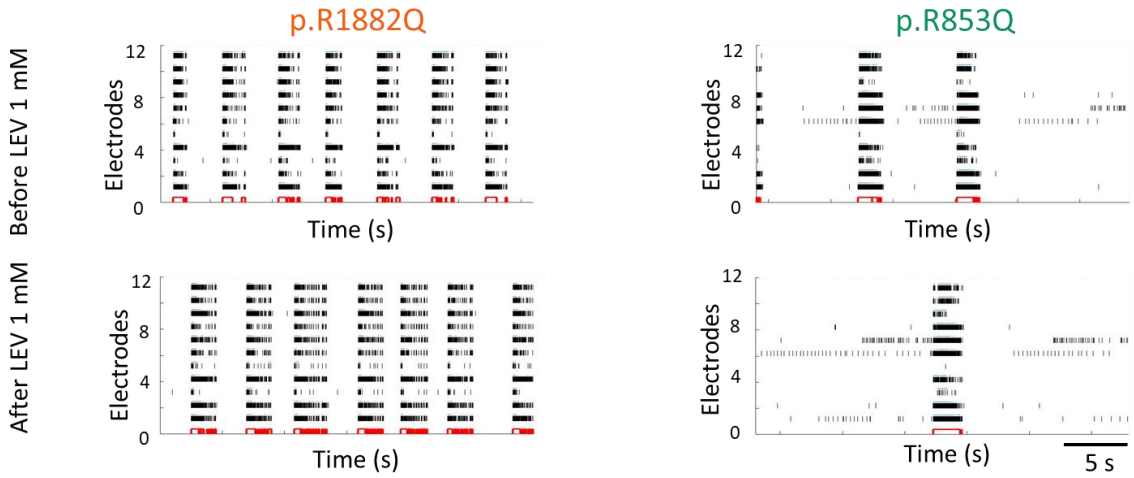

Figure 5.7 Representative raster plots before and after the application of LEV.

Effect of LEV was tested on DIV21 or 22 primary cortical cultures derived from SCN2A p.R1882Q (left) and p.R853Q (right) heterozygous mice. 30 seconds representative raster plots of neuronal activity before (top) and after (bottom) the application of 1 mM LEV in one well are shown.

The changes of firing rate, network bursting rate and duration of bursts are examined here (Figure 5.8). LEV caused no significant changes in the duration of bursts in both early onset and late onset variant cultures. As for the network bursting rate, 0.5 mM LEV caused the biggest change in p.R1882Q networks by increasing 16 ± 15% (p >0.05) of network bursting rate compared to 11 ± 4% of decrease caused by vehicle control. Significant reductions were seen in firing rate in both cultures. In cultures with SCN2A p.R1882Q variant, the percentage reduction was 27 ± 4% (p < 0.01), 29 ± 5% (p < 0.01) and 27 ± 5% (p < 0.05) after the treatment with 0.3 mM, 0.5 mM and 1 mM LEV, respectively. In cultures with the SCN2A p.R853Q variant, the corresponding percent reduction was 11 ± 9% (p > 0.05), 21 ± 4% (p > 0.05) and 31 ± 5% (p < 0.01), respectively.

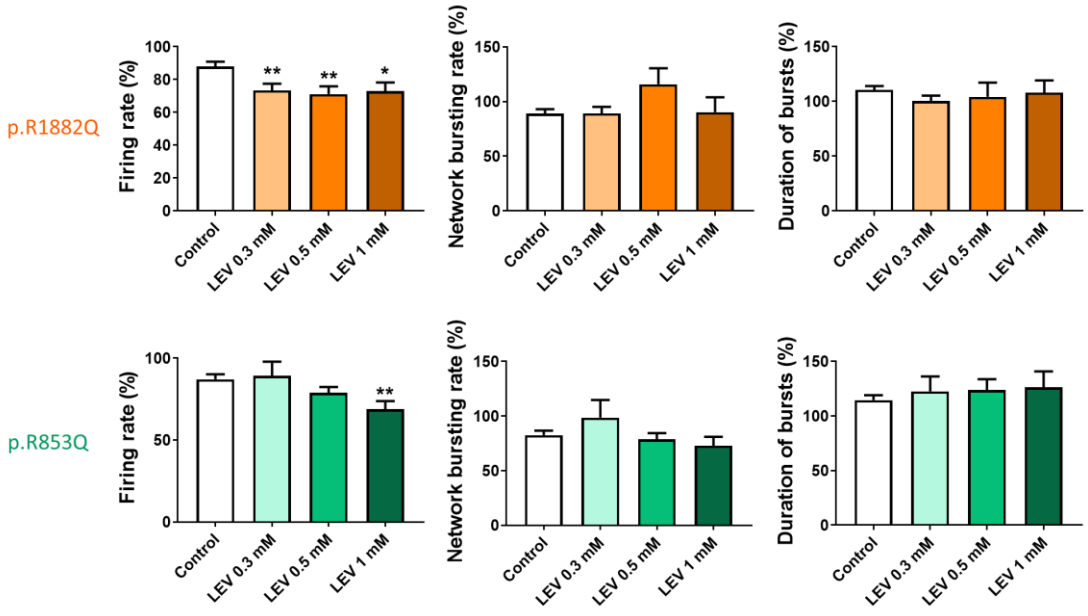

Figure 5.8 The effect of LEV on firing rate, network bursting rate and duration of bursts in cortical neuronal networks carrying SCN2A p.R1882Q and p.R853Q variants.

*Bar graphs on the top row show the drug effect by presenting percentage changes of mean firing rate, mean network bursting rate, and mean duration of single channel bursts of p.R1882Q cultures before and after the application of vehicle control, 0.3, 0.5, 1 mM LEV. Bar graphs on the bottom row show the percentage changes in p.R853Q cultures. p. R1882Q heterozygous under vehicle control, 0.3 mM, 0.5 mM and 1 mM LEV n=38, 20, 19, and 19. p.R853Q heterozygous under vehicle control, 0.3 mM, 0.5 mM and 1 mM LEV n=54, 18, 22, and 19. A Mann-Whitney test was applied on percentage changes to test the significant differences between the drug group and vehicle control group. Results are presented as mean ± SEM. *p < 0.05, **p < 0.01.*

As shown in Figure 5.9, LEV reduced neuronal activity in both cultures with the early onset variant and the late onset variant. In early onset cultures, the amplitude, the firing rate inside of bursts, the number of spikes in bursts and network bursts, and the number of channels participated in spikes or bursts or network bursts were reduced. Similarly, in late onset group, the firing rates inside and outside of bursts were both decreased, along with the amplitude and Kappa.

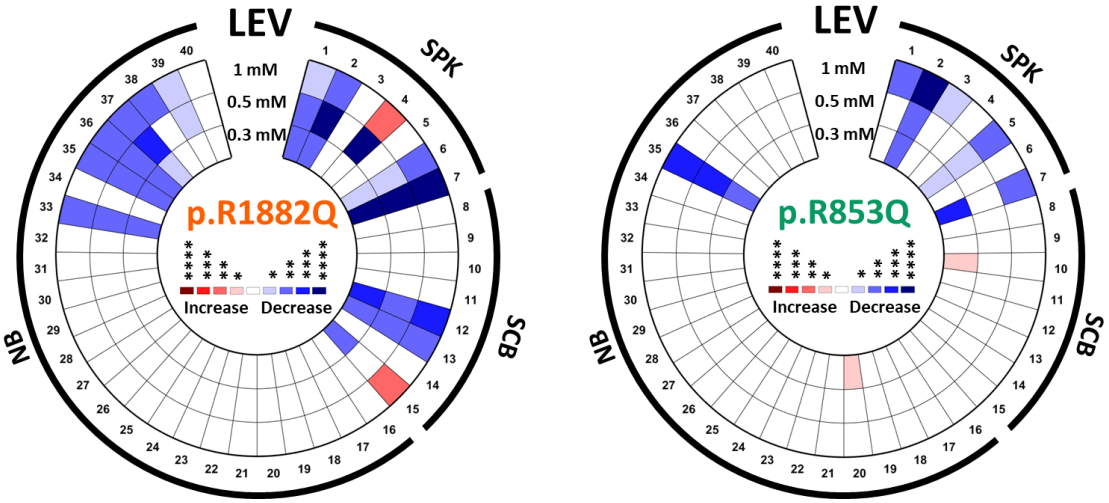

Figure 5.9 The effect of LEV on SCN2A p.R1882Q and p.R853Q networks shown by iris plots.

*The ratio changes of individual culture before and after the application of vehicle control, 0.3, 0.5, 1 mM LEV were calculated. Using Wilcoxon rank sum test, the iris plot on the left shows the differences between the ratio change of vehicle control and the ratio change of 0.3, 0.5, 1 mM LEV in SCN2A p.R1882Q culture. The iris plot on the right shows the SCN2A p.R853Q ratio change of control compared with different concentrations of LEV. p.R1882Q heterozygous under vehicle control, 0.3 mM, 0.5 mM and 1 mM LEV n=38, 20, 19, and 19. p.R853Q heterozygous under vehicle control, 0.3 mM, 0.5 mM and 1 mM LEV n=54, 18, 22, and 19. Results are presented as mean ± SEM. *p < 0.05, **p < 0.01, ***p < 0.001, ****p < 0.0001.*

5.3.3 Retigabine (RTG)

Potassium currents play a balancing role to the sodium currents, therefore we next manipulated the M-current in order to explore its effect on the impairment caused by the mutant sodium channels. Thus, RTG, which works primarily as a Kv7 potassium channel opener, was investigated.

As shown in Figure 5.10, 10 µM RTG reduced the spontaneous activity in the culture containing the SCN2A p.R1882Q variant, while it increased the activity in the culture carrying the SCN2A p.R853Q variant.

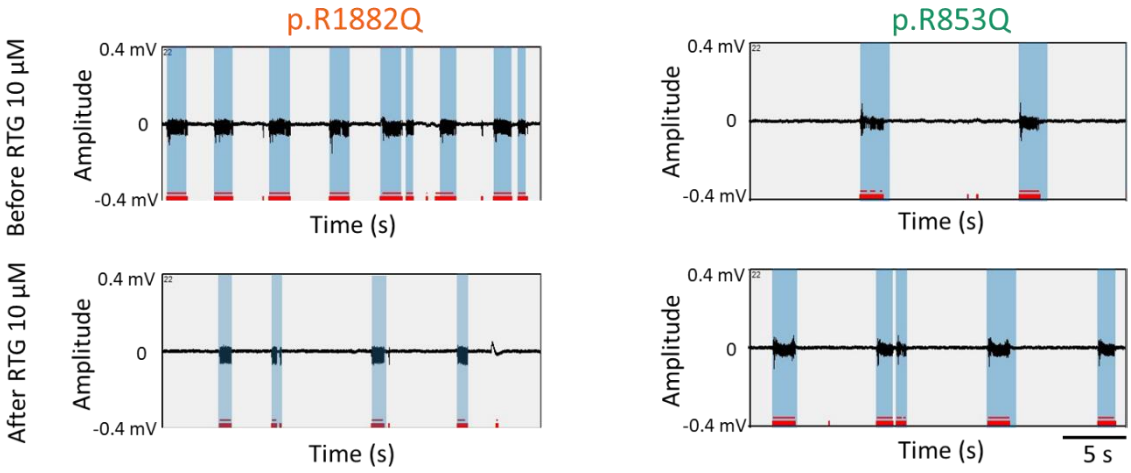

Figure 5.10 Representative raw traces before and after the application of RTG.

Effects of RTG were tested on DIV21 or 22 primary cortical cultures derived from SCN2A p.R1882Q (left) and p.R853Q (right) heterozygous mice. 30 seconds long representative raw traces showing neuronal activity before (top) and after (bottom) the application of 10 µM RTG recorded by one electrode are shown.

The representative rasters plots reveal the same effects of RTG over 12 electrodes (Figure 5.11). RTG inhibited the network bursting and overall firing of p.R1882Q *in vitro* network and enhanced the network bursting, as well as the synchronization of firing in the p.R853Q cultures.

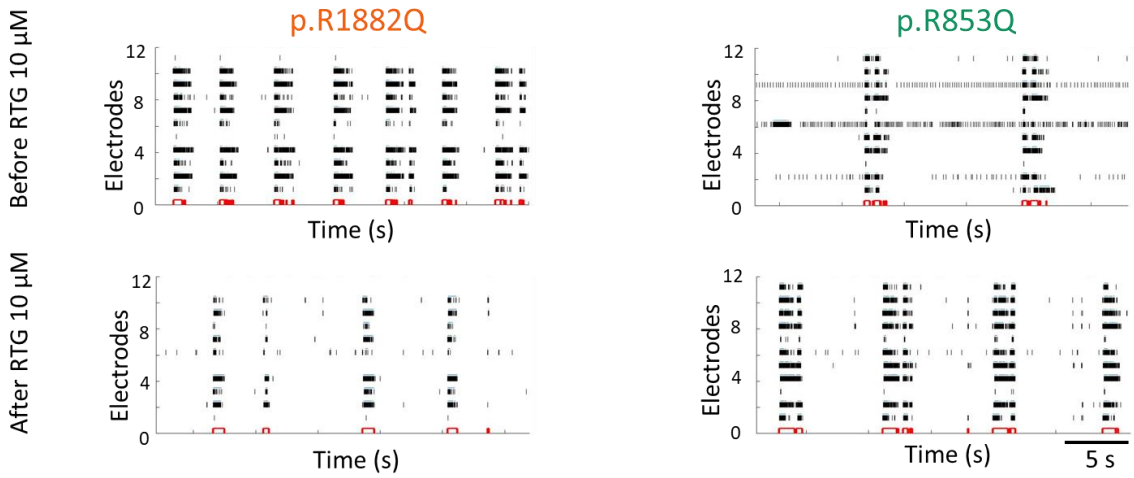

Figure 5.11 Representative raster plots before and after the application of RTG.

Effects of RTG were tested in DIV21 or 22 primary cortical cultures derived from SCN2A p.R1882Q (left) and p.R853Q (right) heterozygous mice. 30 seconds representative raster plots of neuronal activity before (top) and after (bottom) the application of 10 µM RTG recorded by one electrode were shown.

Figure 5.12 showed significant reductions of firing rate in p.R1882Q cultures after applications of 3 µM, 5 µM and 10 µM RTG: 44 ± 8% ($p < 0.001$), 51 ± 6% ($p < 0.0001$) and 65 ± 7% ($p < 0.0001$), respectively. As for the network bursting rate changes in the early onset cultures, the higher dose of RTG caused more than a 50% reduction, 64 ± 6% ($p < 0.0001$) and 66 ± 11% ($p < 0.0001$), respectively. The duration of bursts in the p.R1882Q group increased significantly after application of RTG, by 93 ± 58% ($p > 0.05$), 182 ± 85% ($p < 0.001$) and 364 ± 175% ($p < 0.05$). For the p.R853Q group, only slight reduction was seen in the duration of bursts, with the application of RTG, but big increases were observed for both firing rate and network bursting rate. Compared to the 13 ± 3% reduction in firing rate caused by vehicle control, the significant increases caused by 5 µM and 10 µM RTG were 15 ± 13% ($p < 0.05$) and 20 ± 12% ($p < 0.01$), respectively. The elevations in network bursting rate were more dramatic; from low to high concentrations of RTG the values of increase were 12 ± 23% ($p > 0.05$), 55 ± 21% ($p < 0.001$) and 83 ± 54% ($p < 0.01$).

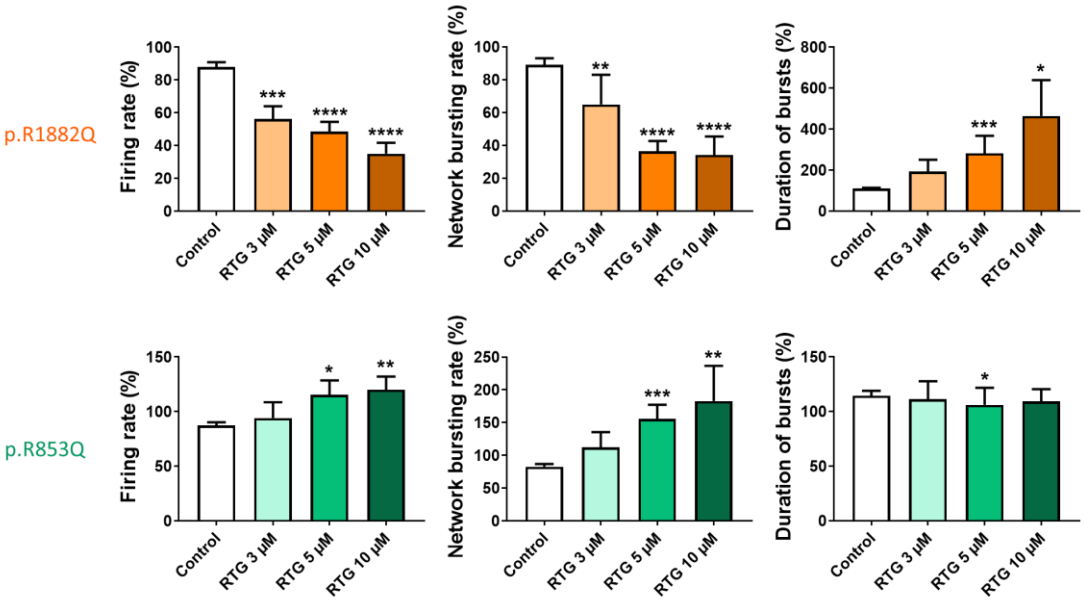

Figure 5.12 The effect of RTG on firing rate, network bursting rate and duration of bursts in cortical neuronal networks carrying SCN2A p.R1882Q and p.R853Q variants.

*Bar graphs on the top show the drug effect as percentage changes for mean firing rate, mean network bursting rate, and mean duration of single channel bursts of p.R1882Q cultures before and after the application vehicle control, 3 µM, 5 µM and 10 µM RTG. Bar graphs on the bottom showed the percentage change in p.R853Q cultures. p.R1882Q heterozygous under vehicle control, 3 µM, 5 µM and 10 µM RTG n=38, 20, 19, and 20. p.R853Q heterozygous under vehicle control, 3 µM, 5 µM and 10 µM RTG n=54, 16, 16, and 16. A Mann-Whitney test was applied on percentage changes to test the significant differences between the drug group and vehicle control group. Results are presented as mean ± SEM. *p < 0.05, **p < 0.01, ***p < 0.001, ****p < 0.0001.*

Unlike the effects of PHT and LEV that alter the cultures with the early onset or late onset DEE variant all in one direction, RTG showed the opposite effects on some parameters (Figure 5.13). For example, RTG increased the firing rate and network bursting rate in p.R853Q networks, while decreasing it in p.R1882Q cultures. The mean interval between network burst starts and the mean inter network burst interval were increased in early onset DEE model, while decreased in late onset DEE. Compared to the phenotype of both cultures, RTG brought them closer to wild type culture parameters.

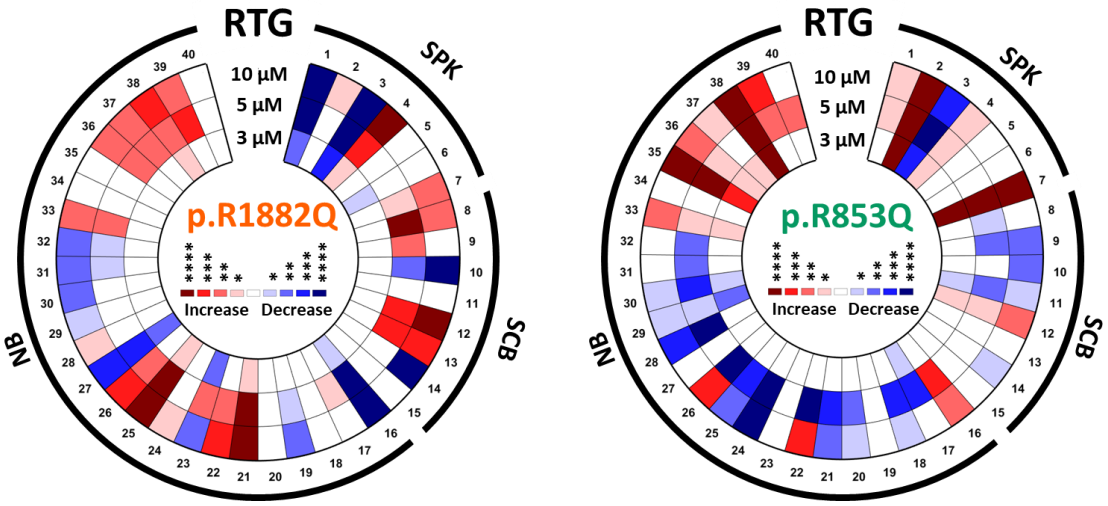

Figure 5.13 The effect of RTG on SCN2A p.R1882Q and p.R853Q networks shown by iris plots.

*The ratio changes of individual cultures before and after the application of vehicle control, 3 µM, 5 µM and 10 µM RTG were calculated. Using Wilcoxon rank sum test, the iris plot on the left shows the differences between the ratio change of vehicle control and the ratio change of 3 µM, 5 µM and 10 µM RTG in SCN2A p.R1882Q culture. The iris plot on the right shows the SCN2A p.R853Q ratio change of control compared with different concentrations of RTG. p.R1882Q heterozygous under vehicle control, 3 µM, 5 µM and 10 µM RTG n=38, 20, 19, and 20. p.R853Q heterozygous under vehicle control, 3 µM, 5 µM and 10 µM RTG n=54, 16, 16, and 16. Results are presented as mean ± SEM. *p < 0.05, **p < 0.01, ***p < 0.001, ****p < 0.0001.*

Some effects of RTG were similar in both cultures. For instance, RTG increased firing frequency of inside/outside ratio of bursts by escalating the firing rate inside of bursts as well as declining the firing rate outside burst. Along with the elevation of the number of spikes in single channel bursts, they showed that RTG regulating the activity by regulating burst firing. Moreover, increase was seen in the mean of amplitudes, the number of spikes and the number of channels participating in network bursts. RTG significantly reduced all the 6 parameters reflecting coefficient of variation in p.R1882Q networks, while decreasing 3 of them in p.R853Q networks. In addition, the elevation of Kappa and decline of Jitter caused by RTG in both cultures showed the enhancement in synchronization. These indicated that RTG promoted the participation of spikes in bursts,

and the participation of spikes and bursts in network bursts, as well as inhibited the variation and increased the synchronization of network activity.

5.4 Discussion and conclusion

With the aim of finding better treatments for *SCN2A* DEE patients, it is necessary to develop models that can be used to predict drug efficacy. My project explored the use of the *in vitro* neuronal networks using a MEA assay to assess the impact of two clinically relevant drugs and explore the potential benefits of drugs that have not previously been tested in these patients. The efficacies of the three compounds (PHT, LEV and RTG) were tested on cultured neuronal networks, derived from mouse lines, carrying heterozygous variants relevant to human SCN2A p.R1882Q (early onset) and p.R853Q (late onset) variants. The tested concentrations of drugs were chosen according to *in vitro* usage [201, 279]. The *in vitro* concentrations of PHT and RTG are at a similar level compared to the plasma or serum concentration in patients, whereas the concentration of LEV used on cultures are much higher than the therapeutic range of serum concentration [201, 279]. The *in vitro* system is very different than the *in vivo* system where drug absorption, distribution, metabolism, excretion, protein-drug binding and blood brain barrier are involved [280]. Acute application of drugs on cultures can also enlarge the differences between *in vitro* and *in vivo* drug dosage [279]. It would be interesting to test the prolonged incubation effect of drugs in future experiments. However, the purpose of our experiment is to test the pharmacological response of different genotypes.

PHT is a classic sodium channel blocker. Voltage-gated sodium channels are closed at resting membrane potential. They open in response to the membrane depolarisation caused by synaptic inputs, and then inactivate within a few milliseconds. The opening of sodium channels allows inward flow of sodium ions that results in the depolarising phase of action potentials. However, about 1% of the sodium channels remains - open for tens of seconds, leading to a persistent sodium current (I_{NaP}), which lowers action potential threshold and sustains bursting in neurons [281]. PHT has higher affinity towards inactivated sodium channels; as the number of inactivated channels increases with membrane depolarization, PHT is believed to suppress abnormal bursting by selectively blocking sodium currents in voltage-dependent, use-dependent and time-dependent

manner and has minimum impacts on normal physiological function [256]. However, in our experiments, PHT showed limited impact on hyper-bursting p.R1882Q cultures, whereas it dramatically inhibited the neuronal activity in the supressed-bursting p.R853Q cultures. In primary p.R1882Q networks, PHT constrained the excitability by reducing firing channels. But it also exhibited enhancement of excitability by escalating the firing frequency inside of bursts, as well as augmenting synchronization by decreasing Jitter and increasing Kappa. This ambiguity might indicate the network level mechanism of why PHT showed variable results in SCN2A p.R1882Q patients [176]. In *in vitro* p.R853Q networks, PHT inhibited firing as well as network bursting. In addition, it reduced the synchronization and prolonged the bursts, moving the properties of the culture further away from the wild type phenotype. The inhibitory effect of PHT, on already less excitable neuronal networks, may explain why PHT exacerbates seizures in p.R853Q patients [176] and has either no effect or exacerbates seizures in patients with *SCN2A* late onset DEE believed to carry other $Na_v1.2$ LoF variants [92]. Our results suggested that the efficacy of PHT in patients with highly hyperexcitable neuronal networks is not very high. However, PHT seems most beneficial for patients with intermediate $Na_v1.2$ GoF. Moreover, the fact that PHT had a larger impact on neuronal networks with less activity, may suggest it should be completely avoided as a treatment for LoF variants.

LEV supresses neurotransmitter release and acts as a neuromodulator by binding to SV2A, a synaptic vesicle glycoprotein, and inhibiting presynaptic calcium channels [257]. LEV is known to have better outcomes in *SCN2A* late onset DEE patients than early onset patients. However, clinical results of LEV in patients carrying p.R1882Q or p.R853Q variant are not known as so far only one p.R1882Q patient was treated with LEV and showed no improvement [92]. After application of LEV, p.R1882Q cultures exhibited smaller spike amplitude, possibly indicating fewer cells were firing near the recording electrodes. Reduced number of firing electrodes also suggested fewer firing neurons. Furthermore, declined spike numbers in bursts showed decreased participation in bursts; reduced number of electrodes, spikes and bursts participating in network bursts showed impaired participation in network activity. Lastly, the overall firing rate, and the firing rate inside of bursts showed decreased excitability of p.R1882Q cultures. Our results demonstrate LEV inhibited the spontaneous neuronal activity of p.R1882Q

cultures by reducing the number of neurons performing single action potentials and bursts, as well as suppressing the participation of neurons in network activity. However, LEV did not reduce the network bursting rate, and this might be the reason for the negative outcome of LEV treatment in patients with early onset DEE. In p.R853Q networks, LEV decreased the firing rate overall, inside of bursts and outside of bursts, reduced the amplitudes, and inhibited the synchronization of firing. But like PHT, LEV also pushed p.R853Q further away from wild type phenotype, and therefore it would be expected to show no effect or exacerbate seizures in patients carrying SCN2A p.R853Q variant.

RTG primarily acts as a K_v7.2-7.5 potassium channel opener, creating a hyperpolarizing shift in the activation of these channels by stabilizing their open state [273]. In brain, K_v7.2 and K_v7.3 channels are known to form heterotetrametric channels that are highly sensitive to RTG [102]. RTG was previously used as an AED to reduce the excitability [102]. The analysis of SCN2A p.R1882Q cultures revealed the same effect. In networks carrying SCN2A GoF variant p.R1882Q, the afterdepolarization and the I_{NaP} caused by repetitive firing were also counteracted by the M current enhanced by RTG. Therefore, RTG supressed the frequency of spontaneous firing and network bursting. Together with prolonging the time duration of bursts, RTG brought the properties of p.R1882Q network activity towards the wild type. Interestingly, in networks carrying SCN2A LoF variant p.R853Q, RTG stabilizes the opened K_v7 channels and therefore hyperpolarizes the resting membrane potential, resulting in rescuing voltage-gated sodium channels from slow inactivation, which leads to increased number of available sodium channels and eventually increases the excitability of neurons. It enhanced the firing and network bursting rate, reduced the time duration of bursts and raised the synchronization. Overall, RTG opposed to the effect caused by p.R853Q variant in *in vitro* neuronal cultures, reverting its effects towards the baseline. RTG also affects synaptic functions and GABA system [244, 245], which might explain why it increased participation in bursts and network bursts, and decreased the variations of both p.R1882Q and p.R853Q networks.

Moreover, the pharmacology of PHT, LEV and RTG have also been tested on wild type cultures (Supplementary Figure 1), showing moderate effects in between the impact of p.R1882Q and p.R853Q phenotypes.

In conclusion, the impact of PHT, LEV and RTG on SCN2A p.R1882Q and p.R853Q *in vitro* networks have been investigated in this chapter. PHT and LEV showed partially limited beneficial effects on cultures carrying the p.R1882Q variant, while pushing the properties of p.R853Q cultures further away from wild type phenotype. On the other hand, RTG counteracted the *in vitro* phenotypes caused by both p.R1882Q and p.R853Q variants, suggesting that RTG could be beneficial to both early and late onset *SCN2A* DEE patients. RTG is also believed to benefit loss-of-function *KCNQ* DEE patients [101]. However, the marketing of RTG was recently discontinued due to causing a blue discolouration of the skin and eye abnormalities [103]. Despite the side effects, RTG may still be worth trying in severe intractable DEE patients under close monitoring. Our findings may help the families and clinicians to bring RTG back to marketing and encouraging the discovery of new K_v7 openers with improved pharmacokinetic and pharmacodynamic properties and reduced unwanted side effects [104, 282]. Moreover, other drugs would be interesting to study using these two *in vitro* models. For instance, we can test T-type calcium channel blockers in p.R1882Q networks, because T-type calcium channels help to generate bursts, and test adrenocorticotropic hormone in p.R853Q cultures because it was beneficial to several p.R853Q patients.

Chapter 6 General discussion and conclusion

6.1 Main findings

A robust workflow for neuronal network analysis using MEA was developed, capable of modelling DEE and separating the phenotypes of early and late seizure onset *SCN2A* DEE. The increased excitability in cultures carrying early onset variant p.R1882Q may reflect the early seizures occurring in patients, and the decreased synchronization in cultures carrying late onset variant p.R853Q may reflect early developmental delay before seizure onset in patients. Our MEA models showed distinct pharmacogenetic responses to existing and potential antiepileptic compounds, and confirmed the clinical observation of PHT benefiting only some DEE patients. These results indicate that signatures of *in vitro* networks can be used as markers of DEE and may assist in identifying drugs that can reverse the signature changes caused by genetic variants. These pharmacology tests also predicted positive clinical outcomes of RTG in both early and late onset *SCN2A* DEE patients, indicating the potential efficacy of potassium channel targeting drugs in *SCN2A* DEE.

6.1.1 Aim 1: Establishing a robust network scale assay

The utilization of MEA in toxicity studies is popular, however few publications have performed phenotypic analysis on MEA [230, 283, 284]. Variability is one of the biggest obstacles for MEA high throughput drug screening. Therefore, the activity level under different conditions and the sources of variability were investigated. Our MEA workflow was designed based on the previous results although large n numbers were still required. In the workflow, cortical neurons were obtained from P0/1 mice, seeded at 300000 cells/well density, and media was changed 48 hours prior to recordings. For phenotyping studies, wild type littermate controls were identified as essential due to litter-to-litter variability. For drug screening, baseline control recordings in the same well were critical.

6.1.2 Aim 2: Use of MEA to model early onset and late onset *SCN2A* DEE

The genotype-phenotype relationship of *SCN2A* DEE has been revealed on the network scale for the first time, indicating that MEA can be used as a model for epilepsy disorders. Early onset DEE variant p.R1882Q and late onset DEE variant p.R853Q were characterized using mouse cortical neuronal networks. Distinct *in vitro* phenotypes were found, showing opposite changes caused by p.R1882Q and p.R853Q. Consistent with p.R1882Q gain-of-function and p.R853Q loss-of-function determined by CHO cell patch clamping, increased excitability and synchronization were observed in p.R1882Q cultured cortical neuronal networks, whereas decreased excitability and synchronization were seen in p.R853Q networks.

A key purpose of using MEA to model DEE is to get a deeper understanding of the disease mechanisms. For early onset *SCN2A* DEE, this study confirmed that the epileptic syndromes may result from the network hyperexcitability caused by the gain of $Na_v1.2$ function. For late onset *SCN2A* DEE, although this study could not explain the mechanism of seizures, it endorses the idea that the developmental delay syndromes may result from the impaired network synchronization.

6.1.3 Aim 3: Determining drug efficacy in MEA models of *SCN2A* DEE

Another fundamental role of MEA DEE modelling is assessing the efficacy of available or potential new treatments by identifying compounds that can reverse *in vitro* phenotypes to the control levels. The efficacy of commonly used antiepileptic drugs PHT and LEV were tested on *SCN2A* p.R1882Q and p.R853Q *in vitro* networks. These drugs showed partially limited beneficial effects on cultures carrying p.R1882Q variant, while driving the properties of p.R853Q cultures further away from wild type. Remarkably, RTG counteracted the *in vitro* phenotypes caused by both p.R1882Q and p.R853Q variants, suggesting that RTG could be beneficial to both early and late onset *SCN2A* DEE patients.

6.2 Is MEA a good platform?

Golden standard single cell patch clamping provides detailed electrophysiological information about ion channels and the activity of individual cells (neurons). However, it does not provide information on neuron interaction, and cell selection can introduce bias. On the other hand, *in vivo* technologies like EEG, MEG and fMRI measure brain activity by detecting changes associated with electricity or blood flow at the whole brain level. However, there are limitations. EEG has good temporal but poor spatial resolution. Whereas MEG and fMRI show better spatial but poor temporal resolution. Dissociated cortical cultures on MEA as a functional neuronal network disease model can fill the gap between single cell and whole brain research, yielding relatively rich information from both single cells and cell interactions at the same time.

6.2.1 Is MEA a good platform for epilepsy modelling?

The most important electrophysiological characteristic of *in vitro* neuronal networks are their synchronized global bursts. While in *in vivo* animals, synchronized bursts happen during development that mostly last for a few days or weeks [250], making networks on MEA a potential model of neural development. Moreover, high frequency bursts of action potentials are also a feature of epileptic activity [285], making MEA a potential model for epilepsy as well. Existing models have established an association between epilepsy and neuronal culture firing, where chemicals such as pentylenetetrazole [214] and 4-aminopyridine [277] have been shown to induce increased bursting activity on MEA. It is more challenging to model genetic disorders due to the variability of MEA analysis. However, mouse primary neurons expressing nicotinic β2-V287L have been used to model autosomal dominant nocturnal frontal lobe epilepsy, showing spontaneous long synaptic induced up state firing events [230].

In our study, dissociated cortical cultures carrying early onset and late onset DEE variants showed distinct MEA features. p.R1882Q cultures displayed increased firing rate and network bursting rate, frequent short bursts, and increased synchronization. In contrast, p.R853Q cultures exhibited decreased firing rate and network bursting rate, sparse long bursts, and reduced synchronization. Compared to patch clamp analysis, increased

excitability of p.R1882Q networks was consistent with the gain of $Na_v1.2$ function in CHO cells, and the reduced excitability of p.R853Q networks was consistent with the loss of $Na_v1.2$ function. Network analysis gave information about synchronization which may reflect the developmental aspect of DEE. Furthermore, MEA enabled us to study the phenotypes over a 2-week time period, allowing the observation of temporal trends. Compared to animal model findings, the increased excitability of p.R1882Q networks was consistent with the spontaneous seizures seen in mice, while p.R853Q network electrophysiology study provided a clear phenotype when the mouse model failed to. This could be due to the large n numbers we can gather for MEA research compared to animal studies; the enlarged differences in 2-dimensional dissociated cultures, or the enhanced developmental stage arrested in MEA that is closely related to DEE. Thus, although requiring large number of repeats due to its variability, MEA analysis has still proved its advantage in modelling DEE.

6.2.3 Is MEA a good platform for drug screening?

Ionic flux through ion channels creates the foundation for membrane excitability. Therefore, ion channels participate in almost all aspects of physiology and play a critical role in diverse processes such as nerve and muscle excitation/relaxation, hormone secretion, sensory transduction, regulation of blood pressure, and cell proliferation. Because of the physiological importance of ion channels, they are involved in a wide range of pathologies spanning all major therapeutic areas. Currently, there are over 60 different inherited ion channel disorders known as “channelopathies” [286], making ion channels the second most popular drug targets after G-protein-coupled receptors [287]. However, the challenge for channelopathy drug development is the lack of electrophysiological high-throughput platforms.

Attempts to automate manual patch clamping started 30 years ago, and several automated electrophysiology platforms have been developed. For example, Robocyte and OpusXpress were made for *Xenopus* oocytes electrophysiological screening, and AutoPatch, Flyscreen and RoboPatch were invented for mammalian cells. Later, the need for higher throughput pushed the development of planar array based automated electrophysiology platforms that can record different channels in parallel. Lastly, the intention to screen drugs through higher level models such as neuronal networks

promoted the birth of MEA. For example, MEA has been used on iPSC derived cardiomyocytes to test over 30 drugs for prediction of chemical induced arrhythmia [226]. However, pharmacology studies pose additional challenges than toxicity assays due to the requirement to test multiple doses, and the large n numbers necessary to capture the effect size, which is smaller than that seen in toxicity.

In our study, it was important to assess the impact of drugs that are already in clinical use and compare the effects of MEA analysis to observations from the clinic. In this regard, the fact that the two *in vitro* models showed different sensitivity to PHT, which is consistent with clinical observation, indicated that these *in vitro* models are a good predictors of drug efficacy and could be useful for drug screening and development of novel therapies.

6.3 What is the mechanism and potential treatment for *SCN2A* DEE?

6.3.2 How can GoF and LoF variant of *SCN2A* both cause DEE in patients?

$Na_v1.2$ is mainly present in excitatory neurons and is essential for the generation and propagation of action potentials early in life. The GoF of $Na_v1.2$ therefore results in highly excitable neurons, and causes hyperexcitability in neuronal networks that leads to seizures in DEE patients. In contrast, LoF of $Na_v1.2$ may reduce bursting and decrease dendritic excitability that causes insufficient synaptic strength [253], thus affecting the formation and maturation of cortical circuits [249]. Later in life, when $Na_v1.6$ takes over the responsibility for generating action potentials, seizures occur in the malfunctioning brain circuits of DEE patients. An alternative hypothesis suggests an imbalance in excitatory/inhibitory inputs based on the expression of $Na_v1.2$ channels in axons of unmyelinated mossy fibres in mature brains [92, 156, 237]. Because mossy fibres predominately target inhibitory basket cells [254], LoF $Na_v1.2$ channels would decrease the activity of mossy fibres that lead to inhibitory input reduction, and therefore can cause hyperexcitability in brain.

6.3.2 How can potassium channel drugs be beneficial for *SCN2A* DEE?

Although not fully understood, the role of K_v7 channels could be to regulate the function of Na_v channels [261]. These channels are responsible for M current, which is critical in controlling neuronal excitability [268]. They contribute to the medium and slow afterhyperpolarizations of action potentials caused by bursts [269-271], as well as regulating resting membrane potential and synaptic functions [268, 269, 271-273]. RTG primarily acts as a potassium channel opener for $K_v7.2$-7.5 channels, creating a hyperpolarizing shift in the activation of these channels by stabilizing the open channels [273]. In networks carrying *SCN2A* GoF variant, apart from the afterdepolarization, the I_{NaP} caused by repetitive firing can also be counteracted by the enhanced M current. Therefore, RTG supressed the firings and bursts in GoF cultures. In networks carrying *SCN2A* LoF variant, RTG stabilized the opened K_v7 channels and therefore hyperpolarized the resting membrane potential, resulted in rescuing voltage-gated sodium channels from slow inactivation which led to raising the number of available sodium channels and eventually increasing the excitability of neurons.

6.4 Limitations and future directions

My hypothesis was that MEA can be used to identify the *in vitro* phenotype of *SCN2A* DEE and find potential drug therapies. This study validated MEA as a rapid and effective tool for analysing phenotypically different transgenic mouse models. However, some limitations have also been identified: it is not a high throughput method yet, and it requires large n numbers and the establishment of transgenic mouse models. In future studies, we would like to compare the effects of compounds assessed on MEA with the data obtained from *in vivo* analysis in mice and also develop a robust MEA method for iPSC derived neurons. Moreover, it would be interesting to test the regularity in isolated spike activity [288].

6.3.1 Can human iPSC derived cellular models be successfully analysed on MEA?

While the potential of modelling disease using cellular cultures on MEA - from (drug) induced cells, cells obtained from transgenic animals, or cells derived from human iPSCs - is very attractive, this study points at some limitations of such approaches, mainly in regard to reproducibility. In this study using mouse cortical cultures, a robust method was established and showed that the variability can be overcome with proper method development, good controls, and larger n numbers. The applicability of these findings in the context of iPSC-derived models needs further consideration.

iPSC-derived cardiomyocytes have proved to be reliable on MEA in different labs all over the world, including Japan [213], US [289], UK [290] and Netherlands [195]. Furthermore, an inter-facility study performed by well-trained individuals following a standardized protocol after detailed demonstration showed no meaningful qualitative inter-facility variability for the 7 compounds tested among 5 facilities [226]. Whether these ranges of variation are within acceptable limits is still arguable, but the study showed the potential of MEA as a platform for human iPSC models. In addition, Kawatou et. al successfully modelled arrhythmias on MEA using 3D heart tissue that containing a mixture of human iPSC derived cardiomyocytes and non-myocytes [291].

However, the performance of iPSC derived neurons on MEA is not as impressive as that of cardiomyocytes or primary rodent cultures. The challenge for iPSC derived neuronal MEA studies is the maturation of neurons and their ability to form a synchronized network. In literature, probably the most active cultures to date were seen from a Japanese group that analysed human iPSC derived cerebral cortical neurons using the Dual SMAD inhibition protocol from Axol Bioscience Inc. [214]. From the data shown, the firing rate of the cultures increased from week 2 and reached a plateau from week 18, while the synchronized network bursting increased from week 13. The first disadvantage is the long culturing period of iPSC derived neurons can be required prior to cultures displaying synchronized bursting, compared to the 2 weeks in primary mouse cultures. A US group studying epilepsy related *KCNT1* variant studied the activity at DIV11 post plating neurons and found that a variant increased the excitability as well as the synchronicity while shortening the duration of bursts. These neurons were differentiated from human iPSCs by FUJIFILM Cellular Dynamics Inc. [292]. However, from the representative

raster plots of MEA, network bursts were not seen, lacking one of the most important elements. Two autism studies were reported using astrocytes co-cultured with iPSC derived neurons produced by NGN2 induction [283, 284]. The recording period was between weeks 4 and 8. However, as observed from the representative raster plots, almost half of the electrodes were not active. Thus, better methods for iPSC derived neurons on MEA need to be developed before large scale applications are undertaken.

6.3.2 Can MEA be used to study other disorders?

MEA has also been used to model other neurological and cardiac disorders. For example, impaired long-term potentiation (LTP) was observed from MEA analysis of hippocampal slices obtained from Alzheimer's disease transgenic mouse models [293]. In another Alzheimer study using rat primary hippocampal neurons, the interneurons and pyramidal neurons showed different phenotypes/firing patterns after being induced by Aβ oligomers, and spatial firing patterns mapping and cross-correlation were used to evaluate the degeneration of network connectivity [294]. Autism disorder was also studied by MEA on valproic acid (VPA) induced rat lateral amygdaloid nucleus slices and found to show hyperreactivity and hyperplasticity after stimulation [295]. As for cardiac disorders, arrhythmia has been modelled on MEA by many different labs globally. And to describe the phenotype of arrhythmia on MEA, parameters regarding the beat interval [289] and the quantification of I_{Na} modulation, prolongation and triangulation [195] were developed. These studies demonstrate that MEA can not only be used to model epilepsy disorders, but also other diseases relate to excitable cells.

6.5 Conclusion

My thesis has shown that MEA can be used to model DEE disorders following adequate method optimization. Network analysis of early and late seizure onset *SCN2A* DEE variants were consistent with previous single cell patching studies, showing increased excitability in cultures carrying early onset variant p.R1882Q and decreased excitability in cultures carrying late onset variant p.R853Q. Compared to other models, the MEA *in vitro* models showed clear phenotypes and provided further information into functional

parameters such as network synchronization. Moreover, pharmacological results were consistent with the clinical observations for the two clinically tested drugs and suggested RTG as a potential treatment for both early and late seizure onset *SCN2A* DEE patients. The workflow developed here may be applied to studies of different diseases.

Bibliography

1. Hesdorffer, D.C., et al., *Estimating risk for developing epilepsy: a population-based study in Rochester, Minnesota.* Neurology, 2011. 76(1): p. 23-7.
2. Sveinsson, O., et al., *The incidence of SUDEP: A nationwide population-based cohort study.* Neurology, 2017. 89(2): p. 170-177.
3. Kobau, R., et al., *Epilepsy surveillance among adults--19 States, Behavioral Risk Factor Surveillance System, 2005.* MMWR Surveill Summ, 2008. 57(6): p. 1-20.
4. Yoon, D., et al., *Economic impact of epilepsy in the United States.* Epilepsia, 2009. 50(10): p. 2186-91.
5. Maljevic, S., C.A. Reid, and S. Petrou, *Models for discovery of targeted therapy in genetic epileptic encephalopathies.* J Neurochem, 2017. 143(1): p. 30-48.
6. Falco-Walter, J.J., I.E. Scheffer, and R.S. Fisher, *The new definition and classification of seizures and epilepsy.* Epilepsy Res, 2018. 139: p. 73-79.
7. Brodie, M.J., et al., *The 2017 ILAE classification of seizure types and the epilepsies: what do people with epilepsy and their caregivers need to know?* Epileptic Disord, 2018. 20(2): p. 77-87.
8. epilepsy, I.l.a. *EpilepsyDiagnosis.org*. 2019; Available from: www.epilepsydiagnosis.org.
9. Luders, H., et al., *Semiological seizure classification.* Epilepsia, 1998. 39(9): p. 1006-13.
10. Scheffer, I.E., et al., *ILAE classification of the epilepsies: Position paper of the ILAE Commission for Classification and Terminology.* Epilepsia, 2017. 58(4): p. 512-521.
11. Berg, A.T., et al., *Revised terminology and concepts for organization of seizures and epilepsies: report of the ILAE Commission on Classification and Terminology, 2005-2009.* Epilepsia, 2010. 51(4): p. 676-85.
12. Hildebrand, M.S., et al., *Recent advances in the molecular genetics of epilepsy.* J Med Genet, 2013. 50(5): p. 271-9.
13. Waxman, S.G. and G.W. Zamponi, *Regulating excitability of peripheral afferents: emerging ion channel targets.* Nat Neurosci, 2014. 17(2): p. 153-63.
14. Meisler, M.H. and J.A. Kearney, *Sodium channel mutations in epilepsy and other neurological disorders.* J Clin Invest, 2005. 115(8): p. 2010-7.
15. Wulff, H., N.A. Castle, and L.A. Pardo, *Voltage-gated potassium channels as therapeutic targets.* Nat Rev Drug Discov, 2009. 8(12): p. 982-1001.
16. Kearney, J.A., et al., *A gain-of-function mutation in the sodium channel gene Scn2a results in seizures and behavioral abnormalities.* Neuroscience, 2001. 102(2): p. 307-17.
17. Ben-Shalom, R., et al., *Opposing Effects on NaV1.2 Function Underlie Differences Between SCN2A Variants Observed in Individuals With Autism Spectrum Disorder or Infantile Seizures.* Biol Psychiatry, 2017. 82(3): p. 224-232.

18. Estacion, M., et al., *A novel de novo mutation of SCN8A (Nav1.6) with enhanced channel activation in a child with epileptic encephalopathy.* Neurobiol Dis, 2014. 69: p. 117-23.
19. Lopez-Santiago, L.F., et al., *Neuronal hyperexcitability in a mouse model of SCN8A epileptic encephalopathy.* Proc Natl Acad Sci U S A, 2017. 114(9): p. 2383-2388.
20. Mantegazza, M., et al., *Identification of an Nav1.1 sodium channel (SCN1A) loss-of-function mutation associated with familial simple febrile seizures.* Proc Natl Acad Sci U S A, 2005. 102(50): p. 18177-82.
21. Ohmori, I., et al., *Nonfunctional SCN1A is common in severe myoclonic epilepsy of infancy.* Epilepsia, 2006. 47(10): p. 1636-42.
22. Saitsu, H., et al., *De novo mutations in the gene encoding STXBP1 (MUNC18-1) cause early infantile epileptic encephalopathy.* Nat Genet, 2008. 40(6): p. 782-8.
23. Deprez, L., et al., *Clinical spectrum of early-onset epileptic encephalopathies associated with STXBP1 mutations.* Neurology, 2010. 75(13): p. 1159-65.
24. Saitsu, H., et al., *STXBP1 mutations in early infantile epileptic encephalopathy with suppression-burst pattern.* Epilepsia, 2010. 51(12): p. 2397-405.
25. Carvill, G.L., et al., *Targeted resequencing in epileptic encephalopathies identifies de novo mutations in CHD2 and SYNGAP1.* Nat Genet, 2013. 45(7): p. 825-30.
26. Berryer, M.H., et al., *Mutations in SYNGAP1 cause intellectual disability, autism, and a specific form of epilepsy by inducing haploinsufficiency.* Hum Mutat, 2013. 34(2): p. 385-94.
27. Reid, C.A., et al., *Can mutation-mediated effects occurring early in development cause long-term seizure susceptibility in genetic generalized epilepsies?* Epilepsia, 2018. 59(5): p. 915-922.
28. Shen, J., et al., *Mutations in PNKP cause microcephaly, seizures and defects in DNA repair.* Nat Genet, 2010. 42(3): p. 245-9.
29. McKenzie, O., et al., *Aristaless-related homeobox gene, the gene responsible for West syndrome and related disorders, is a Groucho/transducin-like enhancer of split dependent transcriptional repressor.* Neuroscience, 2007. 146(1): p. 236-47.
30. Falace, A., et al., *TBC1D24 regulates neuronal migration and maturation through modulation of the ARF6-dependent pathway.* Proc Natl Acad Sci U S A, 2014. 111(6): p. 2337-42.
31. Steinlein, O.K., et al., *A missense mutation in the neuronal nicotinic acetylcholine receptor alpha 4 subunit is associated with autosomal dominant nocturnal frontal lobe epilepsy.* Nat Genet, 1995. 11(2): p. 201-3.
32. Allen, A.S., et al., *De novo mutations in epileptic encephalopathies.* Nature, 2013. 501(7466): p. 217-21.
33. Reid, C.A., et al., *New therapeutic opportunities in epilepsy: a genetic perspective.* Pharmacol Ther, 2010. 128(2): p. 274-80.
34. Escayg, A., et al., *Mutations of SCN1A, encoding a neuronal sodium channel, in two families with GEFS+2.* Nat Genet, 2000. 24(4): p. 343-5.
35. Gerard, F., et al., *Clinical and genetic analysis of a new multigenerational pedigree with GEFS+ (Generalized Epilepsy with Febrile Seizures Plus).* Epilepsia, 2002. 43(6): p. 581-6.

36. Marini, C., et al., *Genetic architecture of idiopathic generalized epilepsy: clinical genetic analysis of 55 multiplex families.* Epilepsia, 2004. 45(5): p. 467-78.
37. Winawer, M.R., et al., *Familial clustering of seizure types within the idiopathic generalized epilepsies.* Neurology, 2005. 65(4): p. 523-8.
38. Kinirons, P., et al., *Phenotypic concordance in 70 families with IGE-implications for genetic studies of epilepsy.* Epilepsy Res, 2008. 82(1): p. 21-28.
39. *Genetic determinants of common epilepsies: a meta-analysis of genome-wide association studies.* Lancet Neurol, 2014. 13(9): p. 893-903.
40. *Genome-wide mega-analysis identifies 16 loci and highlights diverse biological mechanisms in the common epilepsies.* Nat Commun, 2018. 9(1): p. 5269.
41. *Ultra-rare genetic variation in common epilepsies: a case-control sequencing study.* Lancet Neurol, 2017. 16(2): p. 135-143.
42. Rodrigues-Pinguet, N., et al., *Five ADNFLE mutations reduce the Ca2+ dependence of the mammalian alpha4beta2 acetylcholine response.* J Physiol, 2003. 550(Pt 1): p. 11-26.
43. Kalachikov, S., et al., *Mutations in LGI1 cause autosomal-dominant partial epilepsy with auditory features.* Nat Genet, 2002. 30(3): p. 335-41.
44. Senechal, K.R., C. Thaller, and J.L. Noebels, *ADPEAF mutations reduce levels of secreted LGI1, a putative tumor suppressor protein linked to epilepsy.* Hum Mol Genet, 2005. 14(12): p. 1613-20.
45. Howell, K.B., et al., *A population-based cost-effectiveness study of early genetic testing in severe epilepsies of infancy.* Epilepsia, 2018. 59(6): p. 1177-1187.
46. McTague, A., et al., *The genetic landscape of the epileptic encephalopathies of infancy and childhood.* Lancet Neurol, 2016. 15(3): p. 304-16.
47. Yamatogi, Y. and S. Ohtahara, *Early-infantile epileptic encephalopathy with suppression-bursts, Ohtahara syndrome; its overview referring to our 16 cases.* Brain Dev, 2002. 24(1): p. 13-23.
48. Ohtahara, S. and Y. Yamatogi, *Ohtahara syndrome: with special reference to its developmental aspects for differentiating from early myoclonic encephalopathy.* Epilepsy Res, 2006. 70 Suppl 1: p. S58-67.
49. Beal, J.C., K. Cherian, and S.L. Moshe, *Early-onset epileptic encephalopathies: Ohtahara syndrome and early myoclonic encephalopathy.* Pediatr Neurol, 2012. 47(5): p. 317-23.
50. Jeavons, P.M., B.D. Bower, and M. Dimitrakoudi, *Long-term prognosis of 150 cases of "West syndrome".* Epilepsia, 1973. 14(2): p. 153-64.
51. Lux, A.L. and J.P. Osborne, *A proposal for case definitions and outcome measures in studies of infantile spasms and West syndrome: consensus statement of the West Delphi group.* Epilepsia, 2004. 45(11): p. 1416-28.
52. Motte, J., et al., *Lamotrigine for generalized seizures associated with the Lennox-Gastaut syndrome. Lamictal Lennox-Gastaut Study Group.* N Engl J Med, 1997. 337(25): p. 1807-12.
53. Markand, O.N., *Lennox-Gastaut syndrome (childhood epileptic encephalopathy).* J Clin Neurophysiol, 2003. 20(6): p. 426-41.
54. Arzimanoglou, A., et al., *Lennox-Gastaut syndrome: a consensus approach on diagnosis, assessment, management, and trial methodology.* Lancet Neurol, 2009. 8(1): p. 82-93.

55. Wolff, M., C. Casse-Perrot, and C. Dravet, *Severe myoclonic epilepsy of infants (Dravet syndrome): natural history and neuropsychological findings.* Epilepsia, 2006. 47 Suppl 2: p. 45-8.
56. Dravet, C., *The core Dravet syndrome phenotype.* Epilepsia, 2011. 52 Suppl 2: p. 3-9.
57. Palmini, A., et al., *Focal neuronal migration disorders and intractable partial epilepsy: a study of 30 patients.* Ann Neurol, 1991. 30(6): p. 741-9.
58. Coppola, G., et al., *Migrating partial seizures in infancy: a malignant disorder with developmental arrest.* Epilepsia, 1995. 36(10): p. 1017-24.
59. Coppola, G., *Malignant migrating partial seizures in infancy: an epilepsy syndrome of unknown etiology.* Epilepsia, 2009. 50 Suppl 5: p. 49-51.
60. Oguni, H., et al., *Treatment and long-term prognosis of myoclonic-astatic epilepsy of early childhood.* Neuropediatrics, 2002. 33(3): p. 122-32.
61. Kelley, S.A. and E.H. Kossoff, *Doose syndrome (myoclonic-astatic epilepsy): 40 years of progress.* Dev Med Child Neurol, 2010. 52(11): p. 988-93.
62. Ohtahara, S., et al., *Prenatal etiologies of West syndrome.* Epilepsia, 1993. 34(4): p. 716-22.
63. Kurokawa, T., et al., *West syndrome and Lennox-Gastaut syndrome: a survey of natural history.* Pediatrics, 1980. 65(1): p. 81-8.
64. Claes, L., et al., *De novo mutations in the sodium-channel gene SCN1A cause severe myoclonic epilepsy of infancy.* Am J Hum Genet, 2001. 68(6): p. 1327-32.
65. Ostrander, B.E.P., et al., *Whole-genome analysis for effective clinical diagnosis and gene discovery in early infantile epileptic encephalopathy.* NPJ Genom Med, 2018. 3: p. 22.
66. Roizen, N.J. and D. Patterson, *Down's syndrome.* Lancet, 2003. 361(9365): p. 1281-9.
67. Stosser, M.B., et al., *High frequency of mosaic pathogenic variants in genes causing epilepsy-related neurodevelopmental disorders.* Genet Med, 2018. 20(4): p. 403-410.
68. Halvorsen, M., et al., *Mosaic mutations in early-onset genetic diseases.* Genet Med, 2016. 18(7): p. 746-9.
69. Depienne, C., et al., *Sporadic infantile epileptic encephalopathy caused by mutations in PCDH19 resembles Dravet syndrome but mainly affects females.* PLoS Genet, 2009. 5(2): p. e1000381.
70. Terracciano, A., et al., *PCDH19-related epilepsy in two mosaic male patients.* Epilepsia, 2016. 57(3): p. e51-5.
71. Depienne, C. and E. LeGuern, *PCDH19-related infantile epileptic encephalopathy: an unusual X-linked inheritance disorder.* Hum Mutat, 2012. 33(4): p. 627-34.
72. Thiffault, I., et al., *PCDH19-related epileptic encephalopathy in a male mosaic for a truncating variant.* Am J Med Genet A, 2016. 170(6): p. 1585-9.
73. Weckhuysen, S., et al., *KCNQ2 encephalopathy: emerging phenotype of a neonatal epileptic encephalopathy.* Ann Neurol, 2012. 71(1): p. 15-25.
74. Marini, C., et al., *Mosaic SCN1A mutation in familial severe myoclonic epilepsy of infancy.* Epilepsia, 2006. 47(10): p. 1737-40.
75. Selmer, K.K., et al., *Parental SCN1A mutation mosaicism in familial Dravet syndrome.* Clin Genet, 2009. 76(4): p. 398-403.

76. Sun, H., et al., *Analysis of SCN1A mutation and parental origin in patients with Dravet syndrome.* J Hum Genet, 2010. 55(7): p. 421-7.
77. Zerem, A., et al., *Paternal germline mosaicism of a SCN2A mutation results in Ohtahara syndrome in half siblings.* Eur J Paediatr Neurol, 2014. 18(5): p. 567-71.
78. Milh, M., et al., *Variable clinical expression in patients with mosaicism for KCNQ2 mutations.* Am J Med Genet A, 2015. 167a(10): p. 2314-8.
79. Marini, C., et al., *The genetics of Dravet syndrome.* Epilepsia, 2011. 52 Suppl 2: p. 24-9.
80. Depienne, C., et al., *Spectrum of SCN1A gene mutations associated with Dravet syndrome: analysis of 333 patients.* J Med Genet, 2009. 46(3): p. 183-91.
81. Ogiwara, I., et al., *A homozygous mutation of voltage-gated sodium channel beta(I) gene SCN1B in a patient with Dravet syndrome.* Epilepsia, 2012. 53(12): p. e200-3.
82. Shi, X., et al., *Missense mutation of the sodium channel gene SCN2A causes Dravet syndrome.* Brain Dev, 2009. 31(10): p. 758-62.
83. Nava, C., et al., *De novo mutations in HCN1 cause early infantile epileptic encephalopathy.* Nat Genet, 2014. 46(6): p. 640-5.
84. Carvill, G.L., et al., *GABRA1 and STXBP1: novel genetic causes of Dravet syndrome.* Neurology, 2014. 82(14): p. 1245-53.
85. Ishii, A., et al., *Association of nonsense mutation in GABRG2 with abnormal trafficking of GABAA receptors in severe epilepsy.* Epilepsy Res, 2014. 108(3): p. 420-32.
86. Le, S.V., et al., *A mutation in GABRB3 associated with Dravet syndrome.* Am J Med Genet A, 2017. 173(8): p. 2126-2131.
87. Escayg, A., et al., *A novel SCN1A mutation associated with generalized epilepsy with febrile seizures plus--and prevalence of variants in patients with epilepsy.* Am J Hum Genet, 2001. 68(4): p. 866-73.
88. Annesi, G., et al., *Two novel SCN1A missense mutations in generalized epilepsy with febrile seizures plus.* Epilepsia, 2003. 44(9): p. 1257-8.
89. Scheffer, I.E. and S.F. Berkovic, *Generalized epilepsy with febrile seizures plus. A genetic disorder with heterogeneous clinical phenotypes.* Brain, 1997. 120 (Pt 3): p. 479-90.
90. Wallace, R.H., et al., *Sodium channel alpha1-subunit mutations in severe myoclonic epilepsy of infancy and infantile spasms.* Neurology, 2003. 61(6): p. 765-9.
91. Pierson, T.M., et al., *GRIN2A mutation and early-onset epileptic encephalopathy: personalized therapy with memantine.* Ann Clin Transl Neurol, 2014. 1(3): p. 190-198.
92. Wolff, M., et al., *Genetic and phenotypic heterogeneity suggest therapeutic implications in SCN2A-related disorders.* Brain, 2017. 140(5): p. 1316-1336.
93. Wang, J., et al., *Epilepsy-associated genes.* Seizure, 2017. 44: p. 11-20.
94. Bhattacharjee, A., et al., *Slick (Slo2.1), a rapidly-gating sodium-activated potassium channel inhibited by ATP.* J Neurosci, 2003. 23(37): p. 11681-91.
95. Yang, B., et al., *Pharmacological activation and inhibition of Slack (Slo2.2) channels.* Neuropharmacology, 2006. 51(4): p. 896-906.
96. Milligan, C.J., et al., *KCNT1 gain of function in 2 epilepsy phenotypes is reversed by quinidine.* Ann Neurol, 2014. 75(4): p. 581-90.

97. Mikati, M.A., et al., *Quinidine in the treatment of KCNT1-positive epilepsies.* Ann Neurol, 2015. 78(6): p. 995-9.
98. Fukuoka, M., et al., *Quinidine therapy for West syndrome with KCNTI mutation: A case report.* Brain Dev, 2017. 39(1): p. 80-83.
99. Chong, P.F., et al., *Ineffective quinidine therapy in early onset epileptic encephalopathy with KCNT1 mutation.* Ann Neurol, 2016. 79(3): p. 502-3.
100. Mullen, S.A., et al., *Precision therapy for epilepsy due to KCNT1 mutations: A randomized trial of oral quinidine.* Neurology, 2018. 90(1): p. e67-e72.
101. Ihara, Y., et al., *Retigabine, a Kv7.2/Kv7.3-Channel Opener, Attenuates Drug-Induced Seizures in Knock-In Mice Harboring Kcnq2 Mutations.* PLoS One, 2016. 11(2): p. e0150095.
102. Gunthorpe, M.J., C.H. Large, and R. Sankar, *The mechanism of action of retigabine (ezogabine), a first-in-class K+ channel opener for the treatment of epilepsy.* Epilepsia, 2012. 53(3): p. 412-24.
103. Clark, S., A. Antell, and K. Kaufman, *New antiepileptic medication linked to blue discoloration of the skin and eyes.* Ther Adv Drug Saf, 2015. 6(1): p. 15-9.
104. Kalappa, B.I., et al., *Potent KCNQ2/3-specific channel activator suppresses in vivo epileptic activity and prevents the development of tinnitus.* J Neurosci, 2015. 35(23): p. 8829-42.
105. Finkel, R.S., et al., *Treatment of infantile-onset spinal muscular atrophy with nusinersen: a phase 2, open-label, dose-escalation study.* Lancet, 2016. 388(10063): p. 3017-3026.
106. Hua, Y., et al., *Peripheral SMN restoration is essential for long-term rescue of a severe spinal muscular atrophy mouse model.* Nature, 2011. 478(7367): p. 123-6.
107. Hsiao, J., et al., *Upregulation of Haploinsufficient Gene Expression in the Brain by Targeting a Long Non-coding RNA Improves Seizure Phenotype in a Model of Dravet Syndrome.* EBioMedicine, 2016. 9: p. 257-277.
108. Sepp-Lorenzino, L. and M. Ruddy, *Challenges and opportunities for local and systemic delivery of siRNA and antisense oligonucleotides.* Clin Pharmacol Ther, 2008. 84(5): p. 628-32.
109. Zhao, X., et al., *Controlled delivery of antisense oligonucleotides: a brief review of current strategies.* Expert Opin Drug Deliv, 2009. 6(7): p. 673-86.
110. Oyrer, J., et al., *Ion Channels in Genetic Epilepsy: From Genes and Mechanisms to Disease-Targeted Therapies.* Pharmacol Rev, 2018. 70(1): p. 142-173.
111. Armstrong, C.M. and B. Hille, *Voltage-gated ion channels and electrical excitability.* Neuron, 1998. 20(3): p. 371-80.
112. Schwartzkroin, P.A., S.C. Baraban, and D.W. Hochman, *Osmolarity, ionic flux, and changes in brain excitability.* Epilepsy Res, 1998. 32(1-2): p. 275-85.
113. Somlyo, A.P. and A.V. Somlyo, *Signal transduction and regulation in smooth muscle.* Nature, 1994. 372(6503): p. 231-6.
114. Lagnado, L. and D. Baylor, *Signal flow in visual transduction.* Neuron, 1992. 8(6): p. 995-1002.
115. Lang, F., et al., *Ion channels in cell proliferation and apoptotic cell death.* J Membr Biol, 2005. 205(3): p. 147-57.
116. Schwab, A., et al., *Role of ion channels and transporters in cell migration.* Physiol Rev, 2012. 92(4): p. 1865-913.

117. Jia, L., et al., *Inhibition of Calcium-Activated Chloride Channel ANO1/TMEM16A Suppresses Tumor Growth and Invasion in Human Lung Cancer.* PLoS One, 2015. 10(8): p. e0136584.
118. Kaplan, D.I., L.L. Isom, and S. Petrou, *Role of Sodium Channels in Epilepsy.* Cold Spring Harb Perspect Med, 2016. 6(6).
119. Catterall, W.A., *Structure and function of voltage-sensitive ion channels.* Science, 1988. 242(4875): p. 50-61.
120. Hodgkin, A.L. and A.F. Huxley, *A quantitative description of membrane current and its application to conduction and excitation in nerve.* J Physiol, 1952. 117(4): p. 500-44.
121. Armstrong, C.M., *Sodium channels and gating currents.* Physiol Rev, 1981. 61(3): p. 644-83.
122. Oliva, M., S.F. Berkovic, and S. Petrou, *Sodium channels and the neurobiology of epilepsy.* Epilepsia, 2012. 53(11): p. 1849-59.
123. Raman, I.M., et al., *Altered subthreshold sodium currents and disrupted firing patterns in Purkinje neurons of Scn8a mutant mice.* Neuron, 1997. 19(4): p. 881-91.
124. Hartshorne, R.P. and W.A. Catterall, *Purification of the saxitoxin receptor of the sodium channel from rat brain.* Proc Natl Acad Sci U S A, 1981. 78(7): p. 4620-4.
125. Hartshorne, R.P., et al., *The saxitoxin receptor of the sodium channel from rat brain. Evidence for two nonidentical beta subunits.* J Biol Chem, 1982. 257(23): p. 13888-91.
126. Noda, M., et al., *Primary structure of Electrophorus electricus sodium channel deduced from cDNA sequence.* Nature, 1984. 312(5990): p. 121-7.
127. Guy, H.R. and P. Seetharamulu, *Molecular model of the action potential sodium channel.* Proc Natl Acad Sci U S A, 1986. 83(2): p. 508-12.
128. Stuhmer, W., et al., *Structural parts involved in activation and inactivation of the sodium channel.* Nature, 1989. 339(6226): p. 597-603.
129. Kontis, K.J., A. Rounaghi, and A.L. Goldin, *Sodium channel activation gating is affected by substitutions of voltage sensor positive charges in all four domains.* J Gen Physiol, 1997. 110(4): p. 391-401.
130. Shapiro, L., et al., *Crystal structure of the extracellular domain from P0, the major structural protein of peripheral nerve myelin.* Neuron, 1996. 17(3): p. 435-49.
131. Yang, N., A.L. George, Jr., and R. Horn, *Molecular basis of charge movement in voltage-gated sodium channels.* Neuron, 1996. 16(1): p. 113-22.
132. Zhou, Y.Y., et al., *Stabilization of a channel's open state by a hydrophobic residue in the sixth membrane-spanning segment (S6) of rKv1.4.* Pflugers Arch, 1998. 437(1): p. 114-22.
133. Heinemann, S.H., et al., *Calcium channel characteristics conferred on the sodium channel by single mutations.* Nature, 1992. 356(6368): p. 441-3.
134. Goldin, A.L., et al., *Nomenclature of voltage-gated sodium channels.* Neuron, 2000. 28(2): p. 365-8.
135. Noda, M., et al., *Existence of distinct sodium channel messenger RNAs in rat brain.* Nature, 1986. 320(6058): p. 188-92.
136. Kayano, T., et al., *Primary structure of rat brain sodium channel III deduced from the cDNA sequence.* FEBS Lett, 1988. 228(1): p. 187-94.

137. Schaller, K.L., et al., *A novel, abundant sodium channel expressed in neurons and glia.* J Neurosci, 1995. 15(5 Pt 1): p. 3231-42.
138. Burgess, D.L., et al., *Mutation of a new sodium channel gene, Scn8a, in the mouse mutant 'motor endplate disease'.* Nat Genet, 1995. 10(4): p. 461-5.
139. Sangameswaran, L., et al., *A novel tetrodotoxin-sensitive, voltage-gated sodium channel expressed in rat and human dorsal root ganglia.* J Biol Chem, 1997. 272(23): p. 14805-9.
140. Akopian, A.N., L. Sivilotti, and J.N. Wood, *A tetrodotoxin-resistant voltage-gated sodium channel expressed by sensory neurons.* Nature, 1996. 379(6562): p. 257-62.
141. Dib-Hajj, S.D., et al., *Two tetrodotoxin-resistant sodium channels in human dorsal root ganglion neurons.* FEBS Lett, 1999. 462(1-2): p. 117-20.
142. Trimmer, J.S., et al., *Primary structure and functional expression of a mammalian skeletal muscle sodium channel.* Neuron, 1989. 3(1): p. 33-49.
143. Rogart, R.B., et al., *Molecular cloning of a putative tetrodotoxin-resistant rat heart Na+ channel isoform.* Proc Natl Acad Sci U S A, 1989. 86(20): p. 8170-4.
144. George, A.L., Jr., T.J. Knittle, and M.M. Tamkun, *Molecular cloning of an atypical voltage-gated sodium channel expressed in human heart and uterus: evidence for a distinct gene family.* Proc Natl Acad Sci U S A, 1992. 89(11): p. 4893-7.
145. Felipe, A., et al., *Primary structure and differential expression during development and pregnancy of a novel voltage-gated sodium channel in the mouse.* J Biol Chem, 1994. 269(48): p. 30125-31.
146. Patton, D.E., et al., *The adult rat brain beta 1 subunit modifies activation and inactivation gating of multiple sodium channel alpha subunits.* J Biol Chem, 1994. 269(26): p. 17649-55.
147. Isom, L.L., et al., *Primary structure and functional expression of the beta 1 subunit of the rat brain sodium channel.* Science, 1992. 256(5058): p. 839-42.
148. Isom, L.L., et al., *Structure and function of the beta 2 subunit of brain sodium channels, a transmembrane glycoprotein with a CAM motif.* Cell, 1995. 83(3): p. 433-42.
149. Yu, F.H., et al., *Sodium channel beta4, a new disulfide-linked auxiliary subunit with similarity to beta2.* J Neurosci, 2003. 23(20): p. 7577-85.
150. Hinard, V., et al., *ICEPO: the ion channel electrophysiology ontology.* Database (Oxford), 2016. 2016.
151. Shen, H., et al., *Structure of a eukaryotic voltage-gated sodium channel at near-atomic resolution.* Science, 2017. 355(6328).
152. Pan, X., et al., *Molecular basis for pore blockade of human Na(+) channel Nav1.2 by the mu-conotoxin KIIIA.* Science, 2019. 363(6433): p. 1309-1313.
153. Lai, H.C. and L.Y. Jan, *The distribution and targeting of neuronal voltage-gated ion channels.* Nat Rev Neurosci, 2006. 7(7): p. 548-62.
154. Catterall, W.A., *Cellular and molecular biology of voltage-gated sodium channels.* Physiol Rev, 1992. 72(4 Suppl): p. S15-48.
155. Boiko, T., et al., *Compact myelin dictates the differential targeting of two sodium channel isoforms in the same axon.* Neuron, 2001. 30(1): p. 91-104.
156. Kaplan, M.R., et al., *Differential control of clustering of the sodium channels Na(v)1.2 and Na(v)1.6 at developing CNS nodes of Ranvier.* Neuron, 2001. 30(1): p. 105-19.

157. Hu, W., et al., *Distinct contributions of Na(v)1.6 and Na(v)1.2 in action potential initiation and backpropagation.* Nat Neurosci, 2009. 12(8): p. 996-1002.
158. Leterrier, C., et al., *Voltage-gated sodium channel organization in neurons: protein interactions and trafficking pathways.* Neurosci Lett, 2010. 486(2): p. 92-100.
159. Bouza, A.A. and L.L. Isom, *Voltage-Gated Sodium Channel beta Subunits and Their Related Diseases.* Handb Exp Pharmacol, 2018. 246: p. 423-450.
160. Nakamura, K., et al., *Clinical spectrum of SCN2A mutations expanding to Ohtahara syndrome.* Neurology, 2013. 81(11): p. 992-8.
161. Sundaram, S.K., et al., *SCN2A mutation is associated with infantile spasms and bitemporal glucose hypometabolism.* Pediatr Neurol, 2013. 49(1): p. 46-9.
162. Touma, M., et al., *Whole genome sequencing identifies SCN2A mutation in monozygotic twins with Ohtahara syndrome and unique neuropathologic findings.* Epilepsia, 2013. 54(5): p. e81-5.
163. Samanta, D. and R. Ramakrishnaiah, *De novo R853Q mutation of SCN2A gene and West syndrome.* Acta Neurol Belg, 2015. 115(4): p. 773-6.
164. Syrbe, S., et al., *Phenotypic Variability from Benign Infantile Epilepsy to Ohtahara Syndrome Associated with a Novel Mutation in SCN2A.* Mol Syndromol, 2016. 7(4): p. 182-188.
165. Hamdan, F.F., et al., *Mutations in SYNGAP1 in autosomal nonsyndromic mental retardation.* N Engl J Med, 2009. 360(6): p. 599-605.
166. Kim, G.E. and L.K. Kaczmarek, *Emerging role of the KCNT1 Slack channel in intellectual disability.* Front Cell Neurosci, 2014. 8: p. 209.
167. Bras, J., et al., *Mutations in PNKP cause recessive ataxia with oculomotor apraxia type 4.* Am J Hum Genet, 2015. 96(3): p. 474-9.
168. Poulton, C., et al., *Progressive cerebellar atrophy and polyneuropathy: expanding the spectrum of PNKP mutations.* Neurogenetics, 2013. 14(1): p. 43-51.
169. Hamdan, F.F., et al., *De novo STXBP1 mutations in mental retardation and nonsyndromic epilepsy.* Ann Neurol, 2009. 65(6): p. 748-53.
170. Chang, J., et al., *Genotype to phenotype relationships in autism spectrum disorders.* Nat Neurosci, 2015. 18(2): p. 191-8.
171. Heron, S.E., et al., *Sodium-channel defects in benign familial neonatal-infantile seizures.* Lancet, 2002. 360(9336): p. 851-2.
172. Scalmani, P., et al., *Effects in neocortical neurons of mutations of the Na(v)1.2 Na+ channel causing benign familial neonatal-infantile seizures.* J Neurosci, 2006. 26(40): p. 10100-9.
173. Herlenius, E., et al., *SCN2A mutations and benign familial neonatal-infantile seizures: the phenotypic spectrum.* Epilepsia, 2007. 48(6): p. 1138-42.
174. Ogiwara, I., et al., *De novo mutations of voltage-gated sodium channel alphaII gene SCN2A in intractable epilepsies.* Neurology, 2009. 73(13): p. 1046-53.
175. Howell, K.B., et al., *SCN2A encephalopathy: A major cause of epilepsy of infancy with migrating focal seizures.* Neurology, 2015. 85(11): p. 958-66.
176. Berecki, G., et al., *Dynamic action potential clamp predicts functional separation in mild familial and severe de novo forms of SCN2A epilepsy.* Proc Natl Acad Sci U S A, 2018. 115(24): p. E5516-e5525.

177. Misra, S.N., K.M. Kahlig, and A.L. George, Jr., *Impaired NaV1.2 function and reduced cell surface expression in benign familial neonatal-infantile seizures.* Epilepsia, 2008. 49(9): p. 1535-45.
178. Yamashita, S., et al., *Mislocalization of syntaxin-1 and impaired neurite growth observed in a human iPSC model for STXBP1-related epileptic encephalopathy.* Epilepsia, 2016. 57(4): p. e81-6.
179. Feldt Muldoon, S., I. Soltesz, and R. Cossart, *Spatially clustered neuronal assemblies comprise the microstructure of synchrony in chronically epileptic networks.* Proc Natl Acad Sci U S A, 2013. 110(9): p. 3567-72.
180. Ferrea, E., et al., *Large-scale, high-resolution electrophysiological imaging of field potentials in brain slices with microelectronic multielectrode arrays.* Front Neural Circuits, 2012. 6: p. 80.
181. Rosch, R.E., et al., *Calcium imaging and dynamic causal modelling reveal brain-wide changes in effective connectivity and synaptic dynamics during epileptic seizures.* PLoS Comput Biol, 2018. 14(8): p. e1006375.
182. Meyer, M., et al., *Microarray Noninvasive Neuronal Seizure Recordings from Intact Larval Zebrafish.* PLoS One, 2016. 11(6): p. e0156498.
183. Baraban, S.C., M.T. Dinday, and G.A. Hortopan, *Drug screening in Scn1a zebrafish mutant identifies clemizole as a potential Dravet syndrome treatment.* Nat Commun, 2013. 4: p. 2410.
184. Hortopan, G.A., M.T. Dinday, and S.C. Baraban, *Zebrafish as a model for studying genetic aspects of epilepsy.* Dis Model Mech, 2010. 3(3-4): p. 144-8.
185. Baraban, S.C., et al., *A large-scale mutagenesis screen to identify seizure-resistant zebrafish.* Epilepsia, 2007. 48(6): p. 1151-7.
186. Afrikanova, T., et al., *Validation of the zebrafish pentylenetetrazol seizure model: locomotor versus electrographic responses to antiepileptic drugs.* PLoS One, 2013. 8(1): p. e54166.
187. Wong, K., et al., *Modeling seizure-related behavioral and endocrine phenotypes in adult zebrafish.* Brain Res, 2010. 1348: p. 209-15.
188. Loscher, W., *Critical review of current animal models of seizures and epilepsy used in the discovery and development of new antiepileptic drugs.* Seizure, 2011. 20(5): p. 359-68.
189. Frankel, W.N., *Detecting genes in new and old mouse models for epilepsy: a prospectus through the magnifying glass.* Epilepsy Res, 1999. 36(2-3): p. 97-110.
190. Ogiwara, I., et al., *Nav1.2 haplodeficiency in excitatory neurons causes absence-like seizures in mice.* Commun Biol, 2018. 1.
191. Yu, F.H., et al., *Reduced sodium current in GABAergic interneurons in a mouse model of severe myoclonic epilepsy in infancy.* Nat Neurosci, 2006. 9(9): p. 1142-9.
192. Wagnon, J.L., et al., *Convulsive seizures and SUDEP in a mouse model of SCN8A epileptic encephalopathy.* Hum Mol Genet, 2015. 24(2): p. 506-15.
193. Liao, Y., et al., *Molecular correlates of age-dependent seizures in an inherited neonatal-infantile epilepsy.* Brain, 2010. 133(Pt 5): p. 1403-14.
194. Kramer, M.A. and S.S. Cash, *Epilepsy as a disorder of cortical network organization.* Neuroscientist, 2012. 18(4): p. 360-72.
195. Tertoolen, L.G.J., et al., *Interpretation of field potentials measured on a multi electrode array in pharmacological toxicity screening on primary and human*

pluripotent stem cell-derived cardiomyocytes. Biochem Biophys Res Commun, 2018. 497(4): p. 1135-1141.
196. Varghese, K., et al., *A new target for amyloid beta toxicity validated by standard and high-throughput electrophysiology.* PLoS One, 2010. 5(1): p. e8643.
197. Novellino, A., et al., *Development of micro-electrode array based tests for neurotoxicity: assessment of interlaboratory reproducibility with neuroactive chemicals.* Front Neuroeng, 2011. 4: p. 4.
198. Spira, M.E. and A. Hai, *Multi-electrode array technologies for neuroscience and cardiology.* Nat Nanotechnol, 2013. 8(2): p. 83-94.
199. Maccione, A., et al., *A novel algorithm for precise identification of spikes in extracellularly recorded neuronal signals.* J Neurosci Methods, 2009. 177(1): p. 241-9.
200. Mendis, G.D., et al., *Use of adaptive network burst detection methods for multielectrode array data and the generation of artificial spike patterns for method evaluation.* J Neural Eng, 2016. 13(2): p. 026009.
201. Johnstone, A.F., et al., *Microelectrode arrays: a physiologically based neurotoxicity testing platform for the 21st century.* Neurotoxicology, 2010. 31(4): p. 331-50.
202. Barreto-Chang, O.L. and R.E. Dolmetsch, *Calcium imaging of cortical neurons using Fura-2 AM.* J Vis Exp, 2009(23).
203. Shew, W.L., T. Bellay, and D. Plenz, *Simultaneous multi-electrode array recording and two-photon calcium imaging of neural activity.* J Neurosci Methods, 2010. 192(1): p. 75-82.
204. Arnold, F.J., et al., *Microelectrode array recordings of cultured hippocampal networks reveal a simple model for transcription and protein synthesis-dependent plasticity.* J Physiol, 2005. 564(Pt 1): p. 3-19.
205. Wong, R.O., *Calcium imaging and multielectrode recordings of global patterns of activity in the developing nervous system.* Histochem J, 1998. 30(3): p. 217-29.
206. Morefield, S.I., et al., *Drug evaluations using neuronal networks cultured on microelectrode arrays.* Biosens Bioelectron, 2000. 15(7-8): p. 383-96.
207. van Pelt, J., et al., *Dynamics and plasticity in developing neuronal networks in vitro.* Prog Brain Res, 2005. 147: p. 173-88.
208. Wagenaar, D.A., J. Pine, and S.M. Potter, *Searching for plasticity in dissociated cortical cultures on multi-electrode arrays.* J Negat Results Biomed, 2006. 5: p. 16.
209. Pasquale, V., et al., *Self-organization and neuronal avalanches in networks of dissociated cortical neurons.* Neuroscience, 2008. 153(4): p. 1354-69.
210. Marom, S. and G. Shahaf, *Development, learning and memory in large random networks of cortical neurons: lessons beyond anatomy.* Q Rev Biophys, 2002. 35(1): p. 63-87.
211. le Feber, J., J. Stegenga, and W.L. Rutten, *The effect of slow electrical stimuli to achieve learning in cultured networks of rat cortical neurons.* PLoS One, 2010. 5(1): p. e8871.
212. Wagenaar, D.A., J. Pine, and S.M. Potter, *An extremely rich repertoire of bursting patterns during the development of cortical cultures.* BMC Neurosci, 2006. 7: p. 11.

213. Nozaki, Y., et al., *CSAHi study: Validation of multi-electrode array systems (MEA60/2100) for prediction of drug-induced proarrhythmia using human iPS cell-derived cardiomyocytes -assessment of inter-facility and cells lot-to-lot-variability.* Regul Toxicol Pharmacol, 2016. 77: p. 75-86.
214. Odawara, A., et al., *Physiological maturation and drug responses of human induced pluripotent stem cell-derived cortical neuronal networks in long-term culture.* Sci Rep, 2016. 6: p. 26181.
215. Thul, P.J., et al., *A subcellular map of the human proteome.* Science, 2017. 356(6340).
216. Uhlen, M., et al., *Proteomics. Tissue-based map of the human proteome.* Science, 2015. 347(6220): p. 1260419.
217. Atlas, T.H.P. *Tissue expression of SCN2A - Summary - The Human Protein Atlas*. 2017; Available from: https://www.proteinatlas.org/ENSG00000136531-SCN2A/tissue.
218. Reeves AG, S.R., in *Disorders of the nervous system*. 2008.
219. Anand, K.S. and V. Dhikav, *Hippocampus in health and disease: An overview.* Ann Indian Acad Neurol, 2012. 15(4): p. 239-46.
220. Gilbert, P.E. and A.M. Brushfield, *The role of the CA3 hippocampal subregion in spatial memory: a process oriented behavioral assessment.* Prog Neuropsychopharmacol Biol Psychiatry, 2009. 33(5): p. 774-81.
221. Sahu, Madhusmita P., et al., *Culturing primary neurons from rat hippocampus and cortex.* Neuronal Signaling, 2019. 3(2).
222. Beaudoin, G.M., 3rd, et al., *Culturing pyramidal neurons from the early postnatal mouse hippocampus and cortex.* Nat Protoc, 2012. 7(9): p. 1741-54.
223. Kaech, S. and G. Banker, *Culturing hippocampal neurons.* Nat Protoc, 2006. 1(5): p. 2406-15.
224. Clements, M., *Multielectrode Array (MEA) Assay for Profiling Electrophysiological Drug Effects in Human Stem Cell-Derived Cardiomyocytes.* Curr Protoc Toxicol, 2016. 68: p. 22.4.1-22.4.32.
225. Xu, X., et al., *Obtaining Multi-electrode Array Recordings from Human Induced Pluripotent Stem Cell–Derived Neurons.* Bio-protocol, 2017. 7(22): p. e2609.
226. Nozaki, Y., et al., *CSAHi study-2: Validation of multi-electrode array systems (MEA60/2100) for prediction of drug-induced proarrhythmia using human iPS cell-derived cardiomyocytes: Assessment of reference compounds and comparison with non-clinical studies and clinical information.* Regul Toxicol Pharmacol, 2017. 88: p. 238-251.
227. Gross, G.W., et al., *The use of neuronal networks on multielectrode arrays as biosensors.* Biosens Bioelectron, 1995. 10(6-7): p. 553-67.
228. Gopal, K.V. and G.W. Gross, *Unique responses of auditory cortex networks in vitro to low concentrations of quinine.* Hear Res, 2004. 192(1-2): p. 10-22.
229. Martinoia, S., et al., *In vitro cortical neuronal networks as a new high-sensitive system for biosensing applications.* Biosens Bioelectron, 2005. 20(10): p. 2071-8.
230. Gullo, F., et al., *Multi-electrode array study of neuronal cultures expressing nicotinic beta2-V287L subunits, linked to autosomal dominant nocturnal frontal lobe epilepsy. An in vitro model of spontaneous epilepsy.* Front Neural Circuits, 2014. 8: p. 87.

231. Dunlop, J., et al., *High-throughput electrophysiology: an emerging paradigm for ion-channel screening and physiology.* Nat Rev Drug Discov, 2008. 7(4): p. 358-68.
232. McConnell, E.R., et al., *Evaluation of multi-well microelectrode arrays for neurotoxicity screening using a chemical training set.* Neurotoxicology, 2012. 33(5): p. 1048-57.
233. Kenet, T., et al., *Spontaneously emerging cortical representations of visual attributes.* Nature, 2003. 425(6961): p. 954-6.
234. Lin, I.C., et al., *The Nature of Shared Cortical Variability.* Neuron, 2015. 87(3): p. 644-56.
235. Harsch, A. and H.P. Robinson, *Postsynaptic variability of firing in rat cortical neurons: the roles of input synchronization and synaptic NMDA receptor conductance.* J Neurosci, 2000. 20(16): p. 6181-92.
236. Helbig, I. and A.A. Tayoun, *Understanding Genotypes and Phenotypes in Epileptic Encephalopathies.* Mol Syndromol, 2016. 7(4): p. 172-181.
237. Liao, Y., et al., *SCN2A mutation associated with neonatal epilepsy, late-onset episodic ataxia, myoclonus, and pain.* Neurology, 2010. 75(16): p. 1454-8.
238. Sanders, S.J., et al., *De novo mutations revealed by whole-exome sequencing are strongly associated with autism.* Nature, 2012. 485(7397): p. 237-41.
239. Carroll, L.S., et al., *Mutation screening of SCN2A in schizophrenia and identification of a novel loss-of-function mutation.* Psychiatr Genet, 2016. 26(2): p. 60-5.
240. Fromer, M., et al., *De novo mutations in schizophrenia implicate synaptic networks.* Nature, 2014. 506(7487): p. 179-84.
241. Leach, E.L., et al., *Episodic ataxia associated with a de novo SCN2A mutation.* Eur J Paediatr Neurol, 2016. 20(5): p. 772-6.
242. Rauch, A., et al., *Range of genetic mutations associated with severe non-syndromic sporadic intellectual disability: an exome sequencing study.* Lancet, 2012. 380(9854): p. 1674-82.
243. Sakmann, B. and E. Neher, *Patch clamp techniques for studying ionic channels in excitable membranes.* Annu Rev Physiol, 1984. 46: p. 455-72.
244. Lester, H.A. and A. Karschin, *Gain of function mutants: ion channels and G protein-coupled receptors.* Annu Rev Neurosci, 2000. 23: p. 89-125.
245. Schwarz, N., et al., *Mutations in the sodium channel gene SCN2A cause neonatal epilepsy with late-onset episodic ataxia.* J Neurol, 2016. 263(2): p. 334-343.
246. Xu, R., et al., *A childhood epilepsy mutation reveals a role for developmentally regulated splicing of a sodium channel.* Mol Cell Neurosci, 2007. 35(2): p. 292-301.
247. Lossin, C., et al., *Compromised function in the Na(v)1.2 Dravet syndrome mutation R1312T.* Neurobiol Dis, 2012. 47(3): p. 378-84.
248. Kamiya, K., et al., *A nonsense mutation of the sodium channel gene SCN2A in a patient with intractable epilepsy and mental decline.* J Neurosci, 2004. 24(11): p. 2690-8.
249. Shepherd, G.M. and D.M. Katz, *Synaptic microcircuit dysfunction in genetic models of neurodevelopmental disorders: focus on Mecp2 and Met.* Curr Opin Neurobiol, 2011. 21(6): p. 827-33.

250. Zhang, L.I. and M.M. Poo, *Electrical activity and development of neural circuits.* Nat Neurosci, 2001. 4 Suppl: p. 1207-14.
251. Paulsen, O. and T.J. Sejnowski, *Natural patterns of activity and long-term synaptic plasticity.* Curr Opin Neurobiol, 2000. 10(2): p. 172-9.
252. Johnson, K.W., et al., *Sodium channel subtypes are differentially localized to pre- and post-synaptic sites in rat hippocampus.* J Comp Neurol, 2017. 525(16): p. 3563-3578.
253. Spratt, P.W.E., et al., *The Autism-Associated Gene Scn2a Contributes to Dendritic Excitability and Synaptic Function in the Prefrontal Cortex.* Neuron, 2019. 103(4): p. 673-685.e5.
254. Acsady, L., et al., *GABAergic cells are the major postsynaptic targets of mossy fibers in the rat hippocampus.* J Neurosci, 1998. 18(9): p. 3386-403.
255. Keppel Hesselink, J.M., *Phenytoin: a step by step insight into its multiple mechanisms of action-80 years of mechanistic studies in neuropharmacology.* J Neurol, 2017. 264(9): p. 2043-2047.
256. Mantegazza, M., et al., *Voltage-gated sodium channels as therapeutic targets in epilepsy and other neurological disorders.* Lancet Neurol, 2010. 9(4): p. 413-24.
257. Lynch, B.A., et al., *The synaptic vesicle protein SV2A is the binding site for the antiepileptic drug levetiracetam.* Proc Natl Acad Sci U S A, 2004. 101(26): p. 9861-6.
258. Helmstaedter, C. and J.A. Witt, *The effects of levetiracetam on cognition: a non-interventional surveillance study.* Epilepsy Behav, 2008. 13(4): p. 642-9.
259. Schiemann-Delgado, J., et al., *A long-term open-label extension study assessing cognition and behavior, tolerability, safety, and efficacy of adjunctive levetiracetam in children aged 4 to 16 years with partial-onset seizures.* J Child Neurol, 2012. 27(1): p. 80-9.
260. Pan, Z., et al., *A common ankyrin-G-based mechanism retains KCNQ and NaV channels at electrically active domains of the axon.* J Neurosci, 2006. 26(10): p. 2599-613.
261. Cooper, E.C., *Made for "anchorin": Kv7.2/7.3 (KCNQ2/KCNQ3) channels and the modulation of neuronal excitability in vertebrate axons.* Semin Cell Dev Biol, 2011. 22(2): p. 185-92.
262. Kato, M., et al., *Clinical spectrum of early onset epileptic encephalopathies caused by KCNQ2 mutation.* Epilepsia, 2013. 54(7): p. 1282-7.
263. Lehman, A., et al., *Loss-of-Function and Gain-of-Function Mutations in KCNQ5 Cause Intellectual Disability or Epileptic Encephalopathy.* Am J Hum Genet, 2017. 101(1): p. 65-74.
264. Millichap, J.J., et al., *Infantile spasms and encephalopathy without preceding neonatal seizures caused by KCNQ2 R198Q, a gain-of-function variant.* Epilepsia, 2017. 58(1): p. e10-e15.
265. Millichap, J.J., et al., *KCNQ2 encephalopathy: Features, mutational hot spots, and ezogabine treatment of 11 patients.* Neurol Genet, 2016. 2(5): p. e96.
266. Miceli, F., et al., *Early-onset epileptic encephalopathy caused by gain-of-function mutations in the voltage sensor of Kv7.2 and Kv7.3 potassium channel subunits.* J Neurosci, 2015. 35(9): p. 3782-93.
267. Yue, C. and Y. Yaari, *Axo-somatic and apical dendritic Kv7/M channels differentially regulate the intrinsic excitability of adult rat CA1 pyramidal cells.* J Neurophysiol, 2006. 95(6): p. 3480-95.

268. Brown, D.A. and G.M. Passmore, *Neural KCNQ (Kv7) channels.* Br J Pharmacol, 2009. 156(8): p. 1185-95.
269. Koyama, S. and S.B. Appel, *Characterization of M-current in ventral tegmental area dopamine neurons.* J Neurophysiol, 2006. 96(2): p. 535-43.
270. Tzingounis, A.V. and R.A. Nicoll, *Contribution of KCNQ2 and KCNQ3 to the medium and slow afterhyperpolarization currents.* Proc Natl Acad Sci U S A, 2008. 105(50): p. 19974-9.
271. Mateos-Aparicio, P., R. Murphy, and J.F. Storm, *Complementary functions of SK and Kv7/M potassium channels in excitability control and synaptic integration in rat hippocampal dentate granule cells.* J Physiol, 2014. 592(4): p. 669-93.
272. Guan, D., et al., *Contributions of Kv7-mediated potassium current to sub- and suprathreshold responses of rat layer II/III neocortical pyramidal neurons.* J Neurophysiol, 2011. 106(4): p. 1722-33.
273. Corbin-Leftwich, A., et al., *Retigabine holds KV7 channels open and stabilizes the resting potential.* J Gen Physiol, 2016. 147(3): p. 229-41.
274. Nigro, M.J., P. Mateos-Aparicio, and J.F. Storm, *Expression and functional roles of Kv7/KCNQ/M-channels in rat medial entorhinal cortex layer II stellate cells.* J Neurosci, 2014. 34(20): p. 6807-12.
275. Battefeld, A., et al., *Heteromeric Kv7.2/7.3 channels differentially regulate action potential initiation and conduction in neocortical myelinated axons.* J Neurosci, 2014. 34(10): p. 3719-32.
276. Hill, A.J., et al., *Development of multi-electrode array screening for anticonvulsants in acute rat brain slices.* J Neurosci Methods, 2010. 185(2): p. 246-56.
277. Gonzalez-Sulser, A., et al., *The 4-aminopyridine in vitro epilepsy model analyzed with a perforated multi-electrode array.* Neuropharmacology, 2011. 60(7-8): p. 1142-53.
278. Colombi, I., et al., *Effects of antiepileptic drugs on hippocampal neurons coupled to micro-electrode arrays.* Front Neuroeng, 2013. 6: p. 10.
279. Stas, J.I., et al., *The anticonvulsant retigabine suppresses neuronal KV2-mediated currents.* Sci Rep, 2016. 6: p. 35080.
280. Kang, J., et al., *Modern methods for analysis of antiepileptic drugs in the biological fluids for pharmacokinetics, bioequivalence and therapeutic drug monitoring.* Korean J Physiol Pharmacol, 2011. 15(2): p. 67-81.
281. Stafstrom, C.E., *Persistent sodium current and its role in epilepsy.* Epilepsy Curr, 2007. 7(1): p. 15-22.
282. Miceli, F., et al., *Molecular pharmacology and therapeutic potential of neuronal Kv7-modulating drugs.* Curr Opin Pharmacol, 2008. 8(1): p. 65-74.
283. Deneault, E., et al., *Complete Disruption of Autism-Susceptibility Genes by Gene Editing Predominantly Reduces Functional Connectivity of Isogenic Human Neurons.* Stem Cell Reports, 2018. 11(5): p. 1211-1225.
284. Deneault, E., et al., *CNTN5(-)(/+)or EHMT2(-)(/+)human iPSC-derived neurons from individuals with autism develop hyperactive neuronal networks.* Elife, 2019. 8.
285. Litt, B. and J. Echauz, *Prediction of epileptic seizures.* Lancet Neurol, 2002. 1(1): p. 22-30.
286. Ashcroft, F.M., *From molecule to malady.* Nature, 2006. 440(7083): p. 440-7.

287. Overington, J.P., B. Al-Lazikani, and A.L. Hopkins, *How many drug targets are there?* Nat Rev Drug Discov, 2006. 5(12): p. 993-6.
288. Bradley, J.A., et al., *In Vitro Screening for Seizure Liability Using Microelectrode Array Technology.* Toxicol Sci, 2018. 163(1): p. 240-253.
289. Gilchrist, K.H., et al., *High-throughput cardiac safety evaluation and multi-parameter arrhythmia profiling of cardiomyocytes using microelectrode arrays.* Toxicol Appl Pharmacol, 2015. 288(2): p. 249-57.
290. Clements, M. and N. Thomas, *High-throughput multi-parameter profiling of electrophysiological drug effects in human embryonic stem cell derived cardiomyocytes using multi-electrode arrays.* Toxicol Sci, 2014. 140(2): p. 445-61.
291. Kawatou, M., et al., *Modelling Torsade de Pointes arrhythmias in vitro in 3D human iPS cell-engineered heart tissue.* Nat Commun, 2017. 8(1): p. 1078.
292. Quraishi, I.H., et al., *An epilepsy-associated KCNT1 mutation enhances excitability of human iPSC-derived neurons by increasing Slack KNa currents.* J Neurosci, 2019.
293. Chong, S.A., et al., *Synaptic dysfunction in hippocampus of transgenic mouse models of Alzheimer's disease: a multi-electrode array study.* Neurobiol Dis, 2011. 44(3): p. 284-91.
294. Gao, F., et al., *Multi-site dynamic recording for Abeta oligomers-induced Alzheimer's disease in vitro based on neuronal network chip.* Biosens Bioelectron, 2019. 133: p. 183-191.
295. Markram, K., et al., *Abnormal fear conditioning and amygdala processing in an animal model of autism.* Neuropsychopharmacology, 2008. 33(4): p. 901-12.

Supplementary material

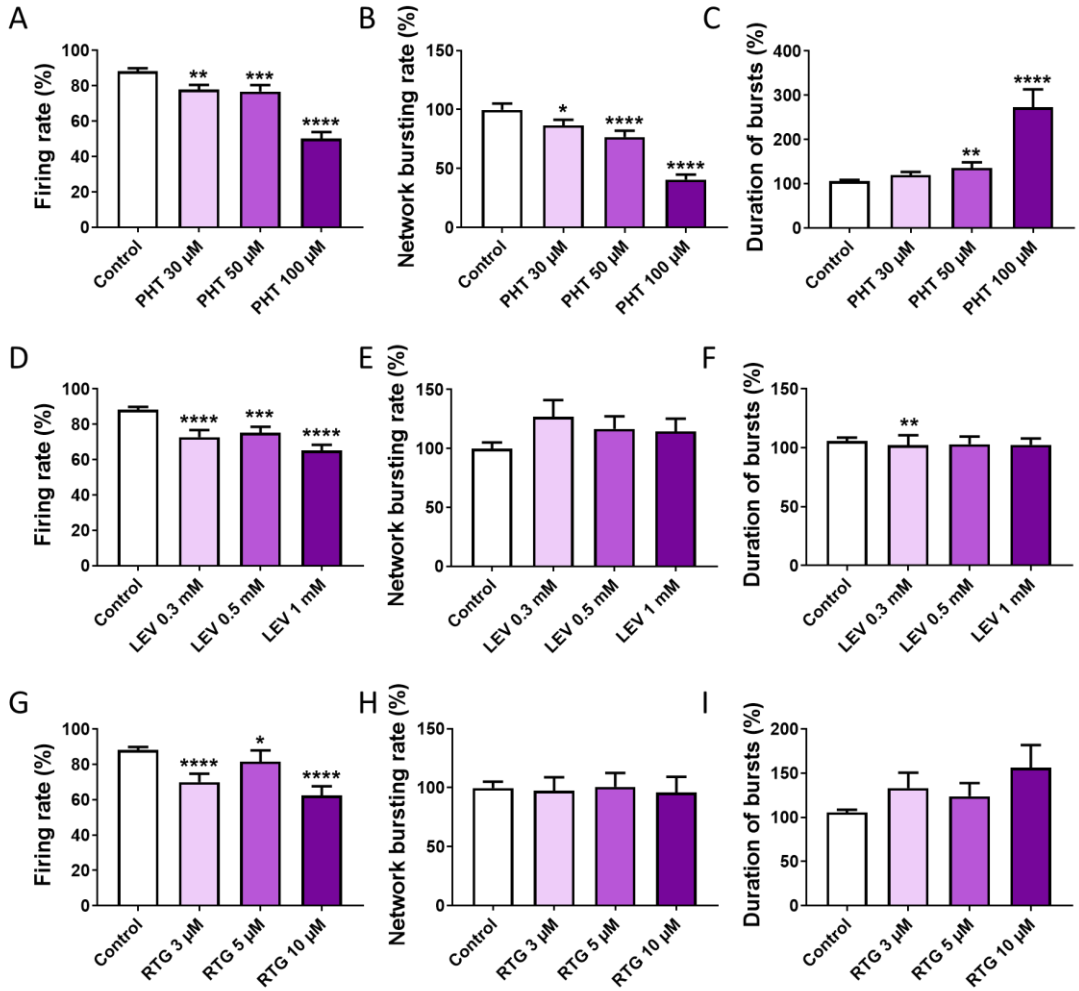

Supplementary Figure 1 The effect of PHT, LEV and RTG on firing rate, network bursting rate and duration of bursts in wild type cortical neuronal networks.

Bar graphs on the top row show the drug effect by presenting percentage changes of A) mean firing rate, B) mean network bursting rate, and C) mean duration of single channel bursts of wild type cultures before and after the application of vehicle control, 30 µM, 50 µM and 100 µM PHT. Bar graphs on the middle row show the drug effect by presenting percentage changes of D) mean firing rate, E) mean network bursting rate, and F) mean duration of single channel bursts of wild type cultures before and after the application of

*vehicle control, 0.3, 0.5, 1 mM LEV. Bar graphs on the bottom row show the drug effect by presenting percentage changes of A) mean firing rate, B) mean network bursting rate, and C) mean duration of single channel bursts of wild type cultures before and after the application of vehicle control, 3 µM, 5 µM and 10 µM RTG. Wild type cultures under vehicle control, 30 µM, 50 µM and 100 µM PHT n=113, 62, 60, and 59. Wild type cultures under vehicle control, 0.3 mM, 0.5 mM and 1 mM LEV n=113, 59, 61, and 59. Wild type cultures under vehicle control, 3 µM, 5 µM and 10 µM RTG n=113, 47, 49, and 49. A Mann-Whitney test was applied on percentage changes to test the significant differences between the drug group and vehicle control group. Results are presented as mean ± SEM. *p < 0.05, **p < 0.01, ***p < 0.001, ****p < 0.0001.*